WAVE PROPAGATION IN SATURATED POROUS MEDIA

Thesis by

Hans van der Kogel

In Partial Fulfillment of the Requirements

For the Degree of

Doctor of Philosophy

California Institute of Technology

Pasadena, California

1977

(Submitted May 16, 1977)

Acknowledgements

The author sincerely thanks his advisor, Professor R.F. Scott for valuable discussions, suggestions and assistance in the course of research and preparation of this thesis.

The author is grateful for the research and teaching assistantships received from the California Institute of Technology. A portion of this work was supported under NSF Grant ERT 74 20407.

Thanks are due to Mrs. Carol Storm for her fast and expert typing of the manuscript.

I am indebted to my wife, Paula, who made many sacrifices during many years of my study.

Abstract

Wave propagation in saturated porous media is investigated in the framework of two models, a theoretical and an experimental one.

The theoretical model has two phases, a fluid phase and a solid phase, both modeled as a continuum. The solid phase consists of incompressible grains forming a compressible skeleton. The fluid phase represents a compressible fluid located between the grains. Interactive forces, due to relative motion between the skeleton and the fluid are taken into account. Non-linear balance laws and equations of state are formulated for plane waves. Linearization of the non-linear balance laws yields a set of equations which in limiting cases reduce to well-known results (e.g. consolidation equation, condition for fluidization). The harmonic solution of the linearized field equations contains two modes: one in which the phases move almost together (which is slightly damped) and one in which the phases move in opposite directions (which is highly damped). Solutions are presented in system form.

Applying a step loading in the variables at the boundary generates, in general, two propagating discontinuities in the variables and these discontinuities decay as they propagate. If we assume that the parameters take "practical" values of wet sand then the jump in pore-pressure is always large with respect to the jump in effective pressure along the faster discontinuity propagating into a medium at rest, while velocity differences between the phases are generated

if the densities of the phases are different. Non-linear effects due to a non-linear constitutive equation for the fluid oppose the decay of gradients in the variables along the faster propagating discontinuity. The influence of non-linear convective terms can be neglected if the phase velocities are small with respect to the velocities of the discontinuities.

The solution to the problem of reflection and refraction of a discontinuity propagating in a fluid and impinging on a two-phase medium is presented. The theory is extended in multi-dimensions, in order to allow shear waves to propagate. The existence of non-propagating discontinuities in dilatant shear is demonstrated.

The experimental model consists of a disc configuration, dry and saturated. The interparticle stresses due to impact are visualized by a photo-elastic technique and recorded by a high-speed camera. Changing stress patterns in the discs behind the wavefront are observed. In the dry case a wavefront emerges, behind which the particles are relatively well stressed, while no such definite stress front can be identified in the saturated case. Phase velocity differences occur and separation of particles was observed to take place due to indirect loading of the discs via the fluid.

Table of Contents

Table of Contents (Continued)

Table of Contents (Continued)

Table of Contents (Continued)

1

INTRODUCTION

Stress propagation in saturated porous media is of practical importance in the protection of structures against earthquakes and other types of ground shock. It is also of theoretical interest in geophysical studies concerned with identifying the properties of rock masses and sedimentary deposits, in which case the determination of wave speeds and reflection coefficients are especially important.

In soil mechanics there is concern about the stability and the displacement of structures located on or in saturated soil, or the stability of soil structures themselves. The loss of strength by a saturated soil during repeated loading, as in the case of an earthquake, and related liquefaction phenomena are of considerable practical importance.

In the present study of wave propagation in saturated sands, a theoretical model and an experimental model are investigated. The theoretical model consists of two phases, a solid phase and a fluid phase, both treated as continua. The compressible solid phase represents the skeleton of sand grains. The compressible fluid phase represents the water located in the pore space between the sand grains which is able to move with respect to the skeleton. Assumptions as to the constituitive relations follow the traditional approaches in soil mechanics. Linearization of the non-linear equations of mass balance, momentum balance, and constituitive relations for the solid and fluid phases in the one-dimensional case yields (Chapter B) four equations with four unknowns (fluid pressure, effective

pressure, average skeleton velocity, average fluid velocity). For limiting cases we generate, in Appendices IV and V, well-known results (e.g. consolidation, fluidization). Because we derive the linear theory from the non-linear theory we have the advantage of testing the validity of the linear theory with respect to the non-linear theory; this is in contrast to other theories (e.g. Biot [1]). The linearized model will enable us to study changes in the variables due to applied loading.

The harmonic solution of the field equations is presented in Chapter C. De Josselin de Jong [4] showed that if the parameters have the "practical" values of wet sand, in the lower frequency range there are two modes, one (first mode) in which the phases move almost together (which is slightly damped) and one (second mode) in which the phases move in opposite directions (which is highly damped). The harmonic solution is presented in system form in Chapter D, which is convenient for further numerical treatment. The eigenfrequencies for a one-dimensional layer are established and it is shown that those of the first mode are very high and those of the second mode are very low for a layer height of 0.2 m.

The propagation of discontinuities due to an applied step loading at the boundary is discussed in Chapter G. We demonstrate the relation between the phase velocity in the harmonic solution, speed of the characteristics (Chapter F) and speed of the discontinuities. Further we show that including non-linear terms due to a non-linear constitutive equation for the fluid opposes the decay of propagating discontinuities in the gradients. The consequence of equal phase velocities

is investigated in Chapter H where it is found that in general equal phase velocities do not occur unless there is a certain ratio between the compressibility of the fluid and the compressibility of the skeleton.

The linear theory is extended to multiple dimensions for the isotropic case in Chapter J, in which the harmonic solution for the plane strain case is investigated. Three modes can exist and the solution can be presented in system form by including a shear deformation. The reflection and refraction of a discontinuity propagating in a fluid and impinging on a two-phase medium is studied in Chapter L. We use here the coupling condition between a fluid and a two-phase medium as established in Chapter K. Near the boundary the skeleton compresses and after that expands to zero effective stress, while the fluid compresses.

In order to derive a more realistic constitutive relation for a sand rather than a linear elastic isotropic material we make an attempt in Chapter M to describe the state of a granular material by including kinematical variables. By using thermodynamic arguments, we construct a constitutive relation which in linearized form will be used for further analysis. A real soil often exhibits contraction or expansion during shear, called dilatancy. Therefore, we study the propagation of discontinuities in the dilatant shear case in Chapter N. There exists a non-propagating discontinuity if the material is present in a state of neutral stability.

The laboratory model consists of a disc configuration, dry and saturated. By shining polarized light through the discs we were

able to visualize the stress patterns in the discs. The discs were impacted and high-speed camera films of the resulting stress patterns were made. In the dry case an area of well-stressed discs emerged after the stress front. No definite stress front in the saturated case was observed. Discs, indirectly loaded by a fluid layer on top of the discs, separated due to impact.

In Chapter A we give a review of some of the work done in the area of wave propagation through saturated porous media and a summary of the main results obtained in this investigation is contained in Chapter P.

A. Literature Review

In this Chapter we will summarize some of the work done on the subject of wave-propagation through saturated porous media.

In the first part we treat the predominantly theoretical work and in the second part the predominantly experimental work.

A.1 Theoretical Work

Biot in a series of papers [1,2,3], treated the problem of wave propagation through saturated porous media.

He assumed that the fluid and the skeleton are linearly elastic. Constitutive equations were established by thermodynamic arguments for the linearized case. For an isotropic skeleton the number of constants in the constitutive equations was four. Further he derived the momentum equations by evaluating the kinetic energy and the dissipation function of the medium, and applying Lagrange's equations. The momentum equations were coupled by inertia coupling terms and terms arising due to different phase velocities.

The harmonic solution of the field equations showed the existence of three kinds of waves: one rotational wave and two dilatational waves (waves of the first kind and waves of the second kind). In the first kind of wave the skeleton and fluid move in phase, while in the second kind of wave the fluid and the skeleton move out of phase. The dilatational wave of the second kind is highly damped and propagates slower than the wave of the first kind.

Biot separated his theory into two parts: low-frequency and high-frequency range. In the low-frequency range the relative motion of the fluid in the pores is of the Poiseuille type and the coefficient in the "Darcy" law is a constant, but in the high-frequency range the coefficient becomes frequency dependent.

He introduced viscoelasticity in order to describe a variety of phenomena, such as interfacial surface tension and physical-chemical interactions. Furthermore he formulated the field equations for an anisotropic skeleton.

This work formed the basis for many subsequent papers on the theory of wave propagation through saturated porous media.

De Josselin de Jong [4] treated one-dimensional wave propagation through a saturated porous medium.

Both the skeleton and the fluid were assumed to be linearly elastic. He derived two momentum balance equations, one for the skeleton and one for the fluid.

For the harmonic solution in the lower frequency range and "practical" values of wet sand he showed that there are two kinds of waves: one in which the phases have almost the same velocity and one in which the phases have velocities in opposite directions. The first wave is almost undamped and the second wave is heavily damped.

Ishihara [5,6] did further work on the Biot theory. He related the Biot coefficients to the compressibilities of the phases and the soil bulk.

He considered harmonic excitation in the lower frequency range with parameters established for saturated soils and he focussed his attention on one of the two kinds of compression waves. This turns out to be the wave in which the phases almost have the same motion and in which the damping is low.

Ishihara suggested the use of elasticity theory as a substitute for poro-elasticity, especially when the medium is stressed in undrained condition as encountered in dynamic problems. However, this statement refers only to the above considered wave.

Hsieh and Yew [7] studied the wave motion in a fluid-saturated porous medium, where the fluid is incompressible.

They used a modified Lubinski stress-strain relation for the skeleton and a Biot equation for the fluid. Further they used the concepts of mixture theory in order to derive the mass balance and momentum balance equations. They assumed that the interaction force between fluid and solid is proportional to the mass flow of the fluid relative to the solid. Further they assumed that the specific flow resistance becomes a function of the frequency for high frequencies. After linearizing the field equations they established the equations for the dilatational and rotational waves.

The harmonic solution revealed two kinds of dilatational waves and one rotational wave.

The effect of the specific flow resistance on the wave speeds was studied.

The airflow through a fiber tangle was treated by Taub [8]. He focussed his interest on a one-dimensional problem and postulated the following nonlinear balance equations: conservation equations for solid mass and fluid mass; conservation equations for solid momentum and fluid momentum and a conservation equation for the fluid energy. Interaction forces were represented by a modified Darcy law, including nonlinearities due to tortuosity of the streamlines through the pores. He assumed that the fiber material was incompressible, but postulated a nonlinear stress-strain relation for the fibers.

The nonlinear equations were solved by the method of characteristics. The flow within a dilation chamber was considered.

Ghaboussi and Wilson [9] formulated the Biot theory numerically by use of finite elements.

A one-dimensional boundary value problem consisting of a steploading of the skeleton at the boundary and keeping the pore-pressure zero at the boundary was considered. Two types of mass representation were used: consistent mass matrix and lumped mass matrix. Results showed a gradual increase in effective stress and pore-pressure. Near the boundary the pore-pressue fell to zero.

Furthermore they applied their numerical scheme to a dam-reservoir system. They noted that in the core of the dam, where the permeability was very low, almost all the oscillations were taken by the fluid and the intergranular stress changed very smoothly.

Liou [10] did a numerical study in order to get insight into liquefaction phenomena in sand deposits.

He first established the field equations for one-dimensional compression. These consist of an equation for the fluid pressure and a constitutive equation for the skeleton, a momentum balance for the total medium and a momentum balance for the relative motion of the pore water with respect to the skeleton. The interaction forces between skeleton and pore water are assumed to be in terms of Darcy's law.

After linearizing the field equations Liou constructed solutions by the method of characteristics.

He established a coupling between the shear modulus and confined compression modulus. In this way he coupled the compression waves with the shear waves. A nonlinear formulation was used in order to investigate the performance of sand deposits during the Niigata earthquake.

Yew and Jogi [11] used the Biot theory in order to study wave motions in fluid-saturated porous rocks. The purpose of their study was to make a comparative study between experimental results of wave-propagation through saturated rocks (sonic-pulse technique) with the results predicted by the Biot theory.

Applying Laplace transformations they were able to solve the appropriate boundary value problem. The inversion integral was evaluated numerically. Two harmonic waves emerged, called the fast and the slow wave. The slow wave was highly dispersive and the fast wave showed very little dispersion. Furthermore the slow wave decayed much faster than the fast wave.

Using the experimentally obtained constants in the Biot equations, they compared the theoretically obtained and the experimentally obtained wave velocities. Because the inertia coupling parameter in

the Biot equations was unknown, they tried to establish this parameter by comparing the experimentally obtained wave speeds and the theoretically obtained wave speeds. It was concluded that the inertia coupling coefficient was small for the cases considered.

Because the recorded waves showed no observable dispersion and because the slow wave damped out rapidly, they stated that they believed that the experimentally observed waves were the fast waves.

O'Connell and Budiansky [12] calculated the elastic moduli of a solid permeated with an isotropic distribution of flat cracks.

They used the argument that the isothermal potential energy of the cracked body is equal to the potential energy of the uncracked body plus the potential energy change due to insertion of cracks. In a similar way they obtained expressions of the elastic moduli of a saturated and partially saturated cracked body.

Increasing the number of cracks in the body decreased the shear modulus and compression modulus of the cracked body. For dry cracks this decrease was larger than for saturated cracks.

Kuster and Toksöz [13] formulated the problem of wave propagation through a two-phase medium in terms of a scattering phenomenon.

They considered the scattering of a plane wave in a solid matrix by a spheroical inclusion. By considering the scattering effect of N spheroical inclusions they derived the composition laws for the effective elastic constants and density (in terms of the elastic constants and densities of the matrix material and the inclusions). Multiple scattering effects were neglected and hence the model is limited to two-phase media where the concentration of inclusions is small.

They stated that the essential result is that the effective elastic moduli depend not only on the concentration but also on the shape of the inclusion.

Numerical results showed that the effective elastic moduli and compressional and shear velocities decrease with increasing concentration of inclusions. Flatter inclusions have a greater effect than the rounder inclusions.

Garg et al. [14] treated the wave propagation in saturated porous media in the framework of the theory of interacting continua.

They considered a one-dimensional problem and formulated four equations: two momentum balance equations and two constitutive equations. The interaction forces were assumed to be proportional to the velocity differences of the phases.

They considered the harmonic solutions, specifically a step-loading in the velocities of the phases at the boundary and were able to construct closed-form analytical solutions with Laplace transforms for two cases: small and strong viscous coupling between the phases. For weak viscous coupling two propagating discontinuities emerged from the boundary and they decayed as they propagated. For strong viscous coupling the two wave fronts coalesced into a single front and the phase velocities were almost equal.

Nikolaevskii [15,16,17,18] studied shock-wave propagation in soft water-saturated soils.

He established five equations for the linearized case, including a porosity perturbation. The skeleton and the fluid are linearly elastic and the grains are compressible. The interaction forces are of the Darcy type. Inertia coupling as in the Biot theory is omitted.

In studying strong shock waves he made the assumption that the pressures in the phases are equal. Then he studied stationary shocks in the framework of his nonlinear equations. These consist of: two mass balance equations, one for the fluid and one for the grains; a momentum equation for the fluid and a momentum equation for the mixture; two nonlinear constitutive equations, one for the fluid and one for the grains.

He concluded that stationary shocks can exist in a coordinate system that moves with the speed of the shock. The shock wave consists of an initial jump in the variables, after which the phase velocities are in general unequal. Behind the jump the phase velocities equalize gradually.

In the linearized equations the stationary shock wave form is impossible. Hence a certain shock strength is needed in order to generate the stationary profile.

Lyakhov et al. [19,20] studied the waves produced by spherical charge in saturated soils.

They concluded that two mechanisms of compression exist simultaneously: transmission of the load through the contacts of the grains and transmission of the load through the compression of air, water and the grains (compression of a three-component medium). For large loads the soils behave like a three-component medium.

By writing down the constitutive equation for the components in the free state, Lyakhov constructed a constitutive equation for a three-component medium. By establishing the equations of motion, a constitutive equation for the detonation products and boundary conditions at the contact discontinuity between detonation products and the three-component medium, they studied the wave propagation due to an explosion.

Solutions were obtained by the method of characteristics for one-dimensional problems and problems with spherical symmetry.

The rate of decay of the maximum pressure with distance increased largely with the increase in the content of the gaseous component in the soil. The rate of decrease of the velocity of the wavefront with distance increased substantially with an increase in air content.

They stated that good agreement between experiment and theory was obtained for very low air content.

A.2 Experimental Work

Wyllie, Gardner and Gregory [21] conducted a series of tests on alundum bars and natural specimens of rock in order to study the wave attenuation in porous media.

They used the resonant bar method and alundum specimens in order to measure sloshing losses and compared these losses with those computed from the Biot theory.

They stated that the attenuation of waves in a fluid-saturated porous medium may be regarded as the sum of the loss due to relative motion of the fluid with respect to the skeleton (sloshing) and the loss

caused by the skeleton (jostling; due to solid friction and viscous loss resulting from the chemical and physical effect of the fluid on the cementing material of the solid).

Alundum was used because a large change in the elastic moduli upon addition of fluids is avoided in that case.

They concluded that by compressing the skeleton and by an increase in the permeability the jostling losses decrease and the sloshing losses become dominant. Furthermore they concluded that there is strong evidence to support the correctness of Biot's theory when applied to resonating bars.

Kuster and Toksöz [22] measured the velocity and attenuation of ultrasonic waves in suspensions of solid spherical particles in fluid matrices as a function of the concentration of inclusions.

A pulse propagation technique was used for velocity measurements. The density of the matrix and inclusions were about the same in order to keep the inclusions in suspension during the test.

They concluded that the wave speed in the composite medium varies with concentration nearly uniformly if the density contrast between particles and fluid is small. If the density contrast is large then there is a minimum in the velocity at some concentration. Furthermore they concluded that the attenuation of the pressure was caused by scattering effects, absorption in the viscous matrix and anelasticity of the filling solid. At the lower frequencies the last two effects dominate.

Gregory [23] investigated the influence of different fluids on the wave propagation in consolidated sedimentary rocks by means of an ultrasonic technique.

He concluded that fluid saturation effects on compressional wave velocity are much larger in low-porosity rocks than in high-porosity rocks. This effect was more pronounced at higher hydrostatic confining pressure.

Gregory stated that the Biot theory predicts that the shear wave velocity of dry rocks is higher than the shear wave velocity in saturated rocks. This observation was confirmed by the experimental data at confining pressures above 9000 psi. For low-porosity rocks at lower confining pressures the experimental data disagreed with the above statement.

Gregory indicated that this discrepancy might be due to the existence of micro-cracks in and around the cementing material of low-porosity rocks.

Hardin and Richart [24] conducted a series of laboratory tests, using the resonant column method, in order to establish longitudinal and shear wave velocities for different sands.

They concluded that the presence of moisture in a sand reduces the velocity of wave propagation due to mass of the water that moves with the skeleton, but that in some materials there is a reduction in the stiffness of the frame due to the moisture. Furthermore they concluded that for saturated granular materials with sufficiently large pores, water flowed through the pores during testing.

Hall and Richard [25] studied the dissipation of wave energy in granular materials by using the vibration decay method. Torsional and longitudinal oscillations were induced.

They found that saturating the specimens with water increased the logarithmic decrement by 1.5 to 4 times that of the dry specimens.

Seed and Lee [26] studied the behavior of saturated sands during repeated loading in a triaxial test under undrained conditions.

The load, deformation and pore pressure were measured as a function of time.

For a loose specimen the pore pressure built up gradually during the first cycles of stress application; however, in this stage there was no noticeable deformation. Quite suddenly the pore pressure increased to a value equal to the externally applied confining pressure and large strains developed.

For a dense sand the pore water pressure increased gradually and no noticeable deformation developed. After the pore water pressure amplitude reached the initial confining pressure the strain amplitude increased relatively slowly with increasing number of cycles.

It was concluded that the susceptibility of a saturated sand to liquefaction as a result of cyclic loading is determined by the void ratio, the confining pressure, the magnitude of cyclic stress or strain and the number of stress cycles.

Castro [27] conducted a series of cyclic loading tests on dense saturated sand samples (cyclic triaxial tests).

He observed that the axial strains were developing mainly in a narrow horizontal zone near the top of the specimen. This zone

consisted of an extremely loose, almost liquid sand-water mixture. He concluded that during the cyclic triaxial test substantial redistribution of pore water took place whenever the magnitude of the cyclic strains reached a few percent and possibly occurred even at much smaller strains.

Ivanov [28] documented information on the action of explosions in water-bearing soils and the processes occurring during compaction of noncohesive soils.

Ivanov pointed out the different wave propagation character in nonsaturated and saturated sand.

For dry sand or partially saturated sand, a steep front in the pressure emerges (which was called shock wave) near the point of explosion. After propagating into the medium, the slope of the front decreases and the profile of the wave expands. Finally it becomes a seismic wave, in which the deformations are mainly elastic. Within the zone of action of the shock wave (near the place of explosion) irreversible deformation of the soil takes place.

For saturated sands the wave due to an explosion was a shock wave at all investigated distances from the place of explosion. The general character of the wave was almost the same as in water.

Observed wave velocities for the wavefront in saturated sands were 1400-1660 m/sec. Small amounts of air (1%-4%) caused a significant decrease in the speed of the wave front (to 200-300 m/sec).

Furthermore it was observed that in saturated sand the amplitude of the pressure did not depend on the orientation of the transducer,

while in dry sand there was a marked difference between radial and lateral pressure (coefficient of lateral pressure 0.3 to 0.5).

The results of several laboratory studies were also reported. In a tank (diameter 1.5 m, height 1.2 m), filled up with fine-grained Volga sand, explosions were performed. Charges (1.5 to 4.5 gm) were placed 30-50 cm under the soil surface. Saturated, loosely packed sands were liquefied during the explosion. It was observed that the pore water pressure increased instantaneously to maximum values during the explosion. After liquefaction took place, compaction of sand with a gradual decrease in excess pore-water pressure and the outflow of water to the surface of the sand took place.

For an initially dense packing of the sand no liquefaction phenomena, no rise in pore pressure and no compaction were observed.

Akai, et al. [29] conducted studies on stress wave propagation through saturated cohesive soils by means of a triaxial shock tube.

By connecting a shock tube to a triaxial chamber which contained a cylindrical saturated clay specimen, they were able to control the loading condition. The input waveform (pressure) was one with a steep front, after which a gradual decay took place. After propagating into the medium the wavefront spread out. Stress and strain gages were imbedded in the specimen in order to obtain stress-strain curves due to stress wave propagation.

At a strain level of 10^{-3} large hysteretic curves (in stress-strain relationship) were observed, while no permanent strain was created during the test.

It was concluded that below a stress level of 20% to 25% of the triaxial compressive strength, the soil behaves elastically or visco-elastically.

True [30,31] conducted a series of tests at the Naval Civil Engineering Laboratory in Port Hueneme.

A vertical pipe (diameter 8 inches, length 12 feet) was connected to a blast simulator. Sand was poured into the pipe. The walls of the pipe were coated with vegetable shortening and a layer of thin rubber sheet isolated the shortening from the sand in order to reduce wall friction. A 12-mesh-per-inch screen 7.8 inches in diameter was put on top of the ion surface. Pore pressure meters were installed in the wall of the pipe. At the same height soil pressure gages were buried in the sand.

The top of the sand column was loaded due to an explosion in the air. The loading (air pressure) had the characteristics of a steep front and a slowly decreasing tail.

The response of the pressure meters at 6 inches below the sand surface for the case the sand was flooded showed a jump in the water pressure similar to the loading (air) pressure; however, the calculated effective stress showed a different pattern. After an initial positive, sometimes small, jump the effective stress decreased and stayed around zero reference stress (equal to the overburden static stress). See Fig. I and Fig. II. Negative reference stresses were observed and there were indications that a quick condition existed in some cases (e.g. migration of pressure meters).

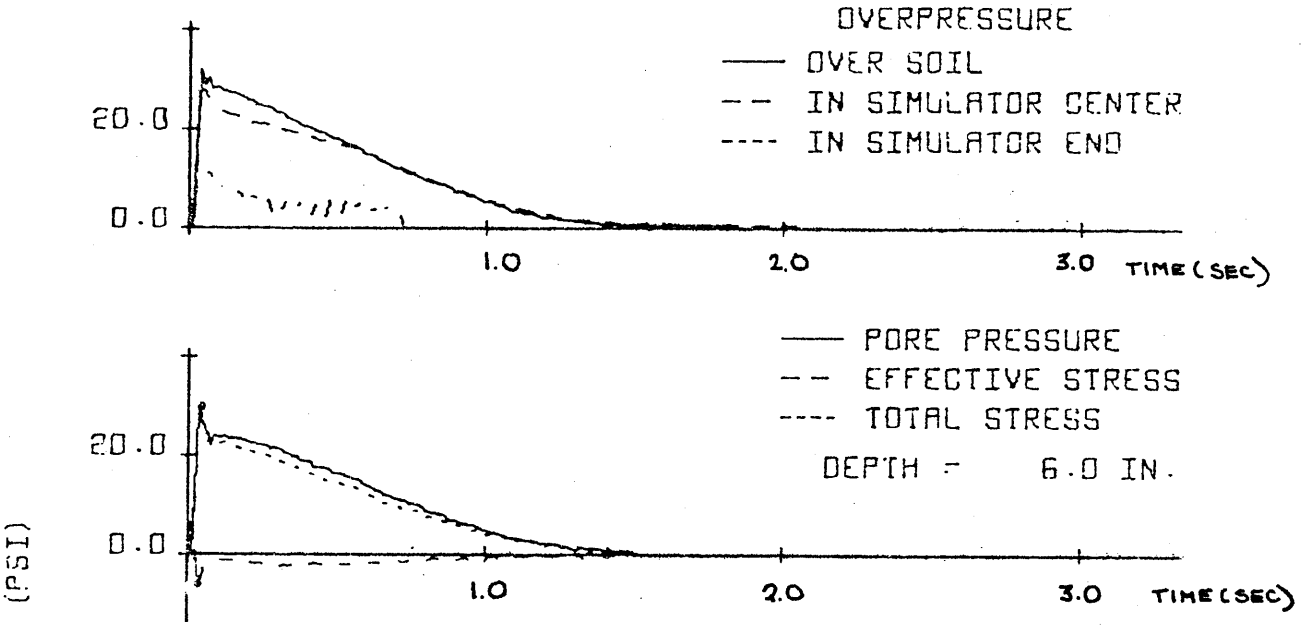

Pore pressure, total stress and calculated effective stress at 6.0 inches below the sand surface, saturated (True [31]).

FIG. I

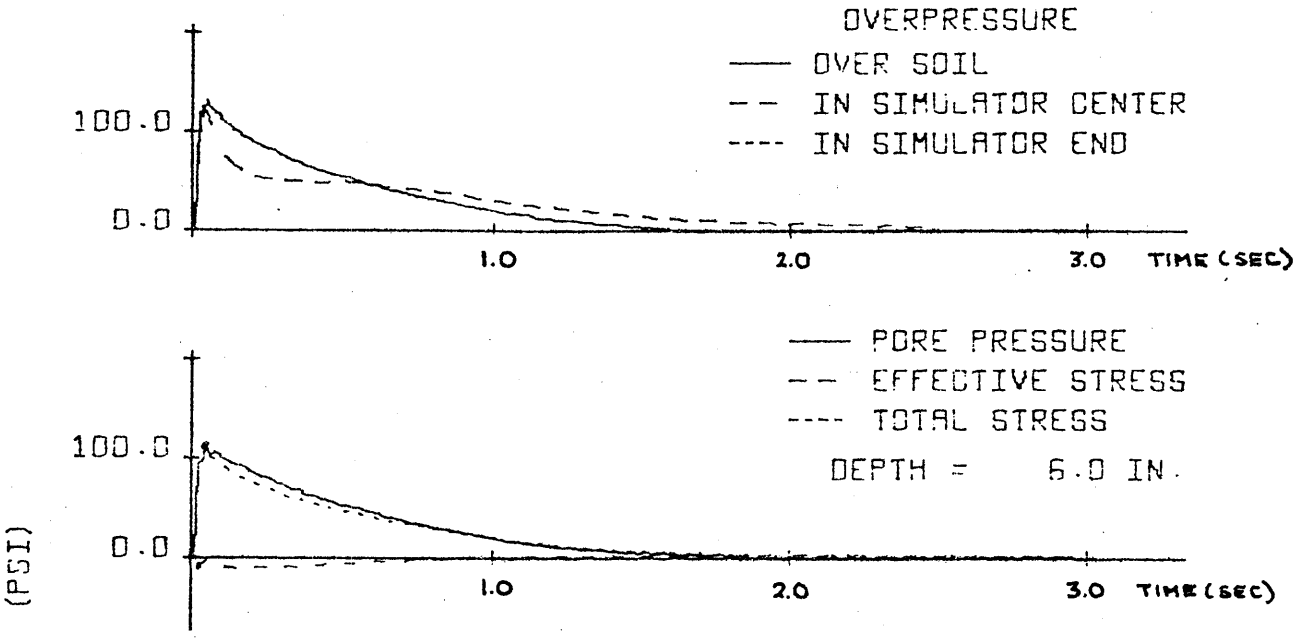

Pore pressure, total pressure and calculated effective stress at 6.0 inches below the sand surface, saturated (True [31]).

FIG. II

Further it was stated that the water pressures measured were probably realistic, but the effective pressures might be affected by wall friction.

Perry [32] studied the effect of blasting on a saturated sand by the movement of inclusions.

A tank (diameter: 4ft and height: 2ft) was partially filled up with a nearly saturated sand or a dry sand. A charge in the remaining portion of the tank supplied the loading.

It was concluded that liquefaction, as evidenced by a loss of shear strength leading to bearing capacity failure, was found to occur in laboratory one-dimensional plane wave loading tests (from movement of inclusions) on nearly saturated and dry sand.

Covering the blast-loaded top surface of the sand with a membrane prevented substantial movement of the inclusions. When the top surface membrane was present, the sand surface moved downward about 0.3 in., but when the membrane was not present the sand surface moved upward about 0.4 in.

B. Dynamics of Porous Media, One-Dimensional Compression

In this chapter we will establish the field equations. The model is a continuous one and is intended to represent the prototype in some important aspects. Basic assumptions will be stated. We will pose the non-linear balance laws and constitutive equations. For further analysis the field equations will be linearized.

Obviously the model forms only an approximation to the prototype (saturated sand). However the study of this model will generate some useful information.

One of the aspects that is not properly modelled is the fact that the real material consists of discrete particles, which are separable. This and other aspects of the behavior will be studied in another, experimental, model.

B.1 Basic Assumptions

The model consists of two media; a fluid in which is immersed a skeleton of solid grains. The fluid occupies nV and the solid occupies (n-1) V of the total volume V. We call n the porosity. The skeleton represents a granular material with constant mass density ρ_p. The fluid represents a compressible fluid with density ρ_w.

The constant density of the solid material and variable density of the fluid is chosen because quartz is 30 times less compressible than pure water (Whitman [33]).

The value for the compressibility of the fluid represents that of the real fluid located between the real grains.

For the equation of state for the skeleton we assume: $n = g(\sigma)$, where σ is the effective stress (Scott [34]). Hence we assume that the above relation does not depend on the fluid pressure. We consider the grains to be incompressible, inert and without cracks.

The real particle configuration (skeleton) will be unable to withstand substantial tensile stresses, therefore we will assume that the skeleton is prestressed at σ_0 and we are interested in the changes with respect to σ_0.

For the equation of state for the fluid we assume: $\rho_w = f(p)$, where p is the pressure in the fluid. We neglect temperature effects.

Separately we pose the momentum conservation equation and the mass conservation equation for the fluid and the skeleton.

The fluid surrounds the grains, except at the small contact areas between the grains.

Relative movement between the skeleton and the fluid is assumed to give rise to forces R.

After linearization of the equations these forces are assumed to follow Darcy's law (Verruijt [35]).

The averaged velocity of the fluid particles in an elementary volume is w and the averaged velocity of the skeleton in an elementary volume is v.

The mass of the fluid and the mass of the skeleton are assumed to be $n\rho_w$ and $(1-n)\rho_p$ respectively in the momentum balance equations.

The independent variables are distance x and time t.

B.2 Field Equations

The field equations consist of the mass conservation equations, the momentum conservation equations and the equation of state for both constituents.

Mass conservation:

$$\frac{\partial}{\partial t}((1-n)\ \rho_p)) + \frac{\partial}{\partial x}\ (\rho_p\ (1-n)\ v) = 0 \qquad \text{(B1)}$$

$$\frac{\partial}{\partial t}\ (\ n\rho_w) + \frac{\partial}{\partial x}\ (\rho_w\ n\ w) = 0 \qquad \text{(B2)}$$

Equation (B1) represents mass conservation for the skeleton and equation (B2) represents mass conservation for the fluid.

Momentum conservation:

$$n\ \rho_w\ (\frac{\partial w}{\partial t} + w\ \frac{\partial w}{\partial x}\ ) = -n\ \frac{\partial p}{\partial x} - R \qquad \text{(B3)}$$

$$(1-n)\ \rho_p\ (\frac{\partial v}{\partial t} + v\ \frac{\partial v}{\partial x}) = -\frac{\partial \sigma}{\partial x} - (1-n)\ \frac{\partial p}{\partial x} + R \qquad \text{(B4)}$$

Equation (B3) represents the momentum conservation equation for the fluid. Equation (B4) is the momentum conservation equation for the skeleton. The term (1-n) $\frac{\partial p}{\partial x}$ is added because the fluid surrounds the solid particles. The term R represents forces due to relative movement of solid and fluid; hence these terms are of opposite sign in (B3) and (B4).

Both the pore pressure p and the effective stress σ are assumed to be positive when compression of their respective phases takes place

and hence the gradients of these quantities appear with negative signs in (B3) and (B4).

Equations of state:

$$\rho_p = \text{constant} \qquad \text{(Scott [34])} \qquad \text{(B5)}$$

$$\rho_w = f(p) \qquad \text{(Bear [36])} \qquad \text{(B6)}$$

$$n = g(\sigma) \qquad \text{(Terzaghi [37])} \qquad \text{(B7)}$$

Equation (B6) states that the density of the fluid ρ_w is a function of the pore pressure p and equation (B7) states that the porosity is a function of the effective stress.

Hence we have six equations: (B1), (B2), (B3), (B4), (B6) and (B7) and we have seven unknowns: ρ_w, n, σ, p, v, w, R. These field equations are non-linear because they contain products of the variables. We will linearize the field equations around an initial state in order to get some insight by solving these linearized equations. An additional equation (Darcy's law) will be added in the linearized case in order to specify R.

We will now rearrange the equations and linearize them.

From (B1) and (B5) there follows:

$$-\frac{\partial n}{\partial t} + (1-n)\frac{\partial v}{\partial x} - v\frac{\partial n}{\partial x} = 0 \qquad \text{(B8)}$$

Equation (B7) gives:

$$\frac{\partial n}{\partial t} = \frac{\partial g}{\partial \sigma}\frac{\partial \sigma}{\partial t} \qquad \text{(B9)}$$

Substitution of (B9) into (B8) gives:

$$-\frac{\partial g}{\partial \sigma}\frac{\partial \sigma}{\partial t} + (1-n)\frac{\partial v}{\partial x} - v\frac{\partial n}{\partial x} = 0 \qquad \text{(B10)}$$

From (B2) it follows that

$$\rho_w \frac{\partial n}{\partial t} + n\frac{\partial \rho_w}{\partial t} + \rho_w \frac{\partial}{\partial x}(nw) + nw \frac{\partial \rho_w}{\partial x} = 0 \qquad \text{(B11)}$$

From (B6) we conclude:

$$\frac{\partial \rho_w}{\partial t} = \frac{\partial f}{\partial p}\frac{\partial p}{\partial t} \qquad \text{(B12)}$$

$$\frac{\partial \rho_w}{\partial x} = \frac{\partial f}{\partial p}\frac{\partial p}{\partial x} \qquad \text{(B13)}$$

substitution of (B12) and (B13) into (B11) gives:

$$\rho_w \frac{\partial n}{\partial t} + n\frac{\partial f}{\partial p}\frac{\partial p}{\partial t} + \rho_w \frac{\partial}{\partial x}(nw) + nw\frac{\partial f}{\partial p}\frac{\partial p}{\partial x} = 0$$

Hence:

$$\frac{\partial n}{\partial t} + n\frac{\frac{\partial f}{\partial p}}{\rho_w}\frac{\partial p}{\partial t} + \frac{\partial}{\partial x}(nw) + nw\frac{\frac{\partial f}{\partial p}}{\rho_w}\frac{\partial p}{\partial x} = 0 \qquad \text{(B14)}$$

adding equation (B14) and (B8) gives:

$$n\frac{\frac{\partial f}{\partial p}}{\rho_w}\frac{\partial p}{\partial t} + \frac{\partial}{\partial x}(nw) + nw\frac{\frac{\partial f}{\partial p}}{\rho_w}\frac{\partial p}{\partial x}$$

$$+ (1-n)\frac{\partial v}{\partial x} - v\frac{\partial n}{\partial x} = 0 \qquad \text{(B15)}$$

The above equations are non-linear because they contain products of the variables n, p, w, v, σ and ρ_w.

We now linearize the equations in the following way:

$$\begin{aligned} p &= p_0 + p_1 \\ w &= w_0 + w_1 \\ v &= v_0 + v_1 \\ \sigma &= \sigma_0 + \sigma_1 \\ n &= n_0 + n_1 \\ \rho_w &= \rho_0 + \rho_1 \end{aligned} \tag{B16}$$

where the variables with subscript zero represent constants and the variables with subscript 1 are the perturbed values.

Now we note that:

$$\frac{\frac{\partial f}{\partial p}}{\rho_w} \approx \frac{\alpha}{\rho_{w_0}} \tag{B17}$$

where α is a constant.

Substitution of (B16) and (B17) into (B15) gives:

$$(n_0 + n_1) \frac{\alpha}{\rho_{w_0}} \frac{\partial (p_1+p_o)}{\partial t} + (n_0 + n_1) \frac{\partial}{\partial x} (w_0+w_1)$$

$$+ (w_0+w_1) \frac{\partial}{\partial x} (n_0+n_1)$$

$$+ (n_0+n_1) (w_0+w_1) \frac{\alpha}{\rho_{w_0}} \frac{\partial}{\partial x} (p_0+p_1) +$$

$$+ (1-n_0-n_1) \frac{\partial}{\partial x} (v_o+v_1)$$

$$- (v_0+v_1) \frac{\partial}{\partial x} (n_0+n_1) = 0$$

Hence to the lowest order:

$$n_0 \frac{\alpha}{\rho_{w_0}} \frac{\partial p_1}{\partial t} + n_o \frac{\partial w_1}{\partial x}$$

$$+ w_0 \frac{\partial n_1}{\partial x} + n_0 w_0 \frac{\alpha}{\rho_{w_0}} \frac{\partial p_1}{\partial x} \qquad \text{(B18)}$$

$$+ (1-n_0) \frac{\partial v_1}{\partial x} - v_0 \frac{\partial n_1}{\partial x} = 0$$

We further assume that:

$$w_0 = 0 \qquad \text{(B19)}$$
$$v_0 = 0$$

substitution of (B19) into (B18) gives:

$$n_0 \frac{\alpha}{\rho_{w_o}} \frac{\partial p_1}{\partial t} + n_0 \frac{\partial w_1}{\partial x} + (1-n_0) \frac{\partial v_1}{\partial x} = 0 \qquad \text{(B20)}$$

We put:

$$\frac{\alpha}{\rho_{w_0}} = \frac{1}{K_w} \qquad \text{(B21)}$$

where K_w is the compression modulus of the liquid.

From (B20) and (B21) there follows:

$$\frac{\partial w_1}{\partial x} + \frac{1-n_0}{n_0} \frac{\partial v_1}{\partial x} = - \frac{1}{K_w} \frac{\partial p}{\partial t} \tag{B22}$$

Equation (B22) can be interpreted as follows: outflow of grains and outflow of fluid in an elementary cube is compensated by a drop in the fluid pressure. This is usually called the storage equation.

Due to the linearization process:

$$\frac{\partial g}{\partial \sigma} \approx \beta \tag{B23}$$

where β is a constant.

Substitution of (B16), (B19) and (B23) into (B10) gives:

$$- \beta \frac{\partial(\sigma_0 + \sigma_1)}{\partial t} + (1-n_0-n_1) \frac{\partial}{\partial x} (0+v_1)$$

$$- (0+v_1) \frac{\partial}{\partial x} (n_o+n_1) = 0$$

Keeping the lowest order terms gives:

$$- \beta \frac{\partial \sigma_1}{\partial t} + (1-n_0) \frac{\partial v_1}{\partial x} = 0 \tag{B24}$$

We put:

$$\frac{\beta}{1-n_0} = -\frac{1}{K_p} \tag{B25}$$

where K_p is the compression modulus of the solid material.

From (B24) and (B25) it follows that:

$$-\frac{1}{K_p}\ \frac{\partial \sigma_1}{\partial t} = \frac{\partial v_1}{\partial x} \tag{B26}$$

Hence in the linearized case the skeleton can be considered as a linear elastic material, with the following one dimensional constitutive relation:

$$\sigma_1 = -K_p\ \varepsilon_1$$

where ε_1 is the strain of the skeleton.

Differentiating of the above expression with respect to t gives equation (B26).

Linearizing equation (B8) gives:

$$-\frac{\partial}{\partial t}(n_0+n_1) + (1-n_0-n_1)\frac{\partial}{\partial x}(v_0+v_1)$$

$$-(v_0+v_1)\ \frac{\partial}{\partial x}(n_0+n_1) = 0$$

Keeping the lowest order terms and putting $v_0=0$ gives:

$$-\frac{\partial n_1}{\partial t} + (1-n_0)\frac{\partial v_1}{\partial x} = 0$$

Hence once we know $v_1(x,t)$, we can calculate n_1 from the above equation and the initial condition for n_1.

Substitution of (B16) and (B19) into (B3) and (B4) gives:

$$(n_0+n_1)\ (\rho_{w_0}+\rho_{w_1})\left[\frac{\partial}{\partial t}(0+w_1) + (0+w_1)\frac{\partial}{\partial x}(0+w_1)\right]$$

$$= -(n_0+n_1)\frac{\partial}{\partial x}(p_0+p_1) - R$$

$$(1-n_0-n_1)\ \rho_p\left[\frac{\partial}{\partial t}(0+v_1) + (0+v_1)\frac{\partial}{\partial x}(0+v_1)\right] =$$

$$= -\frac{\partial}{\partial x}(\sigma_0+\sigma_1) - (1-n_0-n_1)\frac{\partial}{\partial x}(p_0+p_1) + R$$

Keeping the lowest order terms gives:

$$n_0\ \rho_{w_0}\frac{\partial w_1}{\partial t} = -n_0\frac{\partial p_1}{\partial x} - R_0 \qquad \text{(B27)}$$

$$(1-n_0)\ \rho_p\frac{\partial v_1}{\partial t} = -\frac{\partial \sigma_1}{\partial x} - (1-n_0)\frac{\partial p_1}{\partial x} + R_0 \qquad \text{(B28)}$$

Now we assume that R_0 is determined by Darcy's law:

$$n_0\ (w_1-v_1) = -\frac{k'}{\rho_{w_0} g}\frac{\partial p_1}{\partial x} \qquad \text{(Verruijt[35])} \qquad \text{(B29)}$$

where k' is the seepage coefficient and g is the gravitational acceleration.

Hence:

$$R_0 = n_0 \frac{\partial p_1}{\partial x} = n_0^2 \frac{\rho_{w_0} g}{k'} (w_1 - v_1)$$

We put:

$$\frac{\rho_{w_0} g}{k'} = \frac{1}{k} \tag{B30}$$

Hence:

$$R_0 = \frac{n_0^2}{k} (w_1 - v_1) \tag{B31}$$

Substitution of (B31) into (B27) and (B28) gives:

$$n_0 \rho_{w_o} \frac{\partial w_1}{\partial t} = - n_0 \frac{\partial p_1}{\partial x} - \frac{n_0^2}{k} (w_1 - v_1) \tag{B32}$$

$$(1-n_0) \rho_p \frac{\partial v_1}{\partial t} = - \frac{\partial \sigma_1}{\partial x} - (1-n_0) \frac{\partial p_1}{\partial x} + \frac{n_0^2}{k} (w_1 - v_1) \tag{B33}$$

Equations (B32) and (B33) form the linearized momentum balance equations for the fluid and the skeleton respectively.

The coupling terms due to relative movement of fluid and skeleton are given by the last term in (B32) and the last term in (B33).

The third expression in (B33) forms a coupling term due to the fact that the fluid surrounds the grains.

From now on we only use the perturbed variables and we put:

$$w_1 = w$$

$$v_1 = v$$

$$p_1 = p$$

$$\sigma_1 = \sigma$$

$$n_o = n = \text{constant}$$

$$\rho_{w_o} = \rho_w = \text{constant}$$

Hence (B22), (B26), (B32) and (B33) become:

$$n\,\rho_w\,\frac{\partial w}{\partial t} = -\,n\,\frac{\partial p}{\partial x} - \frac{n^2}{k}\,(w-v) \tag{B34}$$

$$(1-n)\rho_p\,\frac{\partial v}{\partial t} = -\,\frac{\partial \sigma}{\partial x} - (1-n)\,\frac{\partial p}{\partial x} + \frac{n^2}{k}\,(w-v) \tag{B35}$$

$$\frac{\partial w}{\partial x} + \frac{(1-n)}{n}\,\frac{\partial v}{\partial x} = -\,\frac{1}{K_w}\,\frac{\partial p}{\partial t} \tag{B36}$$

$$\frac{\partial v}{\partial x} = -\,\frac{1}{K_p}\,\frac{\partial \sigma}{\partial t} \tag{B37}$$

The above four equations form four linear field equations with four unknowns $p(x,t)$, $\sigma(x,t)$, $v(x,t)$ and $w(x,t)$.

These equations are equal to those of de Josselin de Jong [4] and the ones used by van der Kogel [38].

Neglecting the mass coupling and considering the case of incompressible grains and low frequency range, the Biot equations [2] for one dimension form the same set of equations as the above equations.

Considering the case of incompressible grains in Nikolaevkii's equations [15] for one dimension, Nikolaevskii's equations form the same set of equations as the above equations plus a linearized equation (B8).

The field equations (B34) to (B37) are now in a simple form and the constants are easily interpretable. We stress here the fact that the assumptions (B5) and (B7) give rise to considerable simplifications in the two-phase theory. We consider these reasonable assumptions for a saturated sand.

The generation of some familiar results in soil mechanics with field equations (B34) to (B37) will be given in Appendix V.

Because the linear theory is derived from the non-linear balance equations and the non-linear constitutive equations for the two phases, we will be able to test the validity of the linearized field equations (B34) to (B37).

Biot [2] and de Josselin de Jong [4] used only the linear theory. Liou's field equations [10] were motivated partly from non-linear balance equations and partly from linear constitutive equations. Nikolaevskii [39] formulated non-linear balance equations and linear constitutive equations. In other work [15] he used non-linear constitutive equations for the grains and the fluid.

In the case ρ_p is not constant, the non-linear theory becomes more complicated. An additional equation has to be formulated in order to obtain an equal number of equations and variables. Herrmann [40] posed a p-α relation (for dry materials: pressure-porosity relation) and Garg et al., [41] posed a porosity-partial volumetric

strain relation. Garg et al., [42] used the theory of interacting continua in order to study wave propagation through saturated rocks (tuff) in the framework of a non-linear theory, including the above posed relation.

Introduction of gravity forces gives:

$$n\,\rho_w\,\frac{\partial w}{\partial t} = -\,n\,\frac{\partial p}{\partial x} - \frac{n^2}{k}(w-v) + n\,\rho_w\,g \tag{B38}$$

$$(1-n)\,\rho_p\,\frac{\partial v}{\partial t} = -\,\frac{\partial \sigma}{\partial x} - (1-n)\,\frac{\partial p}{\partial x} + \frac{n^2}{k}(w-v) + (1-n)\,\rho_p\,g \tag{B39}$$

$$n\,\frac{\partial w}{\partial x} + (1-n)\,\frac{\partial v}{\partial x} = -\,\frac{1}{K_w}\,\frac{\partial p}{\partial t} \tag{B40}$$

$$\frac{\partial v}{\partial x} = -\,\frac{1}{K_p}\,\frac{\partial \sigma}{\partial t} \tag{B41}$$

This set of equations is the same as those of Liou [10].

It has been pointed out by van der Kogel [38] that the field equations with gravity forces can be reduced to field equations similar to the ones without gravity forces. If we introduce:

$$p^* = p + n\,\rho_w\,g \tag{B42}$$

$$\sigma^* = \sigma + (1-n)\,\rho_p\,g \tag{B43}$$

then the field equations (B38) to (B41) reduce to the form of field equations (B34) to (B37), with variables p^*, σ^*, v and w. We note that introducing p^* is similar to the concept of 'head' (Scott [34]).

In the next chapters we will construct solutions of the field equations (B34) to (B35) by well known methods.

First we will consider harmonic solutions. These are of engineering interest mainly in the lower frequency range (<100 Hz), e.g. vibrating foundations. Further the harmonic solutions contain valuable information, because due to the linearity of the field equations we can by superposition construct solutions to a large number of boundary value problems. Also the harmonic solution gives us information about the modes of vibration and hence we attain physical insight.

In addition we will employ the method of characteristics for formulating the solution. The characteristics carry information from the boundaries into the field and hence the method is especially appropriate to study transient problems.

Finally we will study the propagation of discontinuities. These are important when rapidly changing boundary conditions are involved, such as caused by blasting or during certain earthquake excitations.

We will establish the connections between the harmonic solution, method of characteristics and the propagation of discontinuities and give a physical explanation.

C. Solution of the Field Equations,

Harmonic Response

The field equations (B34) to (B37) will be solved for harmonic response. De Josselin de Jong [4] showed that if the parameters have the practical values of wet sand and the frequency is lower than 1000 Hz, certain simplifications can be made. A derivation of his results will be included for completeness.

The solution will be put in the form of transmission matrices, which are especially convenient for problems with layers and for numerical treatment. We will use the transmission matrices in order to establish the eigenfrequencies of a one-dimensional layer. Let us assume:

$$v(x,t) = V^0 \, e^{\frac{i\omega}{c} x} \, e^{i\omega t} \tag{C9}$$

$$w(x,t) = W^0 \, e^{\frac{i\omega}{c} x} \, e^{i\omega t} \tag{C10}$$

$$p(x,t) = P^0 \, e^{\frac{i\omega}{c} x} \, e^{i\omega t} \tag{C11}$$

$$\sigma(x,t) = \sigma^0 \, e^{\frac{i\omega}{c} x} \, e^{i\omega t} \tag{C12}$$

where c is the wave speed and where V^0, W^0, P^0 and σ^0 are constants and where ω is the frequency.

Substitution of (C9) to (C12) into (B34) to (B37) gives:

$$(n\,\rho_w\,i\omega + \frac{n^2}{k})\,W^0 - \frac{n^2}{k}\,V^0 + n\,\frac{i\omega}{c}\,P^0 = 0 \qquad (C13)$$

$$-\frac{n^2}{k}\,W^0 + (\frac{n^2}{k} + (1-n)\,\rho_p\,i\omega)\,V^0 +$$

$$(1-n)\,\frac{i\omega}{c}\,P^0 + \frac{i\omega}{c}\,\sigma^0 = 0 \qquad (C14)$$

$$n\,\frac{i\omega}{c}\,W^0 + n\,\frac{1-n}{n}\,\frac{i\omega}{c}\,V^0 + \frac{n}{K_w}\,i\omega\,P^0 = 0 \qquad (C15)$$

$$\frac{i\omega}{c}\,V^0 + \frac{1}{K_p}\,i\omega\,\sigma^0 = 0 \qquad (C16)$$

In order to get a solution for the above system we require:

$$\begin{vmatrix} n\rho_w\,i\omega + \frac{n^2}{k} & -\frac{n^2}{k} & n\,\frac{i\omega}{c} & 0 \\ -\frac{n^2}{k} & \frac{n^2}{k} + (1-n)\rho_p\,i\omega & (1-n)\,\frac{i\omega}{c} & \frac{i\omega}{c} \\ n\,\frac{i\omega}{c} & n\,\frac{1-n}{n}\,\frac{i\omega}{c} & \frac{n}{K_w}\,i\omega & 0 \\ 0 & \frac{i\omega}{c} & 0 & \frac{i\omega}{K_p} \end{vmatrix} = 0 \qquad (C18)$$

This gives:

$$1 - c^2 \left[\frac{n\ (1-n)\ \rho_p\ K_w + (1-n)^2\ \rho_w\ K_w + n\ \rho_w\ K_p}{n\ K_w\ K_p} \right.$$

$$\left. + \frac{n}{i\omega\ k} \left(\frac{K_w + n\ K_p}{n\ K_w\ K_p} \right) \right]$$

$$+ c^4 \left[\frac{(1-n)\ \rho_p\ \rho_w}{K_p\ K_w} + \frac{n}{i\omega\ k} \left(\frac{n\rho_w + (1-n)\ \rho_p}{K_p\ K_w} \right) \right] = 0 \qquad \text{(C19)}$$

We can write equation (C19) as:

$$\alpha^4\ c^4 - \beta^2\ c^2 + 1 = 0 \qquad \text{(C20)}$$

where:

$$\alpha^2 = \left[\frac{(1-n)\ \rho_p\ \rho_w}{K_p K_w} + \frac{n}{i\omega\ k} \left(\frac{n\ \rho_w + (1-n)\ \rho_p}{K_w\ K_p} \right) \right]^{1/2} \qquad \text{(C21)}$$

$$\beta = \left[\frac{n\ (1-n)\ \rho_p\ K_w + (1-n)^2\ \rho_w\ K_w + n\ \rho_w\ K_p}{n\ K_p\ K_w} + \right.$$

$$\left. + \frac{n}{i\omega\ k} \left(\frac{K_w + n\ K_p}{n\ K_p\ K_w} \right) \right]^{1/2} \qquad \text{(C22)}$$

From (C20) there follows:

$$c^2 = \frac{\beta^2 \pm \left(\beta^4 - 4\ \alpha^4\right)^{1/2}}{2\alpha^4} \qquad \text{(C23)}$$

Practical values for wet sand are: (Terzaghi [37], Barkan [43], Dorsey [44].)

$$k < 10^{-9} \quad \frac{m^3 \, sec}{kg} \tag{C24}$$

$$\rho_p \approx 2.5 \quad 10^3 \quad kg/m^3 \tag{C25}$$

$$\rho_w \approx 1 \quad 10^3 \quad kg/m^3 \tag{C26}$$

$$K_w \approx 2 \; 10^4 \; kgf/cm^2 = 2 \; 10^9 \; N/m^2 \tag{C27}$$

$$K_p \approx 10^2 \quad kgf/cm^2 = 10^7 \; N/m^2 \tag{C28}$$

$$n = 0.25 \text{ to } 0.50 \tag{C29}$$

Now consider a two-phase medium with the above properties.

We assume:

$$\omega << 10^5 \text{ rad/sec} \tag{C30}$$

This will imply that $\rho_w \, k\omega << 1$, which is required for further approximations.

For further analysis we will consider:

$$\omega < 100 \text{ Hz} \tag{C30a}$$

Substitution of (C24) to (C30) into (C21) and (C22) gives:

$$Re \, \frac{\beta^4}{4\alpha^4} >> 1 \tag{C31}$$

From (C23) and (C31) follows:

$$c^2 = \frac{\beta^2 + \left[4\alpha^4 \left(\frac{\beta^4}{4\alpha^4} - 1 \right) \right]^{1/2}}{2\alpha^4}$$

$$\approx \frac{\frac{\beta^2}{\alpha^2} + \frac{1}{\alpha^2} 2\alpha^2 \frac{\beta^2}{2\alpha^2}}{2\alpha^2} = \frac{\beta^2}{\alpha^4} \qquad \text{(C32)}$$

Substitution of (C24) to (C29) into (C21) and (C22) gives:

$$\left| \frac{4\alpha^4}{\beta^4} \right| << 1 \qquad \text{(C33)}$$

From (C33) there follows:

$$\left(1 - \frac{4\alpha^4}{\beta^4} \right)^{1/2} \approx 1 - \frac{2\alpha^4}{\beta^4} \qquad \text{(C34)}$$

Now (C34) and (C23) give:

$$c^2 = \frac{\beta^2 - \left[\beta^4 \left(1 - \frac{4\alpha^4}{\beta^4} \right) \right]^{1/2}}{2\alpha^4}$$

$$\approx \frac{\beta^2 - \beta^2 \left(1 - \frac{2\alpha^4}{\beta^4} \right)}{2\alpha^4} = \frac{1}{\beta^2} \qquad \text{(C35)}$$

From (C21), (C22) and (C32) it follows that

$$c_1 = \pm \frac{\left[\frac{n\,(1-n)\,\rho_p\,K_w + (1-n)^2\,\rho_w\,K_w + n\,\rho_w\,K_p}{n\,K_w\,K_p} + \frac{n}{i\omega\,k}\;\frac{K_w + n\,K_p}{n\,K_w\,K_p} \right]^{1/2}}{\left[\frac{(1-n)\,\rho_w\,\rho_p}{K_w\,K_p} + \frac{n}{i\omega\,k}\;\frac{n\,\rho_w + (1-n)\,\rho_p}{K_w\,K_p} \right]^{1/2}} \tag{C36}$$

From (C24) and (C30) follows:

$$\rho_w\,\omega k << 1 \tag{C37}$$

Substitution of (C24) to (C29) and (C37) in (C36) shows that the imaginary parts of the denominator and the numerator are very large with respect to the real part of the denominator and the numerator respectively.

so:

$$c_1 \approx \pm \left[\frac{\frac{n}{i\,\omega\,k}\;\frac{K_w + n\,K_p}{n\,K_w\,K_p}}{\frac{n}{i\omega k}\;\frac{n\,\rho_w + (1-n)\,\rho_p}{K_w\,K_p}} \right]^{1/2} \tag{C38}$$

$$= \pm \left(\frac{K_w/n + K_p}{n\,\rho_w + (1-n)\,\rho_p} \right)^{1/2}$$

From (C21), (C22) and (C35) follows:

$$c_2 = \pm \frac{1}{\left[\frac{n\,(1-n)\,\rho_p K_w + (1-n)^2 \rho_w K_w + n\,\rho_w K_p}{n\,K_w K_p}\right. \cdots}$$

$$\cdots \left. + \frac{n}{i\omega k}\left(\frac{K_w + n\,K_p}{n\,K_w K_p}\right)\right]^{1/2} \qquad \text{(C39)}$$

In a similar way as for c_1 we get:

$$c_2 = \pm \left[\frac{1}{\frac{n}{i\omega k}\,\frac{K_w + n\,K_p}{n\,K_p K_w}}\right]^{1/2} = \pm \left(\frac{i\omega \frac{k}{n}}{\frac{1}{K_w} + \frac{1}{n\,K_p}}\right)^{1/2} \qquad \text{(C40)}$$

Inspection of (C38) shows that for practical values of the parameters and the given frequency range the waves with wavespeed c_1 are almost undamped, while inspection of (C40) shows that the waves with wavespeed c_2 are highly damped. For the waves propagating with c_1, the bulk material can be viewed as having a compression modulus of $K_w/n + K_p$. This result agrees with the Gassmann equation [45] if we consider incompressible particles. His equation is frequently employed in the interpretation of seismic data on sedimentary material (Brown and Korringa[46]).

Consider now "practical" values for wet sand:

$$K_p \approx 10^7 \text{ N/m}^2$$

$$K_w \approx 2\ 10^9 \text{ N/m}^2$$

$$k < 10^{-9} \ \frac{\text{m}^3 \text{ sec}}{\text{kg}}$$

$$\rho_p = 2.5 \quad 10^3 \text{ kg/m}^3$$

$$\rho_w = \qquad 10^3 \text{ kg/m}^3$$

Substituting the above values into (C38) gives:

For: $n = 0.3$ $\qquad c_1 \approx 1800$ m/sec

$n = 0.5$ $\qquad c_1 \approx 1500$ m/sec

We note that these wave speeds are higher than the speed of sound in water (1440 m/sec). A lower porosity results in a higher wave speed. The above wavespeeds agree with observed compression-wave-propagation velocities from seismic data in saturated soils. (∿5000 ft/sec, Richart et al. [47].

In Chapter E we will derive the following expression for the wavespeed c_2:

$$c_2 = \frac{1}{2} \left(\omega \, k \, K_p \, 2 \right)^{1/2}$$

Substituting the "practical" values for wet sand in the above expression gives:

For: $T = 1$ sec $\qquad c_2 < 0.18$ m/sec

$T = \frac{1}{10}$ sec $\qquad c_2 < 0.57$ m/sec

$T = \frac{1}{100}$ sec $\qquad c_2 < 1.8$ m/sec

where T is the period of vibration.

Hence we see that the wavespeed c_2 is very small with respect to c_1.

Further in Chapter E we will derive the following expression for the damping of the waves propagating with speed c_2:

$$= \exp \left(- \frac{2\omega^{1/2}}{(2 \, k \, K_p)^{1/2}} \right) \cdot x$$

After substituting the "practical" values for wet sand we obtain the following values for the damping:

For $T = 1$ sec : $\qquad$ damping $< e^{-35 \, x}$

so: $x = 10^{-2}$ m $\Rightarrow e^{-0.35} = 0.7$

$x = 10^{-1}$ m $\Rightarrow e^{-3.5} = 0.03$

For $T = \frac{1}{10}$ sec: $\qquad$ damping $< e^{-110 \, x}$

so: $x = 10^{-2}$ m $\Rightarrow e^{-1.1} = 0.33$

$x = 5 \, 10^{-2}$ m $\Rightarrow e^{-5.50} = 4.10^{-3}$

Hence we see that after a couple of centimeters from the boundary, the waves propagating with speed c_2 are damped out. It should be emphasized that these calculations are given as an example.

From (C38) and (C40) follows:

$$W(x) = W_1^0 e^{\frac{i\omega}{c_1}x} + W_2^0 e^{-\frac{i\omega}{c_1}x} + W_3^0 e^{\frac{i\omega}{c_2}x} + W_4^0 e^{-\frac{i\omega}{c_2}x} \tag{C41}$$

$$V(x) = V_1^0 e^{\frac{i\omega}{c_1}x} + V_2^0 e^{-\frac{i\omega}{c_1}x} + V_3^0 e^{\frac{i\omega}{c_2}x} + V_4^0 e^{-\frac{i\omega}{c_2}x} \tag{C42}$$

$$P(x) = P_1^0 e^{\frac{i\omega}{c_1}x} + P_2^0 e^{-\frac{i\omega}{c_1}x} + P_3^0 e^{\frac{i\omega}{c_2}x} + P_4^0 e^{-\frac{i\omega}{c_2}x} \tag{C43}$$

$$\sigma(x) = \sigma_1^0 e^{\frac{i\omega}{c_1}x} + \sigma_2^0 e^{-\frac{i\omega}{c_1}x} + \sigma_3^0 e^{\frac{i\omega}{c_2}x} + \sigma_4^0 e^{-\frac{i\omega}{c_2}x} \tag{C44}$$

where $(W_1^0, W_2^0, W_3^0, W_4^0)$, $(V_1^0, V_2^0, V_3^0, V_4^0)$,

$(P_1^0, P_2^0, P_3^0, P_4^0)$, $(\sigma_1^0, \sigma_2^0, \sigma_3^0, \sigma_4^0)$

are constants.

The functional relation between W^0 and V^0 is established as follows:

Elimination of P^0 from (C13) and (C15) gives:

$$\left(n \rho_w i\omega + \frac{n^2}{k}\right) W^0 - \frac{n^2}{k} V^0 +$$

$$n \frac{i\omega}{c} \left(-\frac{1}{c} K_w W^0 - \frac{1-n}{n} \frac{1}{c} K_w V^0\right) = 0 \tag{C45}$$

or:

$$\left(-\frac{in}{k} + \rho_w \omega - K_w \frac{\omega}{c^2}\right) W^0$$

$$+ \left(-\frac{1-n}{n} K_w \frac{\omega}{c^2} + \frac{in}{k}\right) V^0 = 0 \qquad \text{(C46)}$$

From (C38) and (C46) follows:

$$\left(-i\frac{n}{k} + \rho_w \omega - K_w \omega \frac{n\rho_w + (1-n)\rho_p}{K_w/n + K_p}\right) W^0 \qquad \text{(C47)}$$

$$\left(-i\frac{n}{k} + \frac{1-n}{n} K_w \omega \frac{n\rho_w + (1-n)\rho_p}{K_w/n + K_p}\right) V^0 \qquad \text{(C47)}$$

In order to see which terms are of first order we substitute (C24) to (C30) into (C47). This gives:

$$-i \frac{n}{k} W^0 \approx -i \frac{n}{k} V^0$$

Hence:

$$V^0 \approx W^0 \qquad \text{(C48)}$$

Hence the waves which travel with wavespeed c_1 have approximately the same phase velocities.

From (C48), (C41) and (C42) follows:

$$W_1^0 \approx V_1^0 \qquad \text{(C49)}$$

$$W_2^0 \approx V_2^0 \qquad \text{(C50)}$$

If $c = c_2$, then from (C46):

$$V^0 = \gamma\, W^0 \tag{C51}$$

where:

$$\gamma = \frac{\left(-\frac{in}{k} + \rho_w \omega - K_w \frac{\omega}{c_2^2}\right)}{\left(\frac{1-n}{n} K_w \frac{\omega}{c_2^2} - \frac{in}{k}\right)} \tag{C52}$$

From (C51) follows:

$$V_3^0 = \gamma\, W_3^0 \tag{C53}$$

$$V_4^0 = \gamma\, W_4^0 \tag{C54}$$

Substitution of (C24) to (C30) into (C52) gives:

$$\gamma \approx -\frac{n}{1-n} \tag{C55}$$

Hence waves which travel with wavespeed c_2 have phase velocities that are opposite in sign. So when the skeleton moves up, the fluid moves down. Because the viscous forces working on the fluid and the skeleton are very high in the case of substantial relative velocity, this wave damps out very rapidly.

The functional relation between σ^0 and W^0 can be determined as follows:

From (C16) follows:

$$\sigma^0 = -\frac{K_p}{c} V^0 \tag{C56}$$

Hence from (C56), (C49), (C50), (C53) and (C54):

$$c = c_1 \quad : \quad \sigma^0 = \sigma_1{}^0 = -\frac{K_p}{c_1} V_1{}^0 = -\frac{K_p}{c_1} W_1{}^0 \tag{C57}$$

$$c = c_1 \quad : \quad \sigma^0 = \sigma_2{}^0 = +\frac{K_p}{c_1} V_2{}^0 = \frac{K_p}{c_1} W_2{}^0 \tag{C58}$$

$$c = c_2 \quad : \quad \sigma^0 = \sigma_3{}^0 = -\frac{K_p}{c_2} V_3{}^0 = -\frac{K_p}{c_2} \gamma W_3{}^0 \tag{C59}$$

$$c = -c_2 \quad : \quad \sigma^0 = \sigma_4{}^0 = +\frac{K_p}{c_2} V_4{}^0 = \frac{K_p}{c_2} \gamma W_4{}^0 \tag{C60}$$

Now we determine the relation between P^0 and W^0.

From (C15) follows:

$$P^0 = -\frac{K_w}{c} (W^0 + \frac{1-n}{n} V^0) \tag{C61}$$

Now from (C61), (C49), (C50), (C53), (C53) and (C54):

$$c = c_1 \quad : \quad P^0 = P_1^0 = -\frac{K_w}{c_1}\left(W_1^0 + \frac{1-n}{n} W_1^0\right) = -\frac{K_w}{c_1 n} W_1^0 \qquad (C62)$$

$$c = -c_1 : \quad P^0 = P_2^0 = +\frac{K_w}{c_1}\left(W_2^0 + \frac{1-n}{n} W_2^0\right) = +\frac{K_w}{c_1 n} W_2^0 \qquad (C63)$$

$$c = +c_2 : \quad P^0 = P_3^0 = -\frac{K_w}{c_2}\left(1 + \frac{1-n}{n}\gamma\right) W_3^0 \qquad (C64)$$

$$c = -c_2 : \quad P^0 = P_4^0 = \frac{K_w}{c_2}\left(1 + \frac{1-n}{n}\gamma\right) W_4^0 \qquad (C65)$$

So we have established the relationship between the constants $(W_1^0, V_1^0, P_1^0, \sigma_1^0)$, $(W_2^0, V_2^0, P_2^0, \sigma_2^0)$, $(W_3^0, V_3^0, P_3^0, \sigma_3^0)$ and $(W_4^0, V_4^0, P_4^0, \sigma_4^0)$.

Substitution of the above relations into (C41) to (C44) gives:

$$W(x) = W_1^0 e^{\frac{i\omega}{c_1}x} + W_2^0 e^{-\frac{i\omega}{c_1}x} + W_3^0 e^{\frac{i\omega}{c_2}x} + W_4^0 e^{-\frac{i\omega}{c_2}x} \qquad (C66)$$

$$V(x) = W_1^0 e^{\frac{i\omega}{c_1}x} + W_2^0 e^{-\frac{i\omega}{c_1}x} + \gamma W_3^0 e^{\frac{i\omega}{c_2}x} + \gamma W_4^0 e^{-\frac{i\omega}{c_2}x} \qquad (C67)$$

$$P(x) = -\frac{K_w}{n\,c_1} W_1^0 e^{\frac{i\omega}{c_1}x} + \frac{K_w}{n\,c_1} W_2^0 e^{-\frac{i\omega}{c_1}x} - \frac{K_w}{c_2}\left(1+\frac{1-n}{n}\gamma\right) e^{\frac{i\omega}{c_2}x} W_3^0$$

$$+ \frac{K_w}{c_2}\left(1+\frac{1-n}{n}\gamma\right) W_4^0 e^{-\frac{i\omega}{c_2}x} \qquad \text{(C68)}$$

$$\sigma(x) = -\frac{K_p}{c_1} W_1^0 e^{\frac{i\omega}{c_1}x} + \frac{K_p}{c_1} W_2^0 e^{-\frac{i\omega}{c_2}x} - \frac{K_p}{c_2}\gamma W_3^0 e^{\frac{i\omega}{c_2}x}$$

$$+ \frac{K_p}{c_2}\gamma W_4^0 e^{-\frac{i\omega}{c_2}x} \qquad \text{(C69)}$$

The constants W_1^0, W_2^0, W_3^0 and W_4^0 can be determined from the boundary conditions.

From substituting (C66) to (C69) into (C1) to (C4) we obtain:

$$w(x,t) = \left(W_1^0 e^{i\frac{\omega}{c_1}x} + W_2^0 e^{-i\frac{\omega}{c_1}x} + W_3^0 e^{i\frac{\omega}{c_2}x} + W_4^0 e^{-i\frac{\omega}{c_2}x} \right) e^{i\omega t} \tag{C70}$$

$$v(x,t) = \left(W_1^0 e^{i\frac{\omega}{c_1}x} + W_2^0 e^{-i\frac{\omega}{c_1}x} + \gamma W_3^0 e^{i\frac{\omega}{c_2}x} + \gamma W_4^0 e^{-i\frac{\omega}{c_2}x} \right) e^{i\omega t} \tag{C71}$$

$$p(x,t) = \left(-\frac{K_w}{nc_1} W_1^0 e^{i\frac{\omega}{c_1}x} + \frac{K_w}{nc_1} W_2^0 e^{-i\frac{\omega}{c_1}x} - \frac{K_w}{c_2}\left(1+\frac{1-n}{n}\gamma\right) W_3^0 e^{i\frac{\omega}{c_2}x} + \frac{K_w}{c_2}\left(1+\frac{1-n}{n}\gamma\right) W_4^0 e^{-i\frac{\omega}{c_2}x} \right) e^{i\omega t} \tag{C72}$$

$$\sigma(x,t) = \left(-\frac{K_p}{c_1} W_1^0 e^{i\frac{\omega}{c_1}x} + \frac{K_p}{c_1} W_2^0 e^{-i\frac{\omega}{c_1}x} - \frac{K_p}{c_2}\gamma W_3^0 e^{i\frac{\omega}{c_2}x} + \frac{K_p}{c_2}\gamma W_4^0 e^{-i\frac{\omega}{c_2}x} \right) e^{i\omega t} \tag{C73}$$

The set of equations (C70) to (C74) forms the solution of the field equations (B34) to (B37) if the parameters have the values of those of wet sand and the frequency is in the low range (conditions (C24) to (C30)).

There are two kinds of waves, one with wave speed c_1 (slightly damped) and one with wavespeed c_2 (heavily damped).

A detailed discussion about the solution and the physical implications will be given in Chapter E.

D. Construction of the Transmission Matrices

In this chapter we will construct the transmission matrices for the system (C66) to (C69). The problem will be approached as an input/output system, with the two stresses σ and p and two velocities w and v as input and output variables. The transmission matrix connects the variables at the two sides of a system of finite length or it connects the variables at the boundary for a system of infinite length.

The presentation of the solution in system form is especially convenient for solving a problem with layers numerically (Pestel and Leckie [48]).

We will use the transmission matrix for a system of finite length in order to generate the eigenfrequencies of a one-dimensional layer.

D.1 Construction of the Transmission Matrix for a System of Finite Length

We put:

$$W_1^0 + W_2^0 = A \tag{D.1.1}$$

$$W_1^0 - W_2^0 = B \tag{D.1.2}$$

$$W_3^0 + W_4^0 = C \tag{D.1.3}$$

$$W_3^0 - W_4^0 = D \tag{D.1.4}$$

Substitution of (D.1.1) to (D.1.4) into (C66) to (C69), after some algebra, gives:

$$W(x) = A \cos\frac{\omega x}{c_1} + i B \sin\frac{\omega x}{c_1} + C \cos\frac{\omega x}{c_2} + i D \sin\frac{\omega x}{c_2} \tag{D.1.5}$$

$$V(x) = A \cos\frac{\omega x}{c_1} + i B \sin\frac{\omega x}{c_1} + \gamma C \cos\frac{\omega x}{c_2} + \gamma i D \sin\frac{\omega x}{c_2} \tag{D.1.6}$$

$$P(x) = -\frac{K_w}{nc_1} B \cos\frac{\omega x}{c_1} - i\frac{K_w}{c_1^n} A \sin\frac{\omega x}{c_1} - \frac{K_w}{c_2}\left(1 + \frac{1-n}{n}\gamma\right) D \cos\frac{\omega x}{c_2}$$

$$- i\frac{K_w}{c_2}\left(1 + \frac{1-n}{n}\gamma\right) C \sin\frac{\omega x}{c_2} \qquad \text{(D.1.7)}$$

$$\sigma(x) = -\frac{K_p}{c_1} B \cos\frac{\omega x}{c_1} - i\frac{K_p}{c_1} A \sin\frac{\omega x}{c_1} - \frac{K_p}{c_2}\gamma D \cos\frac{\omega x}{c_2}$$

$$-i\frac{K_p}{c_2}\gamma C \sin\frac{\omega x}{c_2} \qquad \text{(D.1.8)}$$

At $x = 0$, (D.1.5) to (D.1.8) becomes:

$$W(0) = A + C \qquad \text{(D.1.9)}$$

$$V(0) = A + \gamma C \qquad \text{(D.1.10)}$$

$$P(0) = -\frac{K_w}{c_1^n} B - \frac{K_w}{c_2}\left(1 + \frac{1-n}{n}\gamma\right) D \qquad \text{(D.1.11)}$$

$$\sigma(0) = -\frac{K_p}{c_1} B - \frac{K_p}{c_2}\gamma D \qquad \text{(D.1.12)}$$

Hence:

$$C = \frac{W(0) - V(0)}{1 - \gamma} \tag{D.1.13}$$

$$A = \frac{\gamma\ W(0) - V(0)}{\gamma - 1} \tag{D.1.14}$$

$$D = \frac{K_p\ P(0) - \frac{K_w}{n}\ \sigma(0)}{-\frac{K_p\ K_w}{c_2}\left(1 + \frac{1-n}{n}\gamma\right) + \frac{K_p\ K_w}{n\ c_2}\gamma} \tag{D.1.15}$$

$$B = \frac{-K_p\ \gamma\ P(0) + K_w\left(1 + \frac{1-n}{n}\gamma\right)\sigma(0)}{\frac{K_p\ K_w}{n\ c_1}\gamma - \frac{K_p\ K_w}{c_1}\left(1 + \frac{1-n}{n}\gamma\right)} \tag{D.1.16}$$

Substitution of (D.1.13) to (D.1.16) into (D.15) to (D.18) gives W(x), V(x), P(x) and σ(x) in terms of the constants W(0), V(0), P(0) and $\sigma(0)$.

This substitution gives after some rearrangement:

$$W(x) = \frac{\gamma \cos\frac{\omega x}{c_1} - \cos\frac{\omega x}{c_2}}{\gamma - 1} W(0)$$

$$+ \frac{-\cos\frac{\omega x}{c_1} + \cos\frac{\omega x}{c_2}}{\gamma - 1} V(0)$$

$$+ i \frac{-\frac{K_p}{c_2}\gamma \sin\frac{\omega x}{c_1} + \frac{K_p}{c_1}\sin\frac{\omega x}{c_2}}{\frac{K_w K_p}{n c_1 c_2}\gamma - \frac{K_p K_w}{c_1 c_2}\left(1+\frac{1-n}{n}\gamma\right)} P(0)$$

$$+ i \frac{+\frac{K_w}{c_2}\left(1+\frac{1-n}{n}\gamma\right)\sin\frac{\omega x}{c_2} - \frac{K_w}{c_1 n}\sin\frac{\omega x}{c_2}}{\frac{K_w K_p}{n c_1 c_2}\gamma - \frac{K_w K_p}{c_1 c_2}\left(1+\frac{1-n}{n}\gamma\right)} \sigma(0)$$

(D.1.17)

$$V(x) = \frac{\gamma \cos \frac{\omega x}{c_1} - \gamma \cos \frac{\omega x}{c_2}}{\gamma - 1} W(0)$$

$$+ \frac{- \cos \frac{\omega x}{c_1} + \gamma \cos \frac{\omega x}{c_2}}{\gamma - 1} V(0)$$

$$+ i \frac{\gamma \frac{K_p}{c_1} \sin \frac{\omega x}{c_2} - \gamma \frac{K_p}{c_2} \sin \frac{\omega x}{c_1}}{\frac{K_p K_w}{n c_1 c_2} \gamma - \frac{K_p K_w}{c_1 c_2} \left(1 + \frac{1-n}{n} \gamma\right)} P(0)$$

$$+ i \frac{\frac{K_w}{c_2} \left(1 + \frac{1-n}{n} \gamma\right) \sin \frac{\omega x}{c_1} - \gamma \frac{K_w}{n c_1} \sin \frac{\omega x}{c_2}}{\frac{K_w K_p}{n c_1 c_2} \gamma - \frac{K_w K_p}{c_1 c_2} \left(1 + \frac{1-n}{n} \gamma\right)} \sigma(0)$$

(D.1.18)

$$P(x) = i \frac{-\frac{K_w}{c_1 n}\gamma \sin\frac{\omega x}{c_1} + \frac{K_w}{c_2}\left(1 + \frac{1-n}{n}\gamma\right)\sin\frac{\omega x}{c_2}}{\gamma - 1} W(0)$$

$$+ i \frac{\frac{K_p}{n c_1}\sin\frac{\omega x}{c_1} - \frac{K_p}{c_2}\left(1 + \frac{1-n}{n}\gamma\right)\sin\frac{\omega x}{c_2}}{\gamma - 1} V(0)$$

$$+ \frac{\frac{K_w K_p}{n c_1 c_2}\gamma\cos\frac{\omega x}{c_1} - \frac{K_w K_p}{c_1 c_2}\left(1 + \frac{1-n}{n}\gamma\right)\cos\frac{\omega x}{c_2}}{\frac{K_w K_p}{n c_1 c_2}\gamma - \frac{K_w K_p}{c_1 c_2}\left(1 + \frac{1-n}{n}\gamma\right)} P(0)$$

$$+ \frac{-\frac{K_w K_w}{n c_1 c_2}\left(1 + \frac{1-n}{n}\gamma\right)\cos\frac{\omega x}{c_1} + \frac{K_w K_w}{n c_1 c_2}\left(1 + \frac{1-n}{n}\gamma\right)\cos\frac{\omega x}{c_2}}{\frac{K_w K_p}{n c_1 c_2}\gamma - \frac{K_w K_p}{c_1 c_2}\left(1 + \frac{1-n}{n}\gamma\right)} \sigma(0)$$

(D.1.19)

$$\sigma(x) = -i \frac{\frac{K_p}{c_1}\gamma \sin\frac{\omega x}{c_1} + \frac{K_p}{c_2}\gamma \sin\frac{\omega x}{c_2}}{\gamma - 1} W(0)$$

$$+ i \frac{\frac{K_p}{c_1} \sin\frac{\omega x}{c_1} + \frac{K_p}{c_2}\gamma \sin\frac{\omega x}{c_2}}{\gamma - 1} V(0)$$

$$+ \frac{\frac{K_p K_p}{c_1 c_2}\gamma \cos\frac{\omega x}{c_1} - \frac{K_p K_p}{c_1 c_2}\gamma \cos\frac{\omega x}{c_2}}{\frac{K_p K_w}{n c_1 c_2}\gamma - \frac{K_p K_w}{c_1 c_2}\left(1 + \frac{1-n}{n}\gamma\right)} P(0)$$

$$+ \frac{-\frac{K_w K_p}{c_1 c_2}\left(1 + \frac{1-n}{n}\gamma\right)\cos\frac{\omega x}{c_1} + \frac{K_w K_p}{n c_1 c_2}\gamma \cos\frac{\omega x}{c_2}}{\frac{K_w K_p}{n c_1 c_2}\gamma - \frac{K_w K_p}{c_1 c_2}\left(1 + \frac{1-n}{n}\gamma\right)} \sigma(0)$$

(D.1.20)

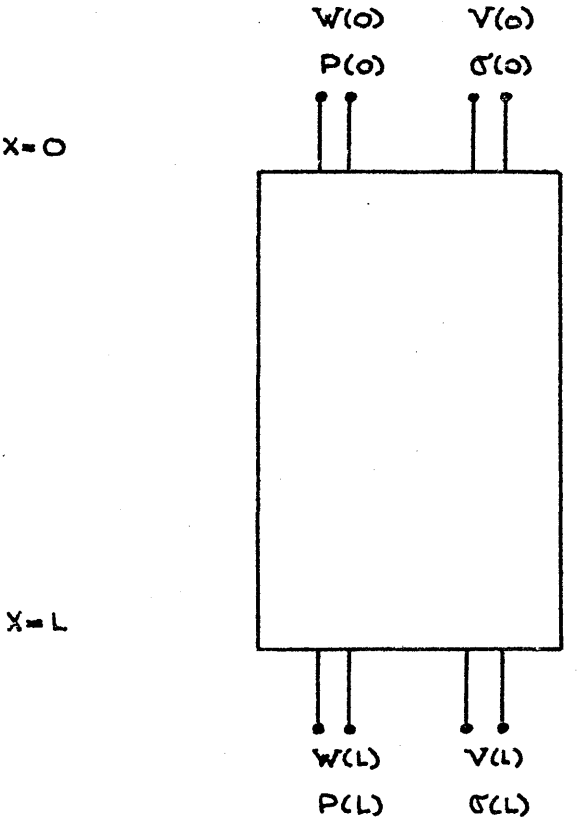

FINITE SYSTEM

FIG. 1

The equations (D.1.17) to (D.1.20) form the input/output system, which we can write in short as follows:

$$W(L) = A\,W(0) + B\,V(0) + C\,P(0) + D\,\sigma(0) \qquad \text{(D.1.21)}$$

$$V(L) = E\,W(0) + F\,V(0) + G\,P(0) + H\,\sigma(0) \qquad \text{(D.1.22)}$$

$$P(L) = K\,W(0) + L^{*}V(0) + M\,P(0) + N\,\sigma(0) \qquad \text{(D.1.23)}$$

$$\sigma(L) = Q\,W(0) + R\,V(0) + S\,P(0) + T\,\sigma(0) \qquad \text{(D.1.24)}$$

We call $\begin{bmatrix} A & B & C & D \\ E & F & G & H \\ K & L^{*} & M & N \\ Q & R & S & T \end{bmatrix}$ the transmission matrix.

Hence we have the picture shown in figure (1).

The input/output system (D.1.21) to (D.1.24) consists of four equations with eight unknowns (W(0), P(0), V(0), σ(0), W(L), P(L), V(L), σ(L)) and gives the relation between the unknowns at x=0 and x=L

Four unknowns have to be described on the boundaries in order to solve the system (D.1.21) to (D.1.24).

D.2 Construction of the Transmission Matrix for a System of Infinite Length

In this system there is no reflection, so we consider only the incoming waves. Then the equations (C66) to (C69) become:

$$W(x) = e^{-\frac{i\omega}{c_1}x} W_2^0 + e^{-\frac{i\omega}{c_2}x} W_4^0 \qquad (D.2.1)$$

$$V(x) = e^{-\frac{i\omega}{c_1}x} W_2^0 + \gamma\, e^{-\frac{i\omega}{c_2}x} W_4^0 \qquad (D.2.2)$$

$$P(x) = \frac{K_w}{n\, c_1} e^{-\frac{i\omega}{c_1}x} W_2^0 + \frac{K_w}{c_2}\left(1 + \frac{1-n}{n}\gamma\right) e^{-\frac{i\omega}{c_2}x} W_4^0 \qquad (D.2.3)$$

$$\sigma(x) = \frac{K_p}{c_1} e^{-\frac{i\omega}{c_1}x} W_2^0 + \frac{K_p}{c_2}\gamma\, e^{-\frac{i\omega}{c_2}x} W_4^0 \qquad (D.2.4)$$

Hence

$$W(0) = W_2^0 + W_4^0 \tag{D.2.5}$$

$$V(0) = W_2^0 + \gamma W_4^0 \tag{D.2.6}$$

$$P(0) = \frac{K_w}{n c_1} W_2^0 + \frac{K_w}{c_2}\left(1 + \frac{1-n}{n}\gamma\right) W_4^0 \tag{D.2.7}$$

$$\sigma(0) = \frac{K_p}{c_1} W_2^0 + \frac{K_p}{c_2} \gamma W_4^0 \tag{D.2.8}$$

From (D.2.5) and (D.2.6) there follows:

$$W_4^0 = \frac{W(0) - V(0)}{1 - \gamma} \tag{D.2.9}$$

$$W_2^0 = \frac{\gamma W(0) - V(0)}{\gamma - 1} \tag{D.2.10}$$

Substitution of (D.2.9) and (D.2.10) into (D.2.1) to (D.2.4) gives $W(x)$, $V(x)$, $P(x)$ and $\sigma(x)$ in terms of the constants $W(0)$ and $V(0)$.

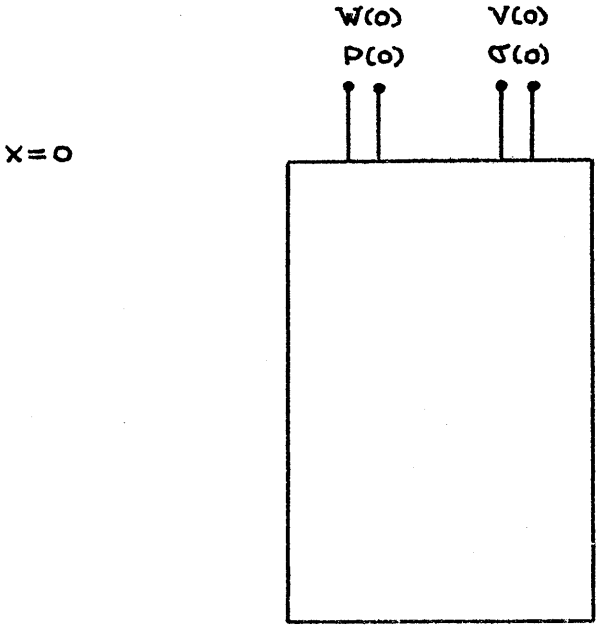

SEMI - INFINITE SYSTEM

FIG. 2

If we now substitute (D.2.9) and (D.2.10) into (D.2.7) and (D.2.8) we obtain

$$P(0) = \frac{\frac{K_w}{n\,c_1}\gamma - \frac{K_w}{c_2}\left(1 + \frac{1-n}{n}\gamma\right)}{\gamma - 1} W(0) + \frac{-\frac{K_w}{n\,c_1} + \frac{K_w}{c_2}\left(1 + \frac{1-n}{n}\gamma\right)}{\gamma - 1} V(0) \qquad \text{(D.2.11)}$$

$$\sigma(0) = \frac{\frac{K_p}{c_1}\gamma - \frac{K_p}{c_2}\gamma}{\gamma - 1} W(0) + \frac{-\frac{K_p}{c_1} + \frac{K_p}{c_2}\gamma}{\gamma - 1} V(0) \qquad \text{(D.2.12)}$$

The equations (D.2.11) and (D.2.12) form the input/output system at x=0 with four unknowns P(0), σ(0), W(0) and V(0). This is shown schematically in figure (2).

We have to describe two unknowns at the boundary x=0 in order to solve (D.2.11) and (D.2.12).

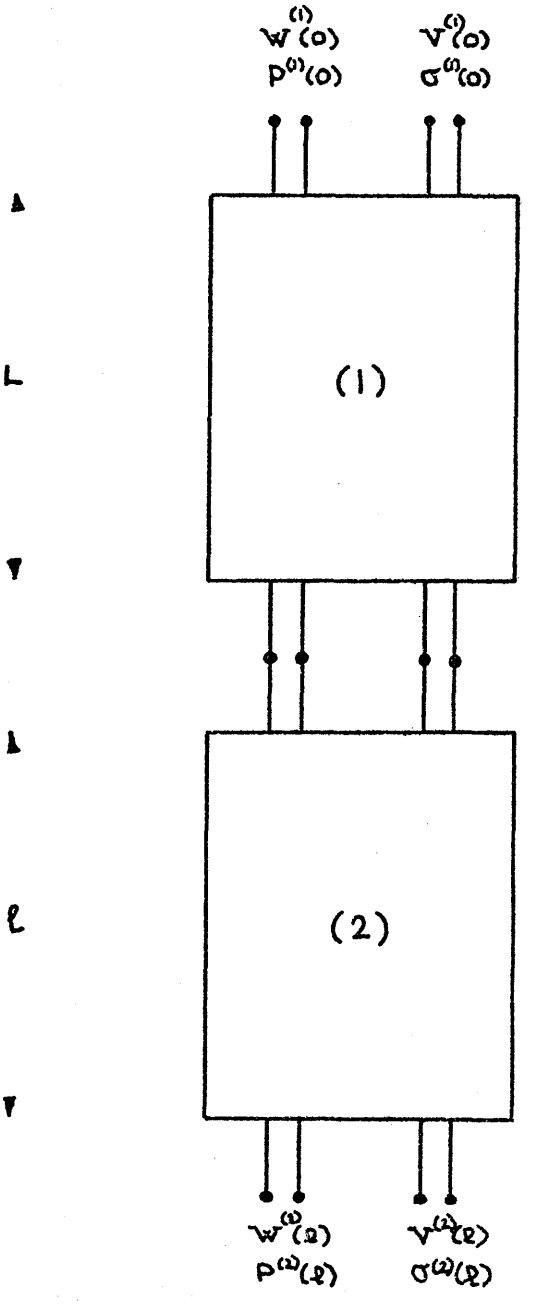

COUPLING OF TWO FINITE SYSTEMS

FIG. 3

The solution of a layered one-dimensional semi-infinite problem can be constructed by a coupling of the individual systems. The actual coupling depends on the coupling conditions. In Chapter K we will derive these coupling conditions.

If we assume: $\sigma^{(1)}(L) = \sigma^{(2)}(0)$, $P^{(1)}(L) = P^{(2)}(0)$, $V^{(1)}(L) = V^{(2)}(0)$ and $W^{(1)}(L) = W^{(2)}(0)$, then the transmission matrix of the total input/output system will be the product of the transmission matrix of system (1) and system (2). This is shown schematically in figure (3).

D.3 Determination of Eigenfrequencies

As an example we will determine the eigenfrequencies of a layer which is stress free at the top and fixed at the bottom. The eigenfrequencies of a layer are interesting parameters for studying forced vibrations, because they determine the resonant frequencies. These are of engineering interest because they generate the most violent motion by fixed input amplitude of the prescribed variables at the boundaries.

We will assume the following boundary conditions:

$$W(0) = V(0) = 0 \tag{D.3.1}$$

$$P(L) = \sigma(L) = 0 \tag{D.3.2}$$

Substitution of (D.3.1) and (D.3.2) into (D.1.21) to (D.1.24) gives:

$$W(L) = C\ P(0) + D\ \sigma(0) \tag{D.3.3}$$

$$V(L) = G\ P(0) + H\ \sigma(0) \tag{D.3.4}$$

$$0 = M\ P(0) + N\ \sigma(0) \tag{D.3.5}$$

$$0 = S\ P(0) + T\ \sigma(0) \tag{D.3.6}$$

In order to solve (D.3.5) and (D.3.6) we require:

$$\begin{vmatrix} M & N \\ S & T \end{vmatrix} = 0 \qquad \text{(D.3.7)}$$

or:

$$M\,T - S\,N = 0 \qquad \text{(D.3.8)}$$

Substitution of the expressions for M, T, S and N gives:

$$\frac{\frac{K_w K_p}{c_1 c_2}\left(1+\frac{1-n}{n}\gamma\right)\cos\frac{\omega L}{c_1}+\frac{K_w K_p}{n c_1 c_2}\gamma\cos\frac{\omega L}{c_2}}{\frac{K_w K_p}{n c_1 c_2}\gamma-\frac{K_w K_p}{c_1 c_2}\left(1+\frac{1-n}{n}\gamma\right)} \quad \frac{\frac{K_w K_p}{n c_1 c_2}\gamma\cos\frac{\omega L}{c_1}-\frac{K_w K_p}{c_1 c_2}\left(1+\frac{1-n}{n}\gamma\right)\cos\frac{\omega L}{c_2}}{\frac{K_w K_p}{n c_1 c_2}\gamma-\frac{K_w K_p}{c_1 c_2}\left(1+\frac{1-n}{n}\gamma\right)}$$

$$-\frac{\frac{K_p K_p}{c_1 c_2}\gamma\cos\left(\frac{\omega L}{c_1}\right)-\frac{K_p K_p}{c_1 c_2}\gamma\cos\frac{\omega L}{c_2}}{\frac{K_w K_p}{n c_1 c_2}\gamma-\frac{K_w K_p}{n c_1 c_2}\left(1+\frac{1-n}{n}\gamma\right)} \quad \frac{-\frac{K_w K_w}{n c_1 c_2}\left(1+\frac{1-n}{n}\gamma\right)\cos\frac{\omega L}{c_1}+\frac{K_w K_w}{n c_1 c_2}\left(1+\frac{1-n}{n}\gamma\right)\cos\frac{\omega L}{c_2}}{\frac{K_w K_p}{n c_1 c_2}\gamma-\frac{K_w K_p}{n c_1 c_2}\left(1+\frac{1-n}{n}\gamma\right)}$$

$$= 0 \qquad \text{(D.3.9)}$$

After some algebra we obtain:

$$\text{factor} * \cos \frac{\omega L}{c_2} * \cos \frac{\omega L}{c_1} = 0 \qquad \text{(D.3.10)}$$

This equation is satisfied for:

$$\cos \frac{\omega L}{c_2} = 0 \qquad \text{(D.3.11)}$$

and also for:

$$\cos \frac{\omega L}{c_1} = 0 \qquad \text{(D.3.12)}$$

From (D.3.11) and (D.3.12) it follows that the lower eigen frequencies are given by the following expressions:

$$\omega = \omega^{*} = \frac{c_1}{L} \left(\frac{\pi}{2} + k^{*} \pi \right) \qquad \text{(D.3.13)}$$

$$\omega = \omega^{**} = \frac{c_2}{L} \left(\frac{\pi}{2} + k^{*} \pi \right) \qquad \text{(D.3.14)}$$

where $k^{*} = 0, 1, 2, \ldots, N$.

The value of N is determined by the upper bound in the frequency given by (C.30a). Hence we are only considering the lower eigen frequencies.

The first set of eigen frequencies (D.3.13) are associated with the first mode (waves with speed c_1) and the second set of eigen frequencies (D.3.14) are associated with the second mode (waves with wave speed c_2).

We note that the eigen motions in the first mode are almost undamped, because c_1 has a very small imaginary part; however, the eigen motions in the second mode are heavily damped, because c_2 has a large imaginary part. This is due to the fact that in the first mode the phase velocities are almost the same and in the second mode the phase velocities have opposite signs.

We observe that in the case of a layer height of 0.2 m the real part of the first eigen frequency ($k^*=0$) in the first mode is very high ($T_1 \approx 10^{-3}$ sec) and in the second mode is low ($T_1 \approx 20$ sec, $T_2 \approx 2$ sec) when we use the practical values of wet sand given by (C24) to (C29).

The contribution of the first and second mode to the eigen motion will depend on the initial conditions; however for long time the first mode will dominate because it is almost undamped.

E. Inspection of Far Field and Near Field Solutions

The waves with wavespeed c_1 are slightly damped, while the waves with wavespeed c_2 are highly damped. Hence in the far field (away from the boundaries) only the waves with wavespeed c_1 will survive.

For the far field equations (C66) to (C69) reduce to:

$$W(x) \approx W_1^0 e^{\frac{i\omega}{c_1}x} + W_2^0 e^{-\frac{i\omega}{c_1}x} \tag{E1}$$

$$V(x) \approx W_1^0 e^{\frac{i\omega}{c_1}x} + W_2^0 e^{-\frac{i\omega}{c_1}x} \tag{E2}$$

$$P(x) \approx -\frac{K_w}{n\,c_1} W_1^0 e^{\frac{i\omega}{c_1}x} + \frac{K_w}{n\,c_1} W_2^0 e^{-\frac{i\omega}{c_1}x} \tag{E3}$$

$$\sigma(x) \approx -\frac{K_p}{c_1} W_1^0 e^{\frac{i\omega}{c_1}x} + \frac{K_p}{c_1} W_2^0 e^{-\frac{i\omega}{c_1}x} \tag{E4}$$

We conclude from (E1) to (E4) that for the far field:

$$W(x) \approx V(x) \tag{E5}$$

$$\frac{P(x)}{\sigma(x)} \approx \frac{K_{w/n}}{K_p} \tag{E6}$$

and from (C38) it follows that:

$$c_1 = \left(\frac{K_w/n + K_p}{n\,\rho_w + (1-n)\,\rho_p} \right)^{1/2} \qquad \text{(E7)}$$

Hence in the far field, waves propagate with wavespeed c_1, which consists of an apparent compression modulus which is the sum of the compression modulus of the grain structure (K_p) and the compression modulus of the fluid (K_w) divided by the porosity. Further c_1 contains a mass term which is the total mass of the system ($n\,\rho_w + (1-n)\,\rho_p$).

In the far field the fluid pressure and the effective pressure have a ratio: $\frac{K_w}{n} / K_p$ and hence for the assumed parameters ($K_w >> K_p$) the fluid pressure will be high and the effective pressure will be low.

Finally we conclude from (E5) that in the far field the velocity of the fluid and the velocity of the grain structure are almost equal. However, they are not exactly equal and so we have an open system in the sense of a multi-phase theory. In fact the inequality of the phase velocities is a crucial condition in the derivation of the wave speeds, because the smallness of the seepage coefficient k gave rise to the approximate wave speeds c_1 and c_2. In chapter H we will explore the implications of the condition $v = w$ in detail.

However, if the boundary conditions are such that the wave with wavespeed c_2 will not be generated (e.g. $v(0,t) \approx w(0,t)$), we can use the reduced form of the field equations in order to generate an approximate solution for the assumed parameters and frequency.

Consider:

$$v \approx w \approx v^* \tag{E8}$$

Addition of (B34) and (B35), and substitution of (E8) gives:

$$(n\ \rho_w + (1-n)\ \rho_p)\ \frac{\partial v^*}{\partial t} = \frac{\partial}{\partial x}-(\sigma+p) = -\frac{\partial \sigma_t}{\partial x} \tag{E9}$$

where: $\sigma_t = \sigma + p$, the total pressure. (E10)

Addition of (B36) and (B37), and substitution of (E8) gives:

$$\left(\frac{K_w}{n} + K_p\right) \frac{\partial v^*}{\partial x} = -\frac{\partial \sigma_t}{\partial t} \tag{E11}$$

After some differentiation and substitution we obtain:

$$((1-n)\ \rho_p + n\ \rho_w)\ \frac{\partial^2 v^*}{\partial t^2} = \left(\frac{K_w}{n} + K_p\right) \frac{\partial^2 v^*}{\partial x^2} \tag{E12}$$

$$((1-n)\ \rho_p + n\ \rho_w)\ \frac{\partial^2 \sigma_t}{\partial t^2} = \left(\frac{K_w}{n} + K_p\right) \frac{\partial^2 \sigma_t}{\partial x^2} \tag{E13}$$

Equations (E12) and (E13) are in the form of the "wave equation", v^* and σ_t propagate with wavespeed $\left(\frac{K_w/n + K_p}{(1-n)\ \rho_p + n\ \rho_w}\right)^{1/2}$, which is consistent with the former solution (E7).

Substitution of (E8) into (B36) and (B37) gives:

$$-\frac{\partial p}{\partial t} = \frac{K_w}{n}\ \frac{\partial v^*}{\partial x} \tag{E14}$$

$$-\frac{\partial \sigma}{\partial t} = K_p\ \frac{\partial v^*}{\partial x} \tag{E15}$$

Hence:

$$\frac{\Delta p}{\Delta \sigma} = \frac{K_w/n}{K_p} \tag{E16}$$

The result (E16) is consistent with the harmonic solution, which generates result (E6).

So for the boundary conditions ($v(o,t) \approx w(o,t)$) we can use the reduced form of the field equations to generate the solution in the semi-infinite case. We can use the total pressure σ_t and $v,^*$ solve the wave equation for σ_t and v^*, and thereafter derive the pore pressure p and the effective stress σ from (E16).

In general the boundary conditions will be such that the two kinds of waves will be generated in the vicinity of the boundary in order to satisfy the boundary conditions. Because the phase velocities in this area can be different, damping and momentum exchange due to interaction of the phases takes place in this region.

The area, that we call near field consists of that part of the field near the boundaries, where the waves c_2 can contribute to the solution with respect to the waves c_1.

The waves c_2 are given by:

$$e^{\frac{i\omega}{\pm c_2} x + i\omega t} \tag{E17}$$

Substitution of (C40) in (E17) gives the damping term as: ($x \geq 0$)

$$e^{-\frac{\omega}{Imc_2} x} = e^{-\frac{\omega x}{Im\left(\frac{i\omega \frac{k}{n}}{\frac{1}{K_w} + \frac{1}{n K_p}}\right)^{1/2}}} \tag{E18}$$

Further:

$$\left(\frac{i\omega \frac{k}{n}}{\frac{1}{K_w} + \frac{1}{n K_p}}\right)^{1/2} = \left(\frac{i\omega \frac{k}{n} (K_w n K_p)}{n K_p + K_w}\right)^{1/2}$$

$$\cong \left(\frac{i\omega k K_w K_p}{K_w}\right)^{1/2}$$

$$= \left(i\omega k K_p\right)^{1/2} \tag{E19}$$

So:

$$Im \quad (i\omega k K_p)^{1/2} = \sqrt{k\omega K_p} \; \frac{1}{2} \; \sqrt{2}$$

$$= \frac{1}{2} \sqrt{\omega k K_p 2} = c_2 \tag{E20}$$

Substitution of (E20) into (E18) gives:

$$e^{-\frac{2\omega}{\sqrt{2\ \omega\ k\ K_p}}\ x} = e^{-\frac{2\sqrt{\omega}}{\sqrt{2\ k\ K_p}}\ x} \qquad \text{(E21)}$$

The expression (E21) represents the damping of the waves with wavespeed c_2.

Hence a more permeable (larger k) and a less compressible (larger K_p) grain structure has a larger near field than a less permeable (smaller k) and a more compressible (smaller K_p) grain structure.

A larger near field means a larger area where velocity differences between the components might be generated. The actual velocity differences will of course depend on the boundary conditions and the parameters in the field equations.

F. Field Equations Viewed as a System of Hyperbolic Equations

In the former chapter we viewed the field equations as a class which we call dispersive; this means there exists a solution in the form:

$$\underset{\sim}{u}(x,t) = \underset{\sim}{u}^0 \exp\,(ikx-i\omega t) \tag{F1}$$

where:

$$\underset{\sim}{u}^0 = \begin{bmatrix} V^0 \\ W^0 \\ P^0 \\ \sigma^0 \end{bmatrix}$$

and where $\underset{\sim}{u}^0$ is a vector with four elements which are constants, called amplitudes. $k\,(=\frac{\omega}{c})$ is called the wave number and ω the frequency. We established a relation between k and ω:

$$G(\omega,k) = 0 \tag{F2}$$

This is called the dispersion relation.

Now we will view the field equations from a different standpoint and establish a relation between the different approaches.

The field equations can be written in the following form:

$$\frac{\partial u_i}{\partial t} + a_{ij} \frac{\partial u_j}{\partial x} + b_i = 0 \qquad i=1,..,4 \qquad \text{(F3)}$$

where the matrix a_{ij} and the vector b_i may be functions of $u_1,..,u_4$ (we use summation convection over repeated subscript).

Now we look for solutions in the following way (Whitham [49]):

We seek the linear combination

$$L_i \frac{\partial u_i}{\partial t} + L_i a_{ij} \frac{\partial u_j}{\partial x} + L_i b_i = 0 \qquad \text{(F4)}$$

which takes the characteristic form:

$$L_i \frac{du_i}{dt} + L_i b_i = 0 \qquad \text{(F5)}$$

on

$$\frac{dx}{dt} = \lambda \qquad \text{where: } x = X(t) \qquad \text{(F6)}$$

This is the case if:

$$L_i a_{ij} = L_j \lambda \qquad \text{(F7)}$$

Then the characteristic velocity λ must satisfy:

$$\left| a_{ij} - \lambda \, \delta_{ij} \right| = 0 \tag{F8}$$

where:

$$\begin{aligned} \delta_{ij} &= 0 \qquad i \neq j \\ &= 1 \qquad i = j \end{aligned} \tag{F9}$$

The system (F3) is called hyperbolic if (F8) has 4 different real roots.

Now we rewrite the field equations (B34) to (B37) on the form (F3):

$$\begin{bmatrix} (1-n)\rho_p & 0 & 0 & 0 \\ 0 & n\rho_w & 0 & 0 \\ 0 & 0 & \frac{n}{K_w} & 0 \\ 0 & 0 & 0 & \frac{1}{K_p} \end{bmatrix} \begin{bmatrix} \frac{\partial v}{\partial t} \\ \frac{\partial w}{\partial t} \\ \frac{\partial p}{\partial t} \\ \frac{\partial \sigma}{\partial t} \end{bmatrix} + \begin{bmatrix} 0 & 0 & 1-n & 1 \\ 0 & 0 & n & 0 \\ 1-n & n & 0 & 0 \\ 1 & 0 & 0 & 0 \end{bmatrix} \begin{bmatrix} \frac{\partial v}{\partial x} \\ \frac{\partial w}{\partial x} \\ \frac{\partial p}{\partial x} \\ \frac{\partial \sigma}{\partial x} \end{bmatrix} + \begin{bmatrix} -\frac{n^2}{k}(w-v) \\ \frac{n^2}{k}(w-v) \\ 0 \\ 0 \end{bmatrix} = \begin{bmatrix} 0 \\ 0 \\ 0 \\ 0 \end{bmatrix} \tag{F10}$$

So:

$$[a_{ij}] = \begin{bmatrix} 0 & 0 & \frac{1}{\rho_p} & \frac{1}{(1-n)\rho_p} \\ 0 & 0 & \frac{1}{\rho_w} & 0 \\ \frac{(1-n)K_w}{n} & K_w & 0 & 0 \\ K_p & 0 & 0 & 0 \end{bmatrix} \qquad \text{(F11)}$$

Hence the characteristic velocity is determined by:

$$\begin{vmatrix} -\lambda & 0 & \frac{1}{\rho_p} & \frac{1}{(1-n)\rho_p} \\ 0 & -\lambda & \frac{1}{\rho_w} & 0 \\ \frac{(1-n)K_w}{n} & K_w & -\lambda & 0 \\ K_p & 0 & 0 & -\lambda \end{vmatrix} = 0 \qquad \text{(F12a)}$$

or:

$$\lambda^4 - \left(\frac{n K_w (1-n) \rho_p + (1-n)^2 K_w \rho_w + n K_p \rho_w}{n \rho_w \rho_p (1-n)} \right) \lambda^2 \qquad \text{(F12)}$$

$$+ \frac{K_w K_p}{(1-n) \rho_w \rho_p} = 0$$

Comparing the equation for the characteristic velocity (F12) with the equation for the wavespeed c (C19), we observe that both equations

are equal for $\omega \to \infty$ (infinity).

Rewriting (F12) gives:

$$\frac{(1-n)\ \rho_w\ \rho_p}{K_w\ K_p}\ \lambda - \left(\frac{n\ (1-n)\ \rho_p\ K_w + (1-n)^2 \rho_w\ K_w + n\ \rho_w\ K_p}{n\ K_w\ K_p}\right) \lambda^2 + 1 = 0 \qquad \text{(F13)}$$

(F13) can be written as:

$$\alpha^4\ \lambda^4 - \beta^2\ \lambda^2 + 1 = 0 \qquad \text{(F14)}$$

$$\alpha^4 = \frac{(1-n)\ \rho_w\ \rho_p}{K_w\ K_p} \qquad \text{(F15)}$$

$$\beta^2 = \frac{n\ (1-n)\ \rho_p\ K_w + (1-n)^2\ \rho_w\ K_w + n\ \rho_w\ K_p}{n\ K_w\ K_p} \qquad \text{(F16)}$$

For practical values of wet sand (C24) to (C29) we observe:

$$\frac{\beta^4}{4\,\alpha^4} >> 1 \qquad \text{(F17)}$$

Hence from (F16) and (F14) there follows:

$$\lambda^2 = \frac{\beta^2 + \left\{4\alpha^4 \left(\frac{\beta^4}{4\alpha^4} - 1\right)\right\}^{1/2}}{2\alpha^4} \approx \qquad \text{(F18)}$$

$$\approx \frac{\frac{\beta^2}{\alpha^2} + 2\alpha^2\ \frac{1}{\alpha^2}\ \frac{\beta^2}{2\alpha^2}}{2\alpha^2} = \frac{\beta^2}{\alpha^4}$$

also:

$$\lambda^2 = \frac{\beta^2 - \left\{\beta^4 \left(1 - \frac{4\alpha^4}{\beta^4}\right)\right\}^{1/2}}{2\alpha^4}$$

$$\approx \frac{\beta^2 - \beta^2 \left(1 - \frac{2\alpha^4}{\beta^4}\right)}{2\alpha^4} = \frac{1}{\beta^2} \qquad \text{(F19)}$$

Substitution of (F15) and (F16) into (F18) and (F19) gives:

$$\lambda_{1,2} = \pm \left\{\frac{n\ (1-n)\ \rho_p\ K_w + (1-n)^2\ \rho_w\ K_w + n\ \rho_w\ K_p}{n\ (1-n)\ \rho_w\ \rho_p}\right\}^{1/2}$$

$$= \pm \left\{\frac{n\ \rho_p\ K_w + (1-n)\ \rho_w\ K_w}{n\ \rho_w\ \rho_p}\right\}^{1/2} \qquad \text{(F20)}$$

$$\lambda_{3,4} = \pm \left\{\frac{n\ K_w\ K_p}{n\ (1-n)\ \rho_p\ K_w + (1-n)^2\ \rho_w\ K_w + n\ \rho_w\ K_p}\right\}^{1/2}$$

$$= \pm \left\{\frac{n\ K_p}{n\ (1-n)\ \rho_p + (1-n)^2\ \rho_w}\right\}^{1/2} \qquad \text{(F21)}$$

Now we will compute the left-hand eigenvalues $\underset{\sim}{L}$ of $[a_{ij}]$:

$$(L_1 \quad L_2 \quad L_3 \quad L_4)\begin{bmatrix} -\lambda_i & 0 & \frac{1}{\rho_p} & \frac{1}{(1-n)\rho_p} \\ 0 & -\lambda_i & \frac{1}{\rho_w} & 0 \\ (1-n)\frac{K_w}{n} & K_w & -\lambda_i & 0 \\ K_p & 0 & 0 & -\lambda_i \end{bmatrix} = \begin{bmatrix} 0 \\ 0 \\ 0 \\ 0 \end{bmatrix} \tag{F22}$$

After some algebra we obtain:

$$L_2 = \frac{-\rho_w K_w}{\rho_p K_w - \lambda_i^2 \rho_w \rho_p} L_1 \tag{F23}$$

$$L_3 = \frac{-\rho_w \lambda_i}{\rho_p K_w - \lambda_i^2 \rho_w \rho_p} L_1 \tag{F24}$$

$$L_4 = \frac{1}{\lambda_i (1-n) \rho_p} L_1 \tag{F25}$$

From (F23) to (F25) we conclude that the characteristic form of the field equations (B34) to (B37) is given by:

$$\left(\frac{\partial}{\partial t} + \lambda_i \frac{\partial}{\partial x}\right)\left(1\ v + \frac{-\rho_w K_w}{\rho_p K_w - \lambda_i^2 \rho_w \rho_p}\ w\right.$$

$$\left. + \frac{-\rho_w \lambda_i}{\rho_p K_w - \lambda_i^2 \rho_w \rho_p}\ p + \frac{1}{\lambda_i (1-n) \rho_p}\ \sigma\right) = \qquad \text{(F26)}$$

$$= 1\ \frac{-\frac{n^2}{k}(w-v)}{(1-n)\rho_p} + \frac{-\rho_w K_w}{\rho_p K_w - \lambda_i^2 \rho_w \rho_p}\ \frac{-\frac{n^2}{k}(w-v)}{n \rho_w}$$

for: $i = 1,..,4$

where the characteristic velocities are given by (F20) and (F21).

If we put:

$$R_i = v + \frac{-\rho_w K_w}{\rho_p K_w - \lambda_i^2 \rho_w \rho_p}\ w + \frac{-\rho_w \lambda_i}{\rho_p K_w - \lambda_i^2 \rho_w \rho_p}\ p + \frac{1}{\lambda_i (1-n) \rho_p}\ \sigma \qquad \text{(F27)}$$

we can bring (F26) into the following form:

$$\frac{dR_i}{dt} = \frac{-n^2 (w-v)}{k (1-n) \rho_p} + \frac{-\rho_w K_w}{\rho_p K_w - \lambda_i^2 \rho_w \rho_p} \frac{\frac{n^2}{k} (w-v)}{n \rho_w} \qquad \text{(F28)}$$

$$\text{on } \frac{dx}{dt} = \lambda_i, \text{ for } i=1,\ldots,4$$

or:

$$\frac{dR_i}{dt} = f_i (R_1, R_2, R_3, R_4) \qquad \text{(F29)}$$

$$\text{on } \frac{dx}{dt} = \lambda_i, \text{ for } i=1,\ldots,4$$

The set of ordinary differential equations (F29) can now be solved by stepwise numerical integration. The advantage of this approach is that non-linear problems can be treated in the same way and detailed proofs of existence and uniqueness are available (Courant and Hilbert [50])

The method of characteristics has been used by Liou [10] to solve the field equations (B34) to (B37) with a variable K_p. Some care should be observed in the process of piecewise linearization of the field equations, because the dependent variables w and v are the perturbed variables at the rest state ($w_0 = 0$, $v_0 = 0$, (B19)). If the

terms with w_0 and v_0 become of first order, we have a different set of field equations. Therefore in certain cases it might be worthwhile to do the linear and non-linear analysis on this different set of equations or on the full set of non-linear equations directly.

In Chapter H.2 and H.3 we will explore the conditions under which the terms with w_0 and v_0 can be neglected.

G. The Propagation of Discontinuities

In this Chapter we will discover that applying a step loading at the boundary will in general generate two propagating discontinuities in the variables. We will make a comparison between the speed of the discontinuities, the characteristic velocities and the velocities of the waves in the harmonic solution. We will draw some general conclusions about the change in variables during the fastest propagating discontinuity in the special case that the parameters have the "practical" values of wet sand (e.g. the jump in the pore pressure is large with respect to the jump in effective stress along the fastest discontinuity).

By using a wavefront approximation we will show that the discontinuities decay as they propagate, due to the generation of velocity differences along the discontinuity. However, we will demonstrate that non-linearities due to a non-linear constitutive equation for the fluid opposes the decay of the gradients in the variables along the fastest propagating discontinuity.

G.1. Derivation of the Jump Conditions

We derive the jump condition of a conservation equation in the following way (Whitham [49]):

Consider the following conservation equation:

$$\frac{d}{dt}\int_{x_2}^{x_1} \rho(x,t)\,dx + q(x_1,t) - q(x_2,t) = 0 \qquad \text{(G.1.1)}$$

where $q(x,t)$ is the flux and $\rho(x,t)$ is the density.

Suppose there is a discontinuity at $x = s(t)$ such that: $x_1 > s(t) > x_2$, then from (G.1.1) follows:

$$q(x_2,t) - q(x_1,t) = \frac{d}{dt}\int_{x_2}^{s(t)} \rho(x,t)\,dx + \frac{d}{dt}\int_{s(t)}^{x_1} \rho(x,t)\,dx$$

$$= \rho(s^-,t)\,\dot{s} - \rho(s^+,t)\,\dot{s}$$

$$+ \int_{x_2}^{s(t)} \rho_t\,dx + \int_{s(t)}^{x_1} \rho_t\,dx \qquad \text{(G.1.2)}$$

If $x_1 \to s^+$ and $x_2 \to s^-$, then the last two integrals approach zero and hence:

$$q(s^-,t) - q(s^+,t) = \{\rho(s^-,t) - \rho(s^+,t)\} \quad \dot{s}$$

or:

$$q_2 - q_1 = U(\rho_2 - \rho_1) \tag{G.1.3}$$

This is called the jump condition for the variables with subscript 1 before the discontinuity with respect to the variables with subscript 2 after the discontinuity. U is the speed of the propagation of discontinuity.

We write (G.1.3) as:

$$-U\,[\rho] + [q] = 0 \tag{G.1.4}$$

where:

$$[\rho] = \rho_2 - \rho_1 \tag{G.1.5}$$

$$[q] = q_2 - q_1 \tag{G.1.6}$$

G.2 Jump Conditions for the Field Equations (B34) to (B37)

The field equations are : (B34) to (B37)

$$n \rho_w \frac{\partial w}{\partial t} = - n \frac{\partial p}{\partial x} - \frac{n^2}{k} (w-v) \tag{G.2.1}$$

$$(1-n) \rho_p \frac{\partial v}{\partial t} = - \frac{\partial \sigma}{\partial x} - (1-n) \frac{\partial p}{\partial x} + \frac{n^2}{k} (w-v) \tag{G.2.2}$$

$$\frac{\partial w}{\partial x} + \frac{1-n}{n} \frac{\partial v}{\partial x} = - \frac{1}{K_w} \frac{\partial p}{\partial t} \tag{G.2.3}$$

$$\frac{\partial v}{\partial x} = - \frac{1}{K_p} \frac{\partial \sigma}{\partial t} \tag{G.2.4}$$

Now we rewrite the field equations in integral form:

$$\frac{d}{dt} \int_{x_2}^{x_1} n \rho_w w \, dx - [n \, p] + \int_{x_2}^{x_1} \frac{n^2}{k} (w-v) \, dx = 0 \tag{G.2.5}$$

$$\frac{d}{dt} \int_{x_2}^{x_1} (1-n) \rho_p v \, dx - \left[\sigma + (1-n) \, p\right] - \int_{x_2}^{x_1} \frac{n^2}{k} (w-v) \, dx = 0 \tag{G.2.6}$$

$$\frac{d}{dt} \int_{x_2}^{x_1} p \, dx - \left[K_w \, w + \frac{1-n}{n} K_w \, v \right] = 0 \qquad (G.2.7)$$

$$\frac{d}{dt} \int_{x_2}^{x_1} \sigma \, dx - \left[K_p \, v \right] = 0 \qquad (G.2.8)$$

In the same way as in Chapter (G.1) we derive the jump conditions for (G.2.5) to (G.2.8):

$$-U \, [\rho_w \, w] + [p] = 0 \qquad (G.2.9)$$

$$-U \, [(1-n) \, \rho_p \, v] + [\sigma + (1-n) \, p] = 0 \qquad (G.2.10)$$

$$-U \, [p] + \left[K_w \, w + \frac{1-n}{n} \, K_w \, v \right] = 0 \qquad (G.2.11)$$

$$-U \, [\sigma] + [K_p \, v] = 0 \qquad (G.2.12)$$

We note that if $x_1 \to s^+$ and $x_2 \to s^-$, then the integral $\int_{x_2}^{x_1} \frac{n^2}{k} (w-v)\, dx$ approaches zero, indicating that during the jump the inertia terms are dominant over the viscous terms.

Rewriting (G.2.9) to (G.2.12) gives:

$$-U \rho_w w_1 + U \rho_w w_2 + p_1 - p_2 = 0 \qquad \text{(G.2.13)}$$

$$-U (1-n) \rho_p v_1 + U (1-n) \rho_p v_2 + \sigma_1 + (1-n) p_1 \qquad \text{(G.2.14)}$$

$$-\sigma_2 - (1-n) p_2 = 0$$

$$-U p_1 + U p_2 + K_w w_1 + \frac{1-n}{n} v_1 K_w - K_w w_2 - \frac{1-n}{n} K_w v_2 = 0 \qquad \text{(G.2.15)}$$

$$-U \sigma_1 + U \sigma_2 + K_p v_1 - K_p v_2 = 0 \qquad \text{(G.2.16)}$$

If we assume that the variables v_1, w_1, σ_1, p_1 before the discontinuity are known then (G.2.13) to (G.2.16) are four equations with five unknowns (U, p_2, σ_2, v_2, w_2). So we have to prescribe one more variable in order to solve (G.2.13) to (G.2.16).

If we choose v_2 as known, then after some algebra we obtain:

$$\sigma_2 = \sigma_1 - \frac{K_p}{U} v_1 + \frac{K_p}{U} v_2 \qquad \text{(G.2.17)}$$

$$p_2 = -U \rho_w w_1 + U \rho_w w_2 + p_1 \qquad \text{(G.2.18)}$$

$$w_2 = w_1 + \frac{(1-n) K_w}{(K_w - U^2 \rho_w) n} v_1 - \frac{(1-n) K_w}{(K_w - U^2 \rho_w) n} v_2 \qquad \text{(G.2.19)}$$

(G.2.17) to (G.2.19) form the equations for the unknown variables after the discontinuity.

Further we obtain an equation for the velocity of the discontinuity:

$$U^4 (1-n) \rho_p \rho_w n - \Big((1-n) \rho_p n K_w + K_p \rho_w n + (1-n)^2 K_w \rho_w\Big) U^2 + \Big(n K_p K_w\Big) = 0 \qquad \text{(G.2.20)}$$

We notice that this is the same equation as the equation for the characteristic velocities (F12) and the same equation for the wave-speed c (C19) for $\omega \to \infty$.

Information from the boundaries is carried along the characteristics (Whitham [49]) so that the characteristics propagate with the speed of discontinuities and hence the first part of the above statement is correct.

Waves with very high frequency ($\omega \to \infty$) are dominated by the inertia of the phases (rapid change of the variables in time) and not by viscous forces between the phases: exactly the same situation as during the jump and hence the second part of the above result becomes clear.

For practical values of wet sand ($K_w >> K_p$) we derive of course the same equations as (F20) and (F21) for the discontinuity velocities U. So:

$$U_{1,2} \approx \pm \left\{ \frac{n \rho_p K_w + (1-n) \rho_w K_w}{n \rho_w \rho_p} \right\}^{1/2} \qquad (G.2.21)$$

$$U_{3,4} \approx \pm \left\{ \frac{n K_p}{n (1-n) \rho_p + (1-n)^2 \rho_w} \right\}^{1/2} \qquad (F.2.22)$$

We observe that (G.2.21) is larger and (G.2.22) is smaller than the speed of sound in water. $\left(= \sqrt{\frac{K_w}{\rho_w}} \right)$ and furthermore that the velocities of the discontinuities are real and hence do exist.

Substitution of the "practical" values for wet sand into (G.2.21) and (G.2.22) gives for $n = 0.4$:

$$U_{1,2} = 1790 \quad \text{m/sec}$$

$$U_{3,4} = 65 \quad \text{m/sec}$$

We see that the speed of the first discontinuity is larger than the speed of sound in water (1440 m/sec) and the speed of the second discontinuity is smaller than the speed of sound in water.

Applying a discontinuity on the boundary will in general generate two discontinuities, which might attenuate as they propagate.

A boundary value problem will be treated in Chapter L.

From (G.2.19) we conclude:

$$w_2 - w_1 = -\frac{(1-n)\, K_w}{(K_w - U^2 \rho_w)\, n} (v_2 - v_1) \qquad \text{(G.2.23)}$$

So:

$$\text{if} \quad U^2 > \frac{K_w}{\rho_w} \quad \Rightarrow \quad w_2 - w_1 = \tilde{\gamma} (v_2 - v_1) \qquad \text{(G.2.24)}$$

$$\text{if} \quad U^2 < \frac{K_w}{\rho_w} \qquad \Rightarrow \qquad w_2 - w_1 = - \tilde{\gamma} \, (v_2 - v_1) \tag{G.2.25}$$

where:

$$\tilde{\gamma} = \left| \frac{(1-n) \, K_w}{(K_w - U^2 \, \rho_w) \, n} \right| \tag{F.2.26}$$

If we assume now that the phase velocities are equal in front of the discontinuity, so $v_1 = w_1 = \tilde{\beta}$, then:

$$\text{if} \quad U^2 > \frac{K_w}{\rho_w} \qquad \Rightarrow \qquad w_2 - \tilde{\beta} = \tilde{\gamma} \quad (v_2 - \tilde{\beta}) \tag{G.2.27}$$

$$\text{if} \quad U^2 < \frac{K_w}{\rho_w} \qquad \Rightarrow \qquad w_2 - \tilde{\beta} = - \tilde{\gamma} \, (v_2 - \tilde{\beta}) \tag{G.2.28}$$

If we further assume that the velocity of the fluid behind the discontinuity is greater than the velocity in front of the discontinuity, so $w_2 > w_1$ or $w_2 - \tilde{\beta} > 0$, then from (G.2.18) follows:

$$p_2 - p_1 = U \, \rho_w \quad (w_2 - \tilde{\beta}) > 0 \tag{G.2.29}$$

if we consider a discontinuity propagating in the positive x-direction.

Furthermore from (G.2.17) there follows:

$$\text{if} \quad U^2 > \frac{K_w}{\rho_w} \quad \Rightarrow \sigma_2 - \sigma_1 = \frac{K_p}{U} \quad (v_2 - v_1) = \frac{1}{\tilde{\gamma}} \frac{K_p}{U} \quad (w_2 - \tilde{\beta}) > 0 \quad \text{(G.2.30)}$$

$$\text{if} \quad U^2 < \frac{K_w}{\rho_w} \quad \Rightarrow \sigma_2 - \sigma_1 = \frac{K_p}{U} \quad (v_2 - v_1) = -\frac{1}{\tilde{\gamma}} \frac{K_p}{U} \quad (w_2 - \tilde{\beta}) < 0 \quad \text{(G.2.31)}$$

Hence if we consider the case where the phase velocities are equal in front of a discontinuity (which is the case for a discontinuity propagating into an area at rest) we come to the following conclusions:

- if the speed of the discontinuity is larger than the speed of sound of the fluid then compressing the fluid during the discontinuity implies compression of the skeleton.
- on the contrary, if the speed of the discontinuity is smaller than the speed of sound of the fluid then compressing the fluid during the discontinuity implies stretching of the skeleton.

Now we consider the case: $\frac{K_w}{K_p} >> 1$, so the speed of the discontinuities are given by (G.2.21) and (G.2.22). Consider further the fastest discontinuity propagating into an area at rest ($v_1 = w_1 = 0$), then:

$$\sigma_2 - \sigma_1 = \Delta\sigma = \frac{K_p}{U} v_2 \qquad \text{(G.2.31)}$$

$$p_2 - p_1 = \Delta p = U \rho_w w_2 \qquad \text{(G.2.32)}$$

$$w_2 = \frac{(1-n) K_w}{(K_w - U^2 \rho_w) n} v_2 \qquad \text{(G.2.33)}$$

Substitution of (G.2.21) into (G.2.31) to (G.2.33) gives:

$$\frac{\Delta p}{\Delta\sigma} = \frac{n \rho_p + (1-n) \rho_w}{n \rho_w} \frac{K_w}{K_p} \qquad \text{(G.2.34)}$$

Note that if $\frac{K_w}{K_p} >> 1$, the fastest propagating discontinuity propagates faster than the speed of sound in the fluid and so result (G.2.27) applies. Also we note that $\tilde{\gamma}$ has the following value in this case:

$$\tilde{\gamma} = \left| \frac{\rho_p}{\rho_w} \right| \qquad \text{(G.2.34a)}$$

Summarizing:

In the case where the parameters have the "practical" values of wet sand, we conclude that behind the first discontinuity propagating into a medium at rest, the change in effective stress is small with respect to the change in pore pressure and that these changes have the same sign. Further velocity differences between the skeleton and the fluid are generated. The fluid velocity has the ratio of $\frac{\rho_p}{\rho_w}$ with respect to the skeleton velocity and both velocities are in the same direction. This result is derived without using specific boundary conditions and hence will hold in general.

The above result is in agreement with Nikolaevskii's [15] results. He states that after the fastest propagating discontinuity the phase mass velocities are equal ($\rho_p \; v = \rho_w \; w$). His result was derived for the case of equal phase stresses.

For the slowest propagating discontinuity we can not make these general statements, because we do not a priori know the conditions in front of this discontinuity as it propagates.

Now we are interested in the following case: A discontinuity propagates into a medium at rest and we assume equal phase velocities behind the discontinuity, then from (G.2.19) follows:

$$\frac{-(1-n)\,K_w}{n\,(K_w - U^2\,\rho_w)} = 1 \qquad \text{(G.2.35)}$$

or:

$$U^2 = \frac{K_w}{n\,\rho_w} \qquad \text{(G.2.36)}$$

We conclude that if the speed of the discontinuity propagating into the rest state is such that $U^2 = \frac{K_w}{n\rho_w}$, then the phase velocities are equal behind this discontinuity.

A detailed discussion about equal phase velocities is given in Chapter H.

In the regions between the discontinuities and between the slowest discontinuity and the boundary, in general momentum exchange takes place, due to different phase-velocities. In these regions viscous forces between the phases play an important role

G.3 The Attenuation of Propagating Discontinuities

So far we have discussed the jumps in the variables relative to each other. In general these jumps will attenuate as they propagate. This question is important in order to assess which parts of the field will be affected by a discontinuity.

We will use a wavefront expansion in order to establish the attenuation.

We introduce the following expansion (Whitham [49]):

$$w(x,t) = W^*(x,t) + W_0(x)\, H_0(S) + W_1(x)\, H_1(S) + \ldots \tag{G.3.1}$$

$$v(x,t) = V^*(x,t) + V_0(x)\, H_0(S) + V_1(x)\, H_1(S) + \ldots \tag{G.3.2}$$

$$p(x,t) = P^*(x,t) + P_0(x)\, H_0(S) + P_1(x)\, H_1(S) + \ldots \tag{G.3.3}$$

$$\sigma(x,t) = \sigma^*(x,t) + \sigma_0(x)\, H_0(S) + \sigma_1(x)\, H_1(S) + \ldots \tag{G.3.4}$$

where:

$$H_0(S) = 0 \quad \text{if } S > 0 \qquad = 1 \quad \text{if } S < 0 \tag{G.3.5}$$

$$H_1(S) = S \quad \text{if } S < 0 \qquad = 0 \quad \text{if } S > 0 \tag{G.3.6}$$

$$H_n(S) = \frac{1}{n!} S^n \quad \text{if } S < 0 \qquad = 0 \quad \text{if } S > 0 \tag{G.3.7}$$

$$S = x - \lambda t \tag{G.3.8}$$

where λ is the speed of the discontinuity.

From the definitions (G.3.5) to (G.3.7) we conclude:

$$H'_{n+1} = H_n \tag{G.3.9}$$

Further $W^*(x,t)$, $V^*(x,t)$, $P^*(x,t)$ and $\sigma^*(x,t)$ satisfy the field equations (B34) to (B37).

The idea is now to consider $|S| << 1$ and hence focus our attention on the neighborhood of the discontinuity. We substitute (G.3.1) to (G.3.4) into the field equations and collect terms of the same order. To each order the field equations have to be satisfied. Executing this process we obtain the following set of equations:

To order $H'_0(S)$:

$$n\rho_w\,(-\lambda)W_0(x) = -nP_0(x) \tag{G.3.10}$$

$$(1-n)\rho_p\,(-\lambda)V_0(x) = -\sigma_0(x) - (1-n)\,P_0(x) \tag{G.3.11}$$

$$W_0(x) + \frac{1-n}{n}\,V_0(x) = -\frac{1}{K_w}\,(-\lambda)P_0(x) \tag{G.3.12}$$

$$V_0(x) = -\frac{1}{K_p}\,(-\lambda)\sigma_0(x) \tag{G.3.13}$$

We identify (G.3.10) to (G.3.13) with (G.2.9) to (G.2.12), which clearly shows that the above variables are indeed the jumps in the variables p, σ, v and w along the discontinuities, whose wave speed is given by (G.2.20).

To order $H_0(S)$:

$$n\,\rho_w(-\lambda)W_1(x) = -n\,P_0'(x) - n\,P_1(x) - \frac{n^2}{k}W_0(x) + \frac{n^2}{k}V_0(x) \tag{G.3.14}$$

$$(1-n)\,\rho_p(-\lambda)V_1(x) = -\sigma_0'(x) - \sigma_1(x) - (1-n)\,P_0'(x) - (1-n)\,P_1(x) + \frac{n^2}{k}W_0(x) - \frac{n^2}{k}V_0(x) \tag{G.3.15}$$

$$W_0'(x) + W_1(x) + \frac{1-n}{n}V_0'(x) + \frac{1-n}{n}V_1(x) = -\frac{1}{K_w}(-\lambda)P_1(x) \tag{G.3.16}$$

$$V_0'(x) + V_1(x) = -\frac{1}{K}(-\lambda)\sigma_1(x) \tag{G.3.17}$$

Regarding the variables with subscript zero as known, the set of equations (G.3.14) to (G.3.17) consists of four equations with four unknowns $W_1(x)$, $V_1(x)$, $P_1(x)$ and $\sigma_1(x)$.

Putting all the variables with subscript zero on the right-hand side and putting all the variables with subscript one on the left-hand side of (G.3.14) to (G.3.17) we identify the matrix of (G.3.14) to (G.3.17) with the matrix of (G.3.10) to (G.3.13). The determinant of the first-order equations was set to zero in order to get nontrivial solutions for the jumps. This implies in the case of the given λ's that the system

(G.3.14) to (G.3.17) cannot in general be solved, unless certain conditions are satisfied.

We proceed here as follows: We reduce (G.3.14) to (G.3.17) to one equation with one variable with subscript one, e.g., W_1.

So

$$(.....)\ W_1(x) = (.....) \qquad (G.3.18)$$

Inspection of (G.3.18) shows that the term in front of W_1 is zero for the given values of λ (G.2.20). Hence the right-hand side of (G.3.18) has to be zero. This right-hand side contains only variables with subscript zero. Now we use the first-order equations (G.3.10) to (G.3.13) in order to express $\sigma_0(x)$, $V_0(x)$ and $W_0(x)$ in terms of $P_0(x)$. Substitution of these expressions into the right-hand side of (G.3.18) gives:

$$\alpha^* P_0'(x) + \beta^* P_0(x) = 0 \qquad (G.3.19)$$

where α^* and β^* are functions of the parameters in the field equations (B24) to (B37). The solution of (G.3.19) is:

$$P_0(x) = \text{constant} \exp(-\frac{\beta^*}{\alpha^*} x) \qquad (G.3.20)$$

Hence the attenuation constant is $\frac{\beta^*}{\alpha^*}$.

Inspection of the expressions for α^* and β^* shows that all terms in β^* contain a factor $\frac{1}{k}$ and that the terms in α^* do not contain k. Hence a smaller permeability (smaller k) will result in higher attenuation.

Substitution of the "practical" values of wet sand (with n = 0.4) into (G.3.19) gives as an example calculation:

$$3.3\ P_0'(x) + 90\ P_0(x) = 0 \qquad \text{(G.3.21)}$$

along the fastest propagating discontinuity and

$$-2.8\ P_0'(x) - 9\times10^3\ P_0(x) = 0 \qquad \text{(G.3.22)}$$

along the slowest propagating discontinuity. So the fastest propagating discontinuity ($\lambda_1 \approx 1800$ m/sec) decays like

$$\sim \exp(-30x) \qquad (x \text{ - in meters}) \qquad \text{(G.3.23)}$$

The slowest propagating discontinuity ($\lambda_2 \approx 70$ m/sec) decays like:

$$\sim \exp(-3300x) \qquad \text{(G.3.24)}$$

Hence we conclude that the first discontinuity decays to $\sim\frac{1}{3}$ of the initial amplitude after $\sim\frac{1}{30}$ m and the second discontinuity decays to $\sim\frac{1}{3}$ of the initial amplitude after $\sim\frac{1}{3300}$ m.

Therefore the second discontinuity decays much more rapidly than the first one. This result is in agreement with conclusions of Gimalitdinov [63], who calculated the decay coefficients of propagating discontinuities in the framework of Nikolaevskii's equations.

G.4 Effect of nonlinearities due to a nonlinear constitutive equation for the fluid on the decay of propagating discontinuities in the gradients.

In this section we will explore the effect of including a nonlinear constitutive equation for the fluid on the decay of propagating discontinuities in the gradients of the variables.

First we note that taking the derivative with respect to x in the linearized field equations (B34) to (B37) and then writing down the jump conditions for propagating discontinuities of the gradients, we get exactly the same result for the gradients of the variables as for the variables themselves.

Particularly we are able to obtain the jumps in the gradients in the field directly after applying two gradients at the boundary for a medium initially at rest. (An example for the jumps in the variables themselves is given in Chapter L.)

Now we focus our interest on the fastest propagating discontinuity. As we have seen in the linear theory the jump in the effective stress (or gradients of effective stress) is small with respect to the jump in the fluid pressure (or gradients of fluid pressure) for "practical" values of wet sand. Therefore we include a nonlinear constitutive equation for the fluid for further analysis.

We recall field equation (B36):

$$\frac{\partial w}{\partial x} + \frac{1-n}{n}\frac{\partial v}{\partial x} = -\frac{1}{K_w}\frac{\partial p}{\partial t} \qquad \text{(G.4.1)}$$

Instead of field equation (B36) we will use:

$$\frac{\partial w}{\partial x} + \frac{1-n}{n} \frac{\partial v}{\partial x} = - \frac{1}{K_w} \frac{\partial p}{\partial t} - \frac{h(p)}{K_w} \frac{\partial p}{\partial t} \qquad (G.4.2)$$

where $h(0) = 0$

$$h'(0) = \alpha < 0$$

so the compressibility is less when p is larger.

Now we proceed as follows (Whitham [49]): We expand the solution in powers of

$$\xi = x - \lambda t \qquad (G.4.3)$$

and further:

$$(\xi < 0) : w(x,t) = \tilde{w}(\xi,x) = \xi \, w_1(x) + \frac{1}{2} \xi^2 \, w_2(x) + \ldots \qquad (G.4.4)$$

$$(\xi > 0) : w(x,t) = \tilde{w}(\xi,x) = 0 \qquad (G.4.5)$$

In a similar way we expand the other variables.

We note that:

$$\frac{\partial w}{\partial x} = 0 \qquad \xi > 0 \qquad (G.4.6)$$

$$\frac{\partial w}{\partial x} = \xi \frac{\partial w_1}{\partial x} + w_1(x) + \xi \, w_2(x) + \ldots \qquad \xi < 0 \qquad (G.4.7)$$

Hence:

$$\left[\frac{\partial w}{\partial x}\right] = w_1(x) \qquad \text{for } \xi \to 0 \qquad (G.4.8)$$

Further:

$$\frac{\partial w}{\partial t} = \frac{\partial \tilde{w}}{\partial \xi}\frac{\partial \xi}{\partial t} = -\left(\lambda\, w_1(x) + \xi\, w_2(x) + \ldots\right)$$

$$= -\lambda\, w_1(x) - \xi\lambda\, w_2(x) + \ldots \qquad \text{(G.4.9)}$$

$$\frac{\partial w}{\partial x} = \frac{\partial \tilde{w}}{\partial \xi}\frac{\partial \xi}{\partial x} + \frac{\partial w}{\partial x}$$

$$= \left(w_1(x) + \xi\, w_2(x) + \ldots\right) 1$$

$$+ \xi\, w_1'(x) + \frac{1}{2}\,\xi^2\, w_2'(x)$$

$$= w_1(x) + \xi\left(w_2(x) + w_1'(x)\right) + \ldots \qquad \text{(G.4.10)}$$

In a similar way we obtain expansions for the derivatives of the other variables.

Furthermore:

$$h(p) = h\left(0 + \xi\, p_1(x) + \ldots\right) =$$

$$= h(0) + \xi p_1(x)\left.\frac{\partial h}{\partial p}\right|_{p=0} + \ldots$$

$$= \xi\, p_1(x)\ \ \alpha + \ldots \qquad \text{(G.4.11)}$$

Now we substitute the expansions for the derivatives of the variables and h(p) into the nonlinear field equations (B34), (B35), (B37) and (G.4.2). We equate equal powers of ξ.

To the zero order we obtain a set of equations like (G.3.10) to (G.3.13). Hence for the nonlinear problem the speed of the fastest propagating discontinuity is given by the largest root of (G.2.20).

The effect of including a nonlinear constitutive equation on terms of order ξ can be seen as follows: The last (nonlinear) term of (G.4.2) becomes:

$$
\begin{aligned}
& - \frac{h(p)}{K_w} \frac{\partial p}{\partial t} = \\
& - \xi \, p_1(x) \, \alpha \left(- \lambda \, p_1(x) - \xi \, \lambda \, p_2(x) + \ldots \right) \frac{1}{K_w} + \ldots \\
& = + \lambda \, \xi \, p_1^2(x) \quad \alpha \, \frac{1}{K_w} + \ldots
\end{aligned}
\tag{G.4.12}
$$

Equating terms with powers ξ gives a set of equations similar to (G.3.14) to (G.3.17), with the exception that (G.3.16) now contains an additional term in its right-hand side. This term is quadratic in $p_1(x)$ and is due to (G.4.12).

Now we proceed in the same way as in section (G.3), but instead of ending up with a linear differential equation we end up with a nonlinear differential equation, which is:

$$
\alpha^* \, p_1'(x) + \beta^* \, p_1(x) + \gamma^* \, p_1^2(x) = 0 \tag{G.4.13}
$$

where α^* and β^* are the same as in section (G.3) and γ^* is a combination of the parameters, including α.

Substitution of the practical values for wet sand (with n = 0.4) into (G.4.13) gives:

$$3.25\ p_1'(x) + 90\ p_1(x) - 1.63\ \alpha\ p_1^2(x) = 0 \qquad \text{(G.4.14)}$$

The equation (G.4.14) is in the form of a Riccati equation which can be solved explicitly (Whitham [49]).

Assume now that the pore pressure increases behind the fastest propagating discontinuity and hence the jump in the gradient of the pore pressure is negative near the boundary.

Inspection of (G.4.14) shows that the third term due to the non-linearity in the constitutive equation for the fluid (with α negative) opposes the decay of the gradient due to the second term in (G.4.14).

If $|p_1(0)| > \left|\frac{90}{1.63\ \alpha}\right|$, then $p_1(0) < 0$ and hence $|p_1(x)|$ grows continually. This leads to $|p_1(x)| \to \infty$ in finite time. Hereafter a shock wave with discontinuities in the variables themselves has to be introduced.

Summarizing: Jumps in the gradients of the variables for the linearized case decay as they propagate for "practical" values of wet sand. Including a nonlinear constitutive equation for the fluid opposes the decay along the fastest discontinuity. If the initial gradients are large enough, a shock wave with discontinuities in the variables will emerge. The initial gradients behind the fastest discontinuity can be calculated from the appropriate gradients at the boundary, because the linear theory can be applied at $t = 0^+$.

H. The Consequences of Equal Phase Velocities

It has been assumed that during dynamic loading saturated earth masses behave as in an undrained condition (Joyner [51]). It is therefore interesting to explore what the consequences are of the assumption of equal phase velocities.

An impact problem will be solved with the non-linear field equations (B1) to (B6), for equal phase velocities, not so much to represent a real physical example but to demonstrate the effect of non-linear terms and the relation to the linear theory. In Chapter I we will comment on a more general non-linear case.

H.1. Equal Phase Velocities; the Linearized Case

The field equations (B34) to (B37) are:

$$n\,\rho_w \frac{\partial w}{\partial t} = -n\frac{\partial p}{\partial x} - \frac{n^2}{k}(w-v) \tag{H.1.1}$$

$$(1-n)\,\rho_p \frac{\partial v}{\partial t} = -\frac{\partial \sigma}{\partial x} - (1-n)\frac{\partial p}{\partial x} + \frac{n^2}{k}(w-v) \tag{H.1.2}$$

$$\frac{\partial w}{\partial x} + \frac{1-n}{n}\frac{\partial v}{\partial x} = -\frac{1}{K_w}\frac{\partial p}{\partial t} \tag{H.1.3}$$

$$\frac{\partial v}{\partial x} = -\frac{1}{K_p}\frac{\partial \sigma}{\partial t} \tag{H.1.4}$$

Putting:

$$w = v \tag{H.1.5}$$

gives:

$$\rho_w \frac{\partial v}{\partial t} = -\frac{\partial p}{\partial x} \tag{H.1.6}$$

$$(1-n)\,\rho_p \frac{\partial v}{\partial t} = -\frac{\partial \sigma}{\partial x} - (1-n)\frac{\partial p}{\partial x} \tag{H.1.7}$$

$$\frac{1}{n}\frac{\partial v}{\partial x} = -\frac{1}{K_w}\frac{\partial p}{\partial t} \qquad \text{(H.1.8)}$$

$$\frac{\partial v}{\partial x} = -\frac{1}{K_p}\frac{\partial \sigma}{\partial t} \qquad \text{(H.1.9)}$$

From (H.1.6) and (H.1.7) follows:

$$(1-n)\,\rho_w\frac{\partial v}{\partial t} = -(1-n)\frac{\partial p}{\partial x} \qquad \text{(H.1.10)}$$

$$(1-n)\,\rho_p\frac{\partial v}{\partial t} = -\frac{\partial \sigma}{\partial x} - (1-n)\frac{\partial p}{\partial x} \qquad \text{(H.1.11)}$$

Subtracting (H.1.10) from (H.1.11) gives:

$$(1-n)\,(\rho_p - \rho_w)\frac{\partial v}{\partial t} = -\frac{\partial \sigma}{\partial x} \qquad \text{(H.1.12)}$$

(H.1.9) states:

$$\frac{\partial v}{\partial x} = -\frac{1}{K_p}\frac{\partial \sigma}{\partial t} \qquad \text{(H.1.13)}$$

From (H.1.12) and (H.1.13) we conclude: If $\rho_p \neq \rho_w$ then a disturbance in the velocity v propagates with velocity:

$$c_\alpha = \pm\left(\frac{K_p}{(1-n)\ (\rho_p - \rho_w)}\right)^{1/2} \tag{H.1.14}$$

From (H.1.6) and (H.1.8) it follows that:

$$\rho_w \ \frac{\partial v}{\partial t} = -\frac{\partial p}{\partial x} \tag{H.1.15}$$

$$\frac{\partial v}{\partial x} = -\frac{n}{K_w}\ \frac{\partial p}{\partial t} \tag{H.1.16}$$

Hence from (H.1.15) and (H.1.16) we see: A disturbance in the velocity v propagates with velocity:

$$c_\beta = \pm\left(\frac{K_w}{n\ \rho_w}\right)^{1/2} \tag{H.1.17}$$

We note that (H.1.17) is equal to the square root of (6.2.36). Because we are looking for a solution of v that satisfies simultaneously (H.1.6) to (H.1.9), we conclude from (H.1.14) and (H.1.17):

$$\frac{K_p}{(1-n)\ (\rho_p - \rho_w)} = \frac{K_w}{n\ \rho_w} \tag{H.1.18}$$

Condition (H.1.18) states:

Only if there is a certain relationship between the compression modulus of the fluid and the compression modulus of the grain structure will the phase velocities in the model be equal. If this relationship does not exist, then if $\rho_p \neq \rho_w$ the phase velocities cannot be equal.

Biot [1] noted the existence of a harmonic solution for compression waves of the Biot equations, where the phase velocities are equal.

Substituting the mass densities for quartz and water into (H.1.18), then for n = 0.4 we obtain:

$$K_w = 0.4\ K_p$$

So the compression modulus of the water has to be of the same order as the compression modulus for the skeleton. For "practical" values of wet sand this is not the case and hence equal phase velocities do not exist. However the presence of small air bubbles can lower the compression modulus of the water considerably (Richart [47]).

Hence in the presence of enough small air bubbles or a more compressible fluid, equation (H.1.18) could be satisfied and equal phase velocities could be possible in that case.

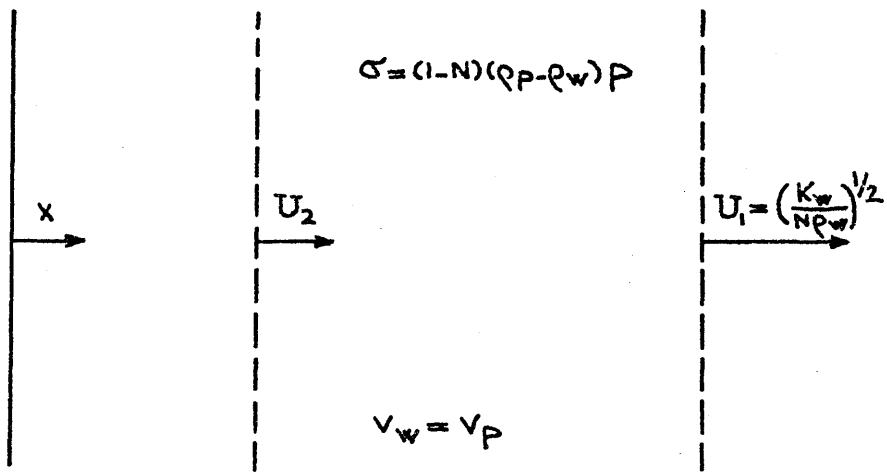

PROPAGATING DISCONTINUITIES

FIG. 4

In Chapter B we showed that there do exist waves with almost equal phase velocities in the lower frequencies for the practical values of wet sand.

Further from (H.1.8) and (H.1.9) we conclude:

$$\frac{\sigma}{p} = \frac{K_p}{K_{w/n}} = \frac{(1-n)\ (\rho_p - \rho_w)}{\rho_w} \qquad \text{(H.1.19)}$$

Substitution of the condition (H.1.18) into (G.2.20) shows that in that case the fastest discontinuity propagates with speed: $\left(\frac{K_w}{n\ \rho_w}\right)^{1/2}$ and hence from (G.2.36) we conclude that if condition (H.1.18) holds the phase velocities behind the fastest discontinuity are equal.

If the phase velocities at the boundaries are not equal, and we apply a step load at the boundary, then a second slower propagating discontinuity will be generated in order to satisfy the boundary conditions. See Fig (4).

If $\rho_p = \rho_w$ and $\frac{K_p}{K_w} >> 1$, then from (G.2.21) it follows that the fastest discontinuity propagates with speed $\left(\frac{K_w}{n\ \rho_w}\right)^{1/2}$ and hence directly behind the discontinuity the phase velocities are equal. Until the next discontinuity or until disturbing influences from the boundaries arise there is no change in the variables and hence $\frac{\partial \sigma}{\partial x} = 0$, which agrees with (H.1.12).

We conclude that equal phase velocities in general do not occur in our model.

H.2. Impact Problem With Non-Linear Field Equations.

We will consider the following problem: A one-dimensional semi-infinite two phase medium has an initial velocity v_1. The properties of the medium are such that the phase velocities are equal and the pore pressure p_1 and effective stress σ_1 are known and constant. At $t = 0$ the boundary $x = 0$ of the medium is stopped, such that $v = w = 0$ at the boundary. We are interested in the changes in the variables for $t > 0$.

Further we assume that the field equations are given by (B.1) to (B.7).

Hence the field equations are:

$$\frac{\partial}{\partial t}\left((1-n)\ \rho_p\right) + \frac{\partial}{\partial x}\left(\rho_p\ (1-n)\ v\right) = 0 \qquad \text{(H.2.1)}$$

$$\frac{\partial}{\partial t}\left(n\ \rho_w\right) + \frac{\partial}{\partial x}\left(\rho_w\ n\ w\right) = 0 \qquad \text{(H.2.2)}$$

$$n\ \rho_w\left(\frac{\partial w}{\partial t} + w\ \frac{\partial w}{\partial x}\right) = -\ n\ \frac{\partial p}{\partial x} - R \qquad \text{(H.2.3)}$$

$$(1-n)\ \rho_p\left(\frac{\partial v}{\partial t} + v\ \frac{\partial v}{\partial x}\right) = -\frac{\partial \sigma}{\partial x} - (1-n)\ \frac{\partial p}{\partial x} + R \qquad \text{(H.2.4)}$$

$$\rho_p = \text{constant} \tag{H.2.5}$$

$$\rho_w = f(p) \tag{H.2.6}$$

$$n = g(\sigma) \tag{H.2.7}$$

Now we attempt to solve the problem in the following way: after impact a discontinuity with speed U will propagate in the opposite direction to v_1. We assume that directly behind the discontinuity the phase velocities are equal and zero, and hence the boundary condition is satisfied. This assumption puts a constraint on the constitutive relation (H.2.7). The analysis will generate the appropriate constitutive relation.

Further we assume that the thickness of the discontinuity is small enough that we may neglect the viscous terms R for the jump conditions. (Hence we allow phase velocities differences during the shock.)

First we develop the mass conservation equations (H.2.1) and (H.2.2), and the momentum conservation equations (H.2.3) and (H.2.4) in integral form:

$$\frac{d}{dt}\int_{x_1}^{x_2} n\,\rho_w\,dx \quad + \quad [\rho_w\, n\, w]_{x_1}^{x_2} \quad = 0 \tag{H.2.5}$$

$$\frac{d}{dt}\int_{x_1}^{x_2} (1-n)\,\rho_p\,dx + \quad [\rho_p\,(1-n)\,v]_{x_1}^{x_2} = 0 \tag{H.2.6}$$

$$\frac{d}{dt}\int_{x_1}^{x_2} (1-n)\ \rho_p\ v\ dx + [(1-n)\ \rho_p\ v^2 + \sigma + (1-n)\ p]_{x_1}^{x_2}$$

$$- \int_{x_1}^{x_2} R\ dx = 0 \qquad \text{(H.2.7)}$$

$$\frac{d}{dt}\int_{x_1}^{x_2} n\ \rho_w\ v\ dx \quad + [\rho_w\ n\ v^2 + p\ n]_{x_1}^{x_2}$$

$$+ \int_{x_1}^{x_2} R\ dx = 0 \qquad \text{(H.2.8)}$$

We assume:

$$v_1 = w_1 \qquad \text{(H.2.9)}$$

$$v_2 = w_2 \qquad \text{(H.2.10)}$$

From (H.2.5) to (H.2.8) we derive the following jump conditions:

$$-U\ [n\ \rho_w] \quad + \quad [n\ \rho_w\ v] \ = 0 \qquad \text{(H.2.11)}$$

$$-U\ [n\ \rho_w\ v] \quad + \quad [n\ \rho_w\ v^2 + p\ n] \ = \ 0 \qquad \text{(H.2.12)}$$

$$-U\ [(1-n)\ \rho_p] \quad + \quad [\rho_p\ (1-n)\ v] \ = 0 \qquad \text{(H.2.13)}$$

$$-U\ [(1-n)\ \rho_p\ v] + [(1-n)\ \rho_p\ v^2 + \sigma + (1-n)\ p] = 0 \qquad \text{(H.2.14)}$$

Now we make the following assumptions:

$$\rho_p = \text{constant} \tag{H.2.15}$$

$$\rho_w = \rho_0 + \rho_0 \beta (p-p_0) \text{ (Bear [36])} \tag{H.2.16}$$

where β is the compressibility and ρ_0 is a reference density.

We do not make any assumption at this point about the form of the constitutive relation for the grain structure. The form of the constitutive relation will be generated by the analysis.

From (H.2.11) to (H.2.16) follows:

$$-U\, n_1\, \rho_{w_1} + U\, n_2\, \rho_{w_2} + n_1\, \rho_{w_1}\, v_1 - n_2\, \rho_{w_2} v_2 = 0 \tag{H.2.17}$$

$$-U\, n_1\, \rho_{w_1}\, v_1 + U\, n_2\, \rho_{w_2} v_2 + n_1\, \rho_{w_1}\, v_1^2 + p_1\, n_1 - n_2\, \rho_{w_2}\, v_2^2 + p_2\, n_2 = 0 \tag{H.2.18}$$

$$-U\,(1-n_1)\,\rho_p + U\,(1-n_2)\,\rho_p + \rho_p\,(1-n_1)\,v_1 - \rho_p\,(1-n_2)\,v_2 = 0 \tag{H.2.19}$$

$$-U\,(1-n_1)\,\rho_p\,v_1 + U\,(1-n_2)\,\rho_p\,v_2 + (1-n_1)\,\rho_p\,v_1^2 + \sigma_1 + (1-n_1)\,p_1 - (1-n_2)\,\rho_p\,v_2^2 - \sigma_2 - (1-n_2)\,p_2 = 0 \tag{H.2.20}$$

$$\rho_{w_2} = \rho_{w_1} + \rho_{w_1}\,\beta\,(p_2-p_1) \tag{H.2.21}$$

We pose the problem in the following way:

Given: $v_1, w_1, \rho_{w_1}, \sigma_1, p_1, n_1$ and $v_2 = w_2 = 0$.

Calculate: $\rho_{w_2}, \sigma_2, p_2, n_2$ and U from (H.2.17) to (H.2.21).

After some algebra we obtain:

$$n_2 = n_1 + (1-n_1)\frac{v_1}{U} \tag{H.2.22}$$

$$\rho_{w_2} = \frac{n_1}{n_2}\rho_{w_1} - \frac{n_1}{n_2}\frac{v_1}{U}\rho_{w_1} \tag{H.2.23}$$

$$\sigma_2 = -U(1-n_1)\rho_p v_1 + (1-n_1)\rho_p v_1^2 + \sigma_1 + (1-n_1)p_1 - (1-n_2)p_2 \tag{H.2.24}$$

$$p_2 = -U\frac{n_1}{n_2}\rho_{w_1} v_1 + \frac{n_1}{n_2}\rho_{w_1} v_1^2 + p_1\frac{n_1}{n_2} \tag{H.2.25}$$

$$U = \frac{1}{2}v_1 \pm \frac{1}{2}\left(v_1^2 + \frac{4}{n_1\rho_{w_1}}\left(-\rho_1(1-n_1) + \frac{1}{\beta}\right)\right)^{1/2} \tag{H.2.26}$$

The variables behind the discontinuity are now known in terms of the variables ahead of the discontinuity and also the speed of the discontinuity is known in terms of the variables in front of the discontinuity.

We observe that we generate n_2 and σ_2. If we take for instance ρ_{w_1}, ρ_1, σ_1, n_1 as constant and we vary the impact velocity v_1, we obtain a relation between σ_2 and n_2 behind the discontinuity. This is a constitutive relation for that case which is required in order to derive equal phase velocities after the discontinuity. Hence we derive a solution for the impact problem with the given assumptions. The solution consists of two uniform regions, both with equal phase velocities and a narrow region in which the variables change rapidly. This region propagates with speed U in a direction opposite v_1.

The generated constitutive relation of the grain structure may have unacceptable features with respect to the prototype. We will explore the character of the constitutive relation in the next section for the case that the fluid has a high compression modulus.

H. 3. Example

We recall from (H.2.22) to (H.2.26):

$$n_2 = n_1 + (1-n_1)\,\frac{v_1}{U} \tag{H.3.1}$$

$$\rho_{w_2} = \frac{n_1}{n_2}\,\rho_{w_1} - \frac{n_1}{n_2}\,\frac{v_1}{U}\,\rho_{w_1} \tag{H.3.2}$$

$$\sigma_2 = -U\,(1-n_1)\,\rho_p\,v_1 + (1-n_1)\,\rho_p\,v_1^2$$

$$+\sigma_1 + (1-n_1)\,p_1 - (1-n_2)\,p_2 \tag{H.3.3}$$

$$p_2 = -U\,\frac{n_1}{n_2}\,\rho_{w_1}\,v_1 + \frac{n_1}{n_2}\,\rho_{w_1}\,v_1^2 + p_1\,\frac{n_1}{n_2} \tag{H.3.34}$$

$$U = \frac{1}{2}\,v_1 \pm \frac{1}{2}\left(v_1^2 + \frac{4}{n_1\,\rho_{w_1}}\left(-p_1\,(1-n_1) + \frac{1}{\beta}\right)\right)^{1/2} \tag{H.3.5}$$

We assume:

$$|U| \gg v_1 \tag{H.3.6}$$

Then (H.3.1) to (H.3.5) become:

$$n_2 \approx n_1 \tag{H.3.7}$$

$$\rho_{w_2} \approx \rho_{w_1} \tag{H.3.8}$$

$$p_2 \approx p_1 - U\, \rho_{w_1}\, v_1 \tag{H.3.9}$$

$$\Delta\sigma \approx -U\, (1-n_1)\, v_1\, (\rho_p - \rho_{w_1}) \tag{H.3.10}$$

We note that in this case the porosity change and the density change of the fluid are small.

We now consider a material with a porosity of 0.25 and a mass density of its grains of $2.5 * 10^3$ kg/m^3. The pores are filled with a fluid with a mass density of 10^3 kg/m^3, an ambient pore pressure of 1 atm and a compressibility twice that of water. The impact velocity is 0.1 m/sec.

So:

$$v_1 = 0.1 \text{ m/sec} \tag{H.3.11}$$

$$n_1 = 0.25 \tag{H.3.12}$$

$$\rho_{w_1} = 10^3 \text{ kg/m}^3 \tag{H.3.13}$$

$$\rho_p = 2.5\ 10^3\ \text{kg/m}^3 \tag{H.3.14}$$

$$p_1 = 10^5\ \text{kg/m sec}^2 = 1\ \text{atm} \tag{H.3.15}$$

$$\frac{1}{\beta} = 10^9\ \text{kg/m sec}^2 \tag{H.3.16}$$

From (H.3.11) to (H.3.6) and (H.3.5) follows:

$$U \approx \pm \frac{1}{2}\left(\frac{4}{0.25\ 10^3}\quad 10^9\right)^{1/2}$$

$$= \pm\ 2000\ \text{m/sec} \tag{H.3.17}$$

From (H.3.17) and (H.3.11) we conclude that the condition (H.3.6) is satisfied and the variables after the discontinuity can be calculated with (H.3.7) to (H.3.10).

We consider the discontinuity propagating in the opposite direction to v_1, hence we take the minus sign in (H.3.17).

So the variables after the discontinuity become:

$$n_2 \approx 0.25 \tag{H.3.11}$$

$$\rho_{w_2} \approx 10^3 \text{ kg/m}^3 \tag{H.3.12}$$

$$p_2 \approx 10^5 + 2\ 10^3\ 10^3\ 0.1 = 3.10^5 \frac{\text{kg}}{\text{m sec}^2}$$
$$= 3 \text{ atm} \tag{H.3.13}$$

$$\Delta\sigma_2 \approx 2\ 10^3\ 0.75\ 0.1\ (2.5\ 10^3 - 10^3)$$
$$= 2.25\ 10^5 \frac{\text{kg}}{\text{m sec}^2} = 2.25 \text{ atm} \tag{H.3.14}$$

Hence the porosity and the density of the water stay almost the same, while the pore pressure jumps 2 atm and the effective pressure jumps 2.25 atm.

Now we make the connection with the linear theory: we define the compression modulus of the grain structure in the same way as in the linearized theory as: (B25)

$$K_p = \frac{n-1}{\frac{\Delta n}{\Delta\sigma}} \tag{H.3.15}$$

From (H.3.1), (H.3.7) and (H.3.10) it follows that for $|U| >> |v_1|$.

$$n-1 \approx n_1-1 \tag{H.3.16}$$

$$\Delta n \approx (1-n_1)\ \frac{v_1}{U} \tag{H.3.17}$$

$$\Delta\sigma \approx -U\ (1-n_1)\ v_1\ (\rho_p-\rho_{w_1}) \tag{H.3.18}$$

Substitution of (H.3.16) to (H.3.18) into (H.3.15) gives:

$$K_p = (n_1-1)\ \frac{-U^2\ (1-n_1)\ v_1\ (\rho_p-\rho_{w_1})}{(1-n_1)\ v_1}$$

$$= (1-n_1)\ U^2\ (\rho_p-\rho_{w_1}) \tag{H.3.19}$$

In (H.3.17) we calculated U as:

$$U = \pm\left(\frac{\frac{1}{\beta}}{n_1\ \rho_{w_1}}\right)^{1/2}$$

$$= \pm\left(\frac{K_w}{n_1\ \rho_{w_1}}\right)^{1/2} \tag{H.3.20}$$

where K_w is defined in the same way as in (B21). So from (H.3.19) and (H.3.20) we conclude:

$$K_p = (1-n_1)\ \frac{K_w}{n_1\ \rho_{w_1}}\ (\rho_p-\rho_{w_1}) \tag{H.3.21}$$

Inspection of (H.1.18) and (H.3.21) shows that the condition for equal phase velocities after the discontinuity is the same in the linear theory and in the given example for the non-linear theory. The result actually suggests that if $|U|>>|v_1|$ the linear theory applies.

Further inspection gives:

For $|U|>>|v_1|$ the non-linear theory generates:

$$\frac{\Delta\sigma}{\Delta p} = \frac{(1-n_1)\ (\rho_p-\rho_{w_1})}{\rho_{w_1}} = \frac{K_p}{K_w/n_1} \tag{H.3.22}$$

$$\begin{aligned}\Delta\sigma_t &= \Delta\sigma + \Delta p = \\ &= -U\ (1-n_1)\ v_1\ \rho_p - U\ n_1\ v_1\ \rho_{w_1} \\ &= -U\ v_1\ \{(1-n_1)\ \rho_p + n_1\rho_{w_1}\}\end{aligned} \tag{H.3.23}$$

$$\begin{aligned}U &= \pm \left(\frac{K_w/n_1}{\rho_{w_1}}\right)^{1/2} \\ &= \pm \left(\frac{K_w/n_1 + K_p}{(1-n_1)\rho_p + n_1\ \rho_{w_1}}\right)^{1/2}\end{aligned} \tag{H.3.24}$$

From the linear theory of Section H.1 we conclude in the same way as in Chapter E:

$$\frac{\sigma}{p} = \frac{K_p}{K_w/n} \tag{H.3.25}$$

$$\sigma_t = -c\ v \left\{(1-n)\ \rho_p + n\ \rho_w\right\} \tag{H.3.26}$$

$$c = \pm \left(\frac{K_w/n + K_p}{(1-n)\ \rho_p + n\ \rho_w} \right)^{1/2} \tag{H.3.27}$$

By inspection of (H.3.22) to (H.3.27) we conclude that in the non-linear theory for $|U| >> |v_1|$ the same results will be derived as in the linear theory and hence if the speed of the discontinuity is much larger than the impact velocity, we can use the linearized equations (B34) to (B37) directly if K_p is constant in the small range of change of n. This also gives a criterion for neglecting "$w_0 = v_0$ terms" in the derivation of the field equations in Chapter B in this case. Hence if condition (H.1.18) is satisfied and the linear theory is applicable then only one discontinuity propagates from the boundary if a step in the velocities is applied and the phase velocities are equal at the boundaries. In the uniform region in front of and behind the discontinuity the phase velocities are equal and the stress ratio of the effective stress to the pore pressure is given by (H.1.19). So if the pore pressure increases the effective stress increase is of the same order (if we take the mass densities of quartz and water).

I. Comment on Discontinuities with Different Phase-Velocities for Non-Linear Field Equations.

When we include equation (B7) as a constitutive relation for the grain structure, we can study the propagation of discontinuities in a medium with field equations (B1) to (B7) in the same way as in Section H-2. The algebra expands rapidly because we have to include an additional equation and an additional variable after the discontinuity (either w_2 or v_2).

If we put (B7) in the form: $\sigma_2 = \sigma_1 - c\,\sigma_1\,(n_2 - n_1)$, where c is a constant, and make the assumptions: $\frac{v_1}{U}$, $\frac{w_1}{U}$, $\frac{w_2}{U}$ and $\frac{v_2}{U} \ll 1$ we retrieve the propagation of discontinuities in the linearized system (B34) to (B37) which is treated on Chapter G.

In fact this gives us a criterion for neglecting the non-linear convective terms in the non-linear balance equations.

So in general the velocities of the phases behind a discontinuity will be different. In the region behind the discontinuity momentum exchange and damping takes place. As we have seen in the linear case the region of substantial velocity differences might be quite small.

J. Dynamics of Porous Media, Multi-Dimensional

So far we have discussed the wave propagation through saturated porous media for the one-dimensional case. In this chapter we will extend the theory for the multi-dimensional case. The field equations (B34) to (B37) for the one-dimensional case will be the basis for the extension into more dimensions. An additional feature with respect to one-dimensional compression is the propagation of shear waves, which is treated in more detail in Appendix III.

For many problems in soil mechanics the plane strain case is appropriate (e.g. long dams). Therefore we will establish the field equations for the plane strain case. We will derive the solution for harmonic excitation and give a system theoretical formulation. This is a summary of work done by van der Kogel [38].

J.1 Interpretation of Field Equations (B36) to (B37)

The one-dimensional field equations (B36) and (B37) are:

$$\frac{\partial w}{\partial x} + \frac{1-n}{n} \frac{\partial v}{\partial x} = - \frac{1}{K_w} \frac{\partial p}{\partial t} \tag{J.1.1}$$

$$\frac{\partial v}{\partial x} = - \frac{1}{K_p} \frac{\partial \sigma}{\partial t} \tag{J.1.2}$$

Equation (J.1.1) is the so called "storage" equation. Equation (J.1.1) states that that the outflow of fluid and the outflow of skeleton material in a unit cube of a two-phase medium are balanced by a drop in fluid pressure.

Equation (J.1.2) represents "Hooke's law" for the grain structure differentiated with respect to t.

We will use the same concept in order to derive the storage equation in more dimensions and a set of equations equivalent to (J.1.2) for a porous linearly elastic isotropic skeleton in more dimensions.

J.2 The Storage Equation and the Continuity Equations for Multiple Dimensions

The storage equation in more dimensions is similar to the one-dimension equation:

$$\nabla \underset{\sim}{w} + \frac{1-n}{n} \nabla \underset{\sim}{v} = -\frac{1}{K_w} \frac{\partial p}{\partial t} \qquad \text{(J.2.1)}$$

where: $\underset{\sim}{w} = (w_x, w_y, w_z)$ and $\underset{\sim}{v} = (v_x, v_y, v_z)$ are the velocity components of fluid and solid materials respectively.

For a linear elastic isotropic homogeneous medium we derive after differentiating with respect to t:

$$\frac{\partial v_x}{\partial x} = -\frac{1}{E}\left\{\frac{\partial \sigma_x}{\partial t} - \nu\left(\frac{\partial \sigma_y}{\partial t} + \frac{\partial \sigma_z}{\partial t}\right)\right\} \qquad \text{(J.2.2)}$$

$$\frac{\partial v_y}{\partial y} = -\frac{1}{E}\left\{\frac{\partial \sigma_y}{\partial t} - \nu\left(\frac{\partial \sigma_x}{\partial t} + \frac{\partial \sigma_z}{\partial t}\right)\right\} \qquad \text{(J.2.3)}$$

$$\frac{\partial v_z}{\partial z} = -\frac{1}{E}\left\{\frac{\partial \sigma_z}{\partial t} - \nu\left(\frac{\partial \sigma_x}{\partial t} + \frac{\partial \sigma_y}{\partial t}\right)\right\} \qquad \text{(J.2.4)}$$

$$\frac{1}{2}\left(\frac{\partial v_x}{\partial y} + \frac{\partial v_y}{\partial x}\right) = \frac{1+\nu}{E} \frac{\partial \tau_{xy}}{\partial t} \qquad \text{(J.2.5)}$$

$$\frac{1}{2}\left(\frac{\partial v_x}{\partial z}+\frac{\partial v_z}{\partial x}\right)=\frac{1+\nu}{E}\frac{\partial \tau_{xz}}{\partial t} \qquad \text{(J.2.6)}$$

$$\frac{1}{2}\left(\frac{\partial v_y}{\partial z}+\frac{\partial v_z}{\partial y}\right)=\frac{1+\nu}{E}\frac{\partial \tau_{yz}}{\partial t} \qquad \text{(J.2.7)}$$

where E is the elasticity modulus and ν is the Poisson's ratio of the grain structure, σ_x, σ_y and σ_z are the normal stresses and τ_{xy}, τ_{xz}, and τ_{yz} the shear stresses; σ_x, σ_y and σ_z are assumed to be positive if they represent a positive pressure.

We added nine new variables (σ_y, σ_z, τ_{xy}, τ_{xz}, τ_{yz}, w_y, w_z, v_y, v_z) and five additional equations with respect to the one-dimensional case. By adding two momentum equations for the fluid and two momentum equations for the grain structure (y and z direction), the number of equations equals the number of variables (σ_x, σ_y, σ_z, τ_{xy}, τ_{xz}, τ_{yz}, p, v_x, v_y, v_z, w_x, w_y, w_z).

J.3 Derivation of the Field Equations for the Plane Strain Case

For the plane strain we have:

$$\frac{\partial v_z}{\partial x} = \frac{\partial v_z}{\partial y} = \frac{\partial v_z}{\partial z} = 0 \qquad \text{(J.3.1)}$$

$$\frac{\partial v_x}{\partial z} = 0 \qquad \text{(J.3.2)}$$

$$\frac{\partial v_y}{\partial z} = 0 \qquad \text{(J.3.3)}$$

For the plane strain case (J.2.2) to (J.2.7) reduce to:

$$\frac{\partial v_x}{\partial x} = -\frac{1-\nu^2}{E}\frac{\partial \sigma_x}{\partial t} + \frac{\nu+\nu^2}{E}\frac{\partial \sigma_y}{\partial t} \qquad \text{(J.3.4)}$$

$$\frac{\partial v_y}{\partial y} = -\frac{1-\nu^2}{E}\frac{\partial \sigma_y}{\partial t} + \frac{\nu+\nu^2}{E}\frac{\partial \sigma_x}{\partial t} \qquad \text{(J.3.5)}$$

$$\frac{\partial v_x}{\partial y} + \frac{\partial v_y}{\partial x} = \frac{2(1+\nu)}{E}\frac{\partial \tau_{xy}}{\partial t} \qquad \text{(J.3.6)}$$

and further:

$$\tau_{xz} = 0 \qquad \text{(J.3.7)}$$

$$\tau_{yz} = 0 \qquad \text{(J.3.8)}$$

$$\sigma_z = \nu\,(\sigma_x + \sigma_y) \qquad \text{(J.3.9)}$$

Because we restrict ourselves to the plane strain case, it is appropriate to choose the boundary conditions such that:

$$w_z = 0 \tag{J.3.10}$$

From (J.3.1), (J.2.1) and J.3.10) it follows that the storage equation has the following form:

$$\frac{\partial w_x}{\partial x} + \frac{\partial w_y}{\partial y} + \frac{1-n}{n} \frac{\partial v_x}{\partial x} + \frac{1-n}{n} \frac{\partial v_y}{\partial y} = - \frac{1}{K_w} \frac{\partial p}{\partial t} \tag{J.3.11}$$

The momentum equations have a similar form as for the one-dimensional case, however we add an additional gradient in the shear stress in the appropriate direction for the skeleton. Hence, we assume that shear stresses are transmitted by the grain structure.

So the momentum equations for the fluid become:

$$n \rho_w \frac{\partial w_x}{\partial t} = - n \frac{\partial p}{\partial x} - \frac{n^2}{k} (w_x - v_x) \tag{J.3.12}$$

$$n \rho_w \frac{\partial w_y}{\partial t} = - n \frac{\partial p}{\partial y} - \frac{n^2}{k} (w_y - v_y) \tag{J.3.13}$$

and the momentum equations for the grain structure become:

$$(1-n)\ \rho_p\ \frac{\partial v_x}{\partial t} = -\frac{\partial \sigma_x}{\partial x} - (1-n)\ \frac{\partial p}{\partial x} + \frac{n^2}{k}\ (w_x - v_x) + \frac{\partial \tau_{yx}}{\partial y} \qquad \text{(J.3.14)}$$

$$(1-n)\ \rho_p\ \frac{\partial v_y}{\partial t} = -\frac{\partial \sigma_y}{\partial y} - (1-n)\ \frac{\partial p}{\partial y} + \frac{n^2}{k}\ (w_y - v_y) + \frac{\partial \tau_{xy}}{\partial x} \qquad \text{(J.3.15)}$$

From (J.3.4) to (J.3.6), (J.2.11) to (J.3.15) follows that the field equations for the plane strain case are given by the following set of equations:

$$\frac{\partial v_x}{\partial x} = -\frac{1-\nu^2}{E}\ \frac{\partial \sigma_x}{\partial t} + \frac{\nu+\nu^2}{E}\ \frac{\partial \sigma_y}{\partial t} \qquad \text{(J.3.16)}$$

$$\frac{\partial v_y}{\partial y} = -\frac{1-\nu^2}{E}\ \frac{\partial \sigma_y}{\partial t} + \frac{\nu+\nu^2}{E}\ \frac{\partial \sigma_x}{\partial t} \qquad \text{(J.3.17)}$$

$$\frac{\partial v_x}{\partial y} + \frac{\partial v_y}{\partial x} = \frac{2(1+\nu)}{E}\ \frac{\partial \tau_{xy}}{\partial t} \qquad \text{(J.3.18)}$$

$$\frac{\partial w_x}{\partial x} + \frac{\partial w_y}{\partial y} + \frac{1-n}{n}\ \frac{\partial v_x}{\partial x} + \frac{1-n}{n}\ \frac{\partial v_y}{\partial y} = -\frac{1}{K_w}\ \frac{\partial p}{\partial t} \qquad \text{(J.3.19)}$$

$$n\ \rho_w\ \frac{\partial w_x}{\partial t} = -n\ \frac{\partial p}{\partial x} - \frac{n^2}{k}\ (w_x - v_x) \qquad \text{(J.3.20)}$$

$$n\ \rho_w\ \frac{\partial w_y}{\partial t} = -n\ \frac{\partial p}{\partial y} - \frac{n^2}{k}\ (w_y - v_y) \qquad \text{(J.3.21)}$$

$$(1-n)\ \rho_p \frac{\partial v_x}{\partial t} = -\frac{\partial \sigma_x}{\partial x} - (1-n)\ \frac{\partial p}{\partial x} + \frac{n^2}{k}\ (w_x - v_x) + \frac{\partial \tau_{yx}}{\partial y} \qquad \text{(J.3.22)}$$

$$(1-n)\ \rho_p \frac{\partial v_y}{\partial t} = -\frac{\partial \sigma_y}{\partial y} - (1-n)\ \frac{\partial p}{\partial y} + \frac{n^2}{k}\ (w_y - v_y) + \frac{\partial \tau_{xy}}{\partial x} \qquad \text{(J.3.23)}$$

(J.3.16) to (J.3.23) form eight equations with eight unknowns (w_x, w_y, v_x, v_y, σ_x, σ_y, $\tau_{xy} = \tau_{yx}$, p).

J.4 Solution of the Field Equations (J.3.16) to (J.3.23), Harmonic Response.

We will construct the solution of (J.3.16) to (J.3.23) in the same way as in the one dimensional case:

Assume:

$$v_x(x,y,t) = V_x^0 e^{i(\omega^* x + \omega y + \bar{\omega}t)} = V_x(x,y) e^{i\bar{\omega}t} \quad \text{(J.4.1)}$$

$$v_y(x,y,t) = V_y^0 e^{i(\omega^* x + \omega y + \bar{\omega}t)} = V_y(x,y) e^{i\bar{\omega}t} \quad \text{(J.4.2)}$$

$$w_x(x,y,t) = W_x^0 e^{i(\omega^* x + \omega y + \bar{\omega}t)} = W_x(x,y) e^{i\bar{\omega}t} \quad \text{(J.4.3)}$$

$$w_y(x,y,t) = W_y^0 e^{i(\omega^* x + \omega y + \bar{\omega}t)} = W_y(x,y) e^{i\bar{\omega}t} \quad \text{(J.4.5)}$$

$$p(x,y,t) = P^0 e^{i(\omega^* x + \omega y + \bar{\omega}t)} = P(x,y) e^{i\bar{\omega}t} \quad \text{(J.4.6)}$$

$$\sigma_x(x,y,t) = \sigma_x^0 e^{i(\omega^* x + \omega y + \bar{\omega}t)} = \sigma_x(x,y) e^{i\bar{\omega}t} \quad \text{(J.4.7)}$$

$$\sigma_y(x,y,t) = \sigma_y^0 e^{i(\omega^* x + \omega y + \bar{\omega}t)} = \sigma_y(x,y) e^{i\bar{\omega}t} \quad \text{(J.4.8)}$$

$$\tau_{xy}(x,y,\tau) = \tau_{yx}(x,y,\tau) = \tau^0 e^{i(\omega^* x + \omega y + \bar{\omega}t)} = \tau(x,y) e^{i\bar{\omega}t} \quad \text{(J.4.9)}$$

Substitution of (J.4.1) to (J.4.9) into the field equations (J.3.16) to (J.3.23) gives:

$$i\omega^* V_x^0 = -\frac{1-\nu^2}{E} i\bar{\omega} \sigma_x^0 + \frac{\nu+\nu^2}{E} i\bar{\omega} \sigma_y^0 \qquad (J.4.10)$$

$$i\omega V_y^0 = -\frac{1-\nu^2}{E} i\bar{\omega} \sigma_y^0 + \frac{\nu+\nu^2}{E} i\bar{\omega} \sigma_x^0 \qquad (J.4.11)$$

$$i\omega V_x^0 + i\omega^* V_y^0 = \frac{2(1+\nu)}{E} i\bar{\omega} \tau^0 \qquad (J.4.12)$$

$$i\omega^* W_x^0 + i\omega W_y^0 + \frac{1-n}{n} V_x^0 i\omega^* + \frac{1-n}{n} V_y^0 i\omega = -\frac{1}{K_w} i\bar{\omega} P^0 \qquad (J.4.13)$$

$$n \rho_w i\bar{\omega} W_x^0 = -n i\omega^* P^0 - \frac{n^2}{k} (W_x^0 - V_x^0) \qquad (J.4.14)$$

$$n \rho_w i\bar{\omega} W_y^0 = -n i\omega P^0 - \frac{n^2}{k} (W_y^0 - V_y^0) \qquad (J.4.15)$$

$$(1-n) \rho_p i\bar{\omega} V_x^0 = -i\omega^* \sigma_x^0 - (1-n) i\omega^* P^0 + \frac{n^2}{k} (W_x^0 - V_x^0) + i\omega \tau^0 \qquad (J.4.16)$$

$$(1-n) \rho_p i\bar{\omega} V_y^0 = -i\omega \sigma_y^0 - (1-n) i\omega P^0 + \frac{n^2}{k} (W_y^0 - V_y^0) + i\omega^* \tau^0 \qquad (J.4.17)$$

In order to solve (J.4.10) to (J.4.17) we require:

$$
\begin{vmatrix}
\frac{1-\nu^2}{E}\,i\bar{\omega} & -\frac{\nu+\nu^2}{E}\,i\bar{\omega} & 0 & 0 & 0 & 0 & i\omega^* & 0 \\
-\frac{\nu+\nu^2}{E}\,i\bar{\omega} & \frac{1-\nu^2}{E}\,i\bar{\omega} & 0 & 0 & 0 & 0 & 0 & i\omega \\
0 & 0 & \frac{2(1+\nu)}{E}\,i\bar{\omega} & 0 & 0 & 0 & -i\omega & -i\omega^* \\
0 & 0 & 0 & n\,\frac{i\bar{\omega}}{K_w} & ni\omega^* & ni\omega & (1-n)\,i\omega^* & (1-n)\,i\omega \\
0 & 0 & 0 & ni\omega^* & \frac{n^2}{k}+n\rho_w i\bar{\omega} & 0 & -\frac{n^2}{k} & 0 \\
0 & 0 & 0 & n\,i\omega & 0 & \frac{n^2}{k}+n\rho_w\,i\bar{\omega} & 0 & -\frac{n^2}{k} \\
i\omega^* & 0 & -i\omega & (1-n)\,i\omega^* & -\frac{n^2}{k} & 0 & (1-n)\rho_p\,i\bar{\omega}+\frac{n^2}{k} & 0 \\
0 & i\omega & -i\omega^* & (1-n)\,i\omega & 0 & -\frac{n^2}{k} & 0 & (1-n)\rho_p\,i\bar{\omega}+\frac{n^2}{k}
\end{vmatrix} = 0
$$

We note the symmetry of the determinant (J.4.18). This is also the case for the determinant (C18) in the one-dimensional case.

Evaluation of the determinant (J.4.18) gives:

$$A\,\omega^6 + B\,\omega^4 + C\,\omega^2 + D = 0 \qquad \text{(J 4.19)}$$

where A,B,C and D are functions of $\bar{\omega}$ and ω^*.

The solution of (F.4.19) is:

$$\omega = \begin{matrix} \pm\,\alpha \\ \pm\,\beta \\ \pm\,\gamma \end{matrix} \qquad \text{(J.4.20)}$$

Inspection of the determinant (J.4.18) shows that ω^* only exists in the following powers: ω^{*2}, ω^{*4} and ω^{*6}. So if α, β, γ are roots of (J.4.19) for $\omega^* = \omega_1$, then α, β and γ are also roots of (F.4.19) for $\omega^* = -\omega_1$.

We consider now a solution in the following form:

$$
\begin{aligned}
W_y(x,y) = {} & W_{y1}^{0}\, e^{i\alpha y}\, e^{i\omega_1 x} + W_{y2}^{0}\, e^{i\beta y}\, e^{i\omega_1 x} + W_{y3}^{0}\, e^{i\gamma y}\, e^{i\omega_1 x} \\
& + W_{y4}^{0}\, e^{-i\alpha y}\, e^{i\omega_1 x} + W_{y5}^{0}\, e^{-i\beta y}\, e^{i\omega_1 x} + W_{y6}^{0}\, e^{-i\gamma y}\, e^{i\omega_1 x} \\
& + W_{y7}^{0}\, e^{i\alpha y}\, e^{-i\omega_1 x} + W_{y8}^{0}\, e^{+i\beta y}\, e^{-i\omega_1 x} + W_{y3}^{0}\, e^{i\gamma y}\, e^{-i\omega_1 x} \\
& + W_{y10}^{0}\, e^{-i\alpha y}\, e^{-i\omega_1 x} + W_{y11}^{0}\, e^{-i\beta x}\, e^{-i\omega_1 x} + W_{y12}^{0}\, e^{-i\gamma y}\, e^{-i\omega_1 x}
\end{aligned}
\qquad \text{(J.4.21)}
$$

where W_{y1}^{0}, ..., W_{y12}^{0} are constants. In the same way we define the other variables.

Due to the linearity of the field equations (F.3.16) to (F.3.23), $W_y(x,y)\, e^{i\bar{\omega}t}$, etc, is a solution of the field equation.

Now for every choice of $\bar{\omega}$ and ω^* with an ω generated by (F.4.19), the system (F.4.10) to (F.4.17) gives the relation between V_y^0, V_x^0, W_x^0, W_y^0, P^0, σ_x^0, σ_y^0 and τ^0. Hence we can write the total solution with the constants W_{y1}^{0}, ..., W_{y12}^{0} (twelve).

Once the solution has been cast in this form we can construct the transmission matrices in the same way as for the one-dimensional case:

e.g:

$$W_y(x,0) = \left\{ W_{y1}^{\ 0} + W_{y2}^{\ 0} + W_{y3}^{\ 0} + W_{y4}^{\ 0} + W_{y5}^{\ 0} + W_{y6}^{\ 0} \right\} e^{i\omega_1 x}$$

$$+ \left\{ W_{y7}^{\ 0} + W_{y8}^{\ 0} + W_{y9}^{\ 0} + W_{y10}^{\ 0} + W_{y11}^{\ 0} + W_{y12}^{\ 0} \right\} e^{-i\omega_1 x} \qquad \text{(J.4.22)}$$

etc.

Now we assume:

$$W_y(x,0) = C_{+w_y}(y=0)\, e^{i\omega_1 x} + C_{-w_y}(y=0)\, e^{-i\omega_1 x} \qquad \text{(J.4.23)}$$

where $W_y(x,0)$ and the other amplitudes of the variables at y=0 are periodic functions of x with frequency ω_1. C_+ and C_- are the Fourier coefficients:

$$C_{+\,w_y}(y=0) = \frac{1}{T} \int_0^T W_y(x,0)\, e^{-i\omega_1 x}\, dx \qquad \text{(J.4.24)}$$

$$C_{-\,w_y}(y=0) = \frac{1}{T} \int_0^T W_y(x,0)\, e^{i\omega_1 x}\, dx \qquad \text{(J.4.25)}$$

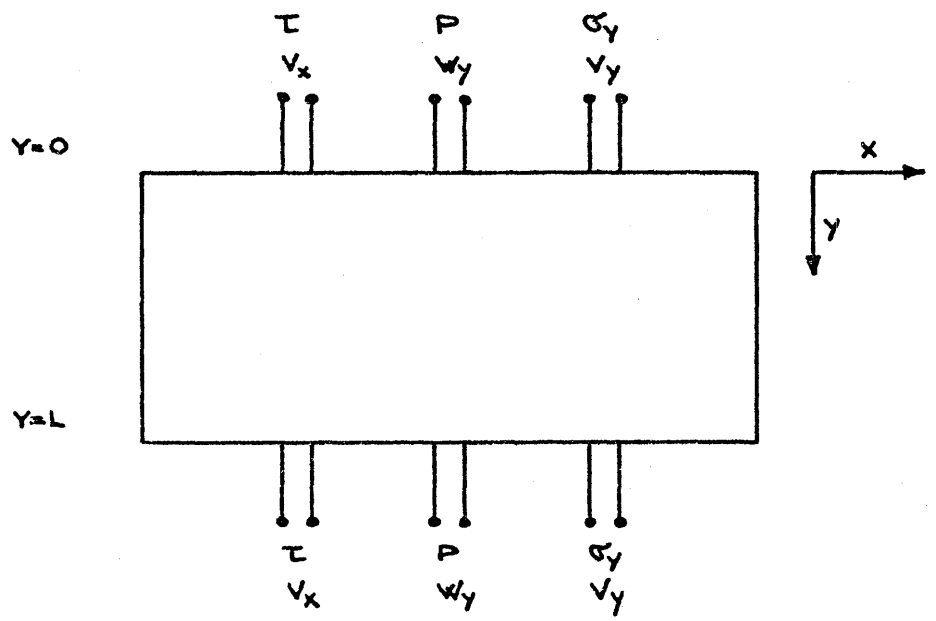

FINITE SYSTEM

FIG. 5

where:

$$\omega_1 = \frac{2\pi}{T} \tag{J.4.26}$$

We can follow a similar procedure at y=L.

Hence we can express the constants W_{y1}^{0} to W_{y6}^{0} in terms of the Fourier coefficients C_+ of six variables at y=0 or at y=L and also we can express the constants W_{y7}^{0} to W_{y12}^{0} in terms of the Fourier coefficients C_- of six variables at y=0 or at y=L. And so we are able to establish two sets of equations which relate the Fourier coefficients at y=L and y=0 (each six). The matrix of this relation can be viewed as the transmission matrix.

In a similar way we can establish the equation for a semi-infinite system (van der Kogel [38]).

Summarizing: for a system of finite length in y and infinite length in x we have to prescribe at the boundaries (y=0 and y=L) a total of six periodic dependent variables. The transmission matrix relates the C_+ or C_- coefficients (six each) of the relevant variables at the boundaries.

This is shown in diagrammatic form in figure (5).

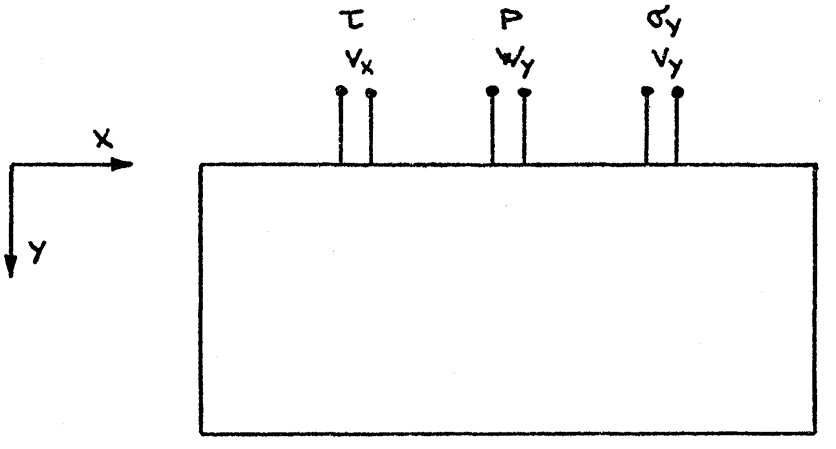

SEMI INFINITE SYSTEM

FIG. 6

For a system of infinite length in y and x we have to prescribe at the boundary (y=0) a total of three dependent variables. The transmission matrix relates the C_+ or C_- coefficients (three each) of the relevant variables at the boundary y=0 (figure (6)).

We can join the systems by the appropriate coupling conditions in order to solve a problem including layers.

K. Jump Conditions Due to Discontinuities in the Parameters

As stated in the former chapters we can join transmission matrices in order to solve a problem with layers. The question arises as to how to join these transmission matrices.

In this chapter we will establish the jump conditions of the dependent variables σ, p, w and v for the one-dimensional case across the interface between two two-phase media (hence with different parameters: n, K_p, K_w, ρ_w, ρ_p, k). The jump conditions are the coupling conditions for the transmission matrices.

Further we will state the jump conditions between a two-phase medium and a fluid medium. These are important because shock loading on soils due to explosions is frequently applied via a fluid (e.g. water or air).

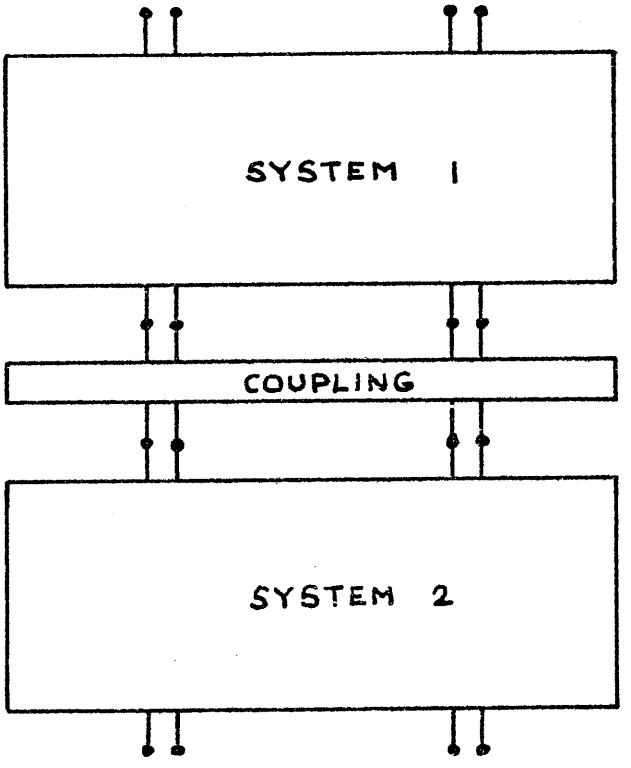

COUPLING OF TWO TWO-PHASE SYSTEMS

FIG. 7

K.1 Jump Conditions at the Interface Between Two Two-Phase Media

The problem of a moving discontinuity has been treated in Chapter G. Following the same procedure and putting U=0 we conclude:

$$[p] = 0 \tag{K.1.1}$$

$$[\sigma] = 0 \tag{K.1.2}$$

$$[n\,w + (1-n)\,v] = 0 \tag{K.1.3}$$

$$[v] = 0 \tag{K.1.4}$$

Diagrammatically the coupling of two finite systems looks like figure (7).

So using the transmission matrices of system 1 and system 2, and the coupling conditions (K.1.1) to (K.1.4) we can solve the equations by applying appropriate boundary conditions (e.g. two at the top and two at the bottom).

We note that (K.1.3) in general gives rise to velocity differences between the phases near the interface.

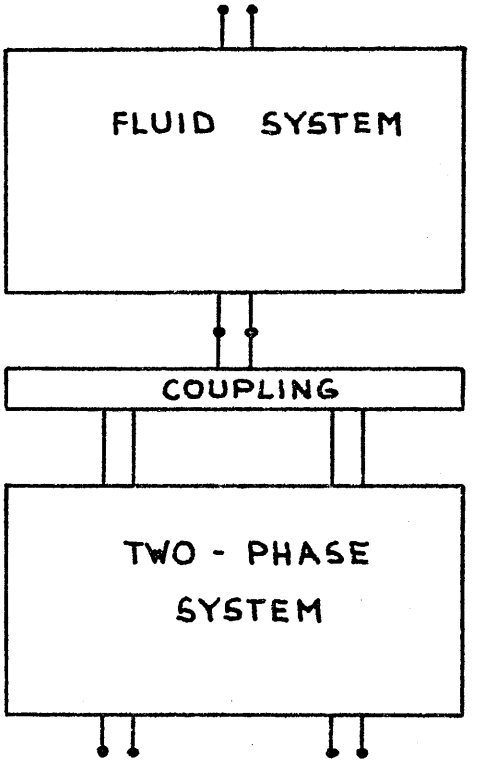

COUPLING OF TWO-PHASE SYSTEM

AND FLUID SYSTEM

FIG. 8

K.2 Jump Conditions at the Interface Between a Two-Phase Medium and a Fluid Medium

Inspection of (K.1.1) and (K.1.4) shows that the first two equations are the "action=reaction" laws and the last two equations are the continuity equations for fluid and grain structure. Because one side of the interface is lacking a grain structure, we delete the continuity equation for the grain structure and put $\sigma_2 = 0$. Hence:

$$p_1 - p_2 = 0 \tag{K.2.1}$$

$$\sigma_1 = 0 \tag{K.2.2}$$

$$n\, w_1 + (1-n)\, v_1 - w_2 = 0 \tag{K.2.3}$$

where the medium 2 is the fluid and the medium 1 is the two-phase medium.

Schematically the coupling of two finite systems looks like figure (8).

Hence by using the transmission matrices of the fluid system (see Appendix I) and the two-phase medium we can solve a problem by applying appropriate boundary conditions (e.g. one at the top and two on the bottom).

We observe that (K.2.3) in general will give rise to velocity differences between the components near the interface and zero effective stress due to (K.2.2).

L. Propagation of Discontinuities Near an Interface Between a Fluid and a Two-Phase Medium

In Chapter G we studied the propagation of discontinuities in a two phase medium in general. In this chapter we study a specific boundary value problem. We focus our interest on an interface between a fluid and a two-phase medium. Both are at rest initially. At $t=t_1$ a discontinuity in the fluid phase with a uniform particle velocity v** behind the discontinuity approaches the interface.

After the discontinuity hits the interface we assume that refraction and reflection take place in the pattern of figure (9). So two discontinuities are propagating into the two-phase medium and one discontinuity is propagating back into the fluid.

We will use coupling conditions along the interface, jump conditions for the discontinuities in the two-phase medium and jump conditions for the discontinuity in the fluid in order to derive the solution.

This is a problem of practical interest. Geophysicists, interested in locating and identifying the sea floor under the oceans by means of sonar want to know how an incoming discontinuity is reflected by a porous medium as a function of the properties of the porous medium. The solution presented gives this function in the framework of the assumed models for the two-phase medium and the fluid.

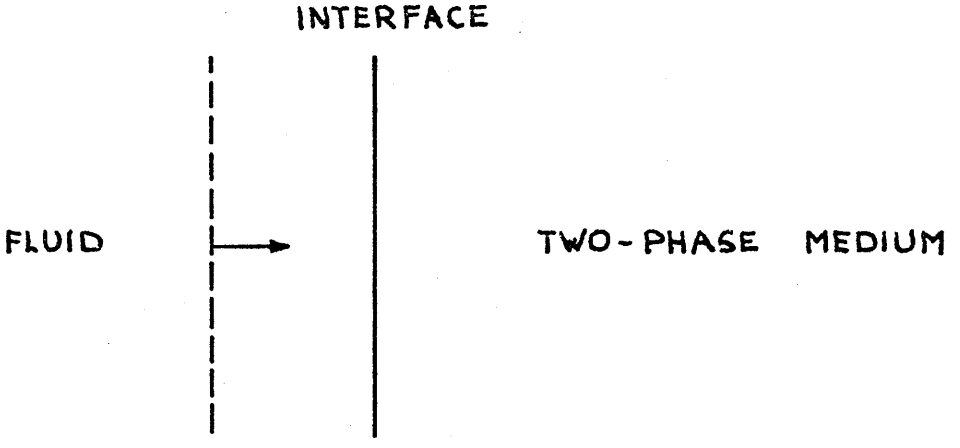

PATTERN BEFORE REFLECTION

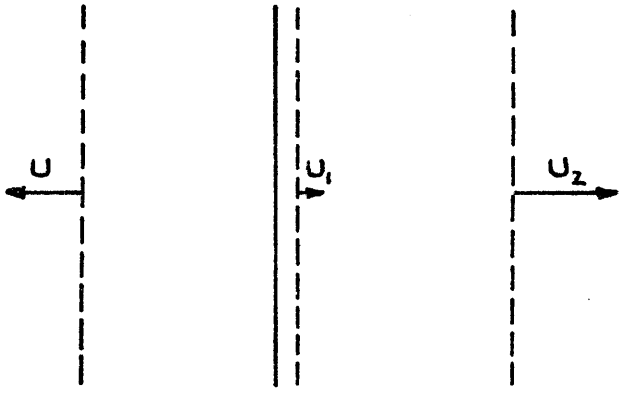

PATTERN AFTER REFLECTION

FIG. 9

Engineers are interested in the initialization of liquefaction by shock loading and the efficiency of compaction due to shock loading. The solution presented gives insight into the distribution of effective stresses and velocity differences among skeleton and fluid near the boundary for this special, but probably frequently encountered, boundary value problem.

Jump Condition for the Fluid

From (I.31) it follows that:

$$p_1 - p_2 = U \rho_w (v_1 - v_2) \tag{L.1}$$

where (I.30):

$$U = \pm \left(\frac{K_w}{\rho_w} \right)^{1/2} \tag{L.2}$$

For the incoming discontinuity we have a situation as in figure (10).

So the pressure behind the incoming discontinuity is:

$$p_2 = U\ \rho_w\ v^{**} \tag{L.3}$$

After reflection the picture looks like figure (11).

So from (L.1) and (L.3) there follows:

$$p_1 = -U\ \rho_w\ v_1 + 2\ U\ \rho_w\ v^{**} \tag{L.4}$$

This is the jump condition for the fluid.

Coupling Condition Along the Interface (figure (12)).

We will use the coupling conditions (K.2.1) to (K.2.3), so:

$$\bar{p}_1 = \bar{p}_2 \tag{L.5}$$

$$\bar{\sigma}_1 = 0 \tag{L.6}$$

$$n\ \bar{w}_1 + (1-n)\ \bar{v}_1 - \bar{w}_2 = 0 \tag{L.7}$$

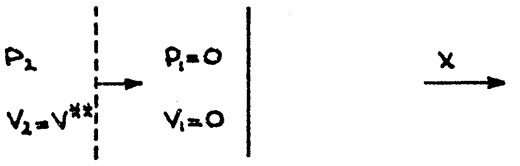

FIG. 10

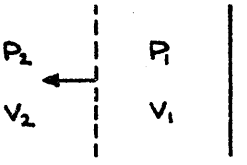

FIG. 11

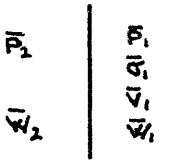

FIG. 12

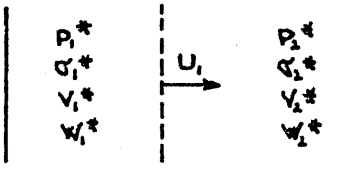

FIG. 13

Jump Condition in the Two-phase medium in the case of the Lower Speed U_1 (figure (13)).

We use the jump conditions (G.2.17) to (G.2.19) and hence:

$$\sigma_1^* = \sigma_2^* - \frac{K_p}{U} v_2^* + \frac{K_p}{U} v_1^* \tag{L.8}$$

$$p_1^* = - U_1 \rho_w w_2^* + U_1 \rho_w w_1^* + p_2^* \tag{L.9}$$

$$w_1^* = w_2^* + \frac{(1-n) K_w}{(K_w - U_1^2 \rho_w) n} v_2^* - \frac{(1-n) K_w}{(K_w - U_1^2 \rho_w) n} v_1^* \tag{L.10}$$

Jump Condition in the Two-Phase Medium in the Case of the Higher Speed U_2 (figure (14)).

Again we use (G.2.17) to (G.2.19) and hence:

$$\hat{\sigma}_2 = \frac{K_p}{U_2} \hat{v}_2 \tag{L.11}$$

$$\hat{p}_2 = U_2 \rho_w \hat{w}_2 \tag{L.12}$$

$$\hat{w}_2 = - \frac{(1-n) K_w}{\left(K_w - U_2^2 \rho_w\right) n} \hat{v}_2 \tag{L.13}$$

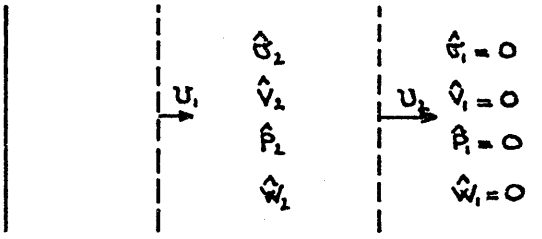
$\hat{\sigma}_2$
$\hat{V}_2$
$\hat{P}_2$
$\hat{W}_2$
U_1
U_2
$\hat{\sigma}_1 = 0$
$\hat{V}_1 = 0$
$\hat{P}_1 = 0$
$\hat{W}_1 = 0$

FIG. 14

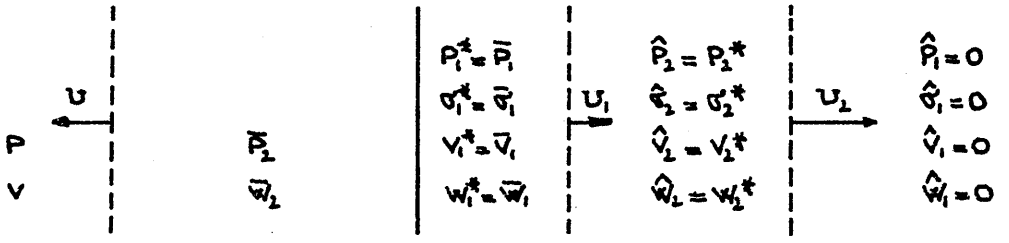
P
V
U
$\bar{P}_2$
$\bar{W}_2$
$P_1^* = \bar{P}_1$
$\sigma_1^* = \bar{\sigma}_1$
$V_1^* = \bar{V}_1$
$W_1^* = \bar{W}_1$
U_1
$\hat{P}_2 = P_2^*$
$\hat{\sigma}_2 = \sigma_2^*$
$\hat{V}_2 = V_2^*$
$\hat{W}_2 = W_2^*$
U_2
$\hat{P}_1 = 0$
$\hat{\sigma}_1 = 0$
$\hat{V}_1 = 0$
$\hat{W}_1 = 0$

FIG. 15

So we have the picture explained in figure (15).

Hence:

$$\bar{p}_1 = p_1^* \; ; \; \bar{\sigma}_1 = \sigma_1^* \; ; \; \bar{v}_1 = v_1^* \; ; \; \bar{w}_1 = w_1^* \tag{L.14}$$

$$p_2^* = \hat{p}_2 \; ; \sigma_2^* = \hat{\sigma}_2 \; ; \; v_2^* = \hat{v}_2 \; ; \; w_2^* = \hat{w}_2 \tag{L.15}$$

Now we substitute (L.4) to (L.7), (L.11) to (L.13) into (L.8) to (L.10) and we use the conditions (L.14) and (L.15). This results in three equations with three unknowns (e.g. $\hat{v}_2$, v_1^*, $\bar{w}_2$). Once $\hat{v}_2$, v_1^* and $\bar{w}_2$ have been determined in terms of the parameters and v^{**}, we can determine all the other variables from (L.4) to (L.15). If we assume $\frac{K_p}{K_w} \ll 1$, we can use the approximate expressions for U_1 and U_2 given by (G.2.22) and (G.2.21) respectively. In that case we obtain the following qualitative picture (figure (16)).

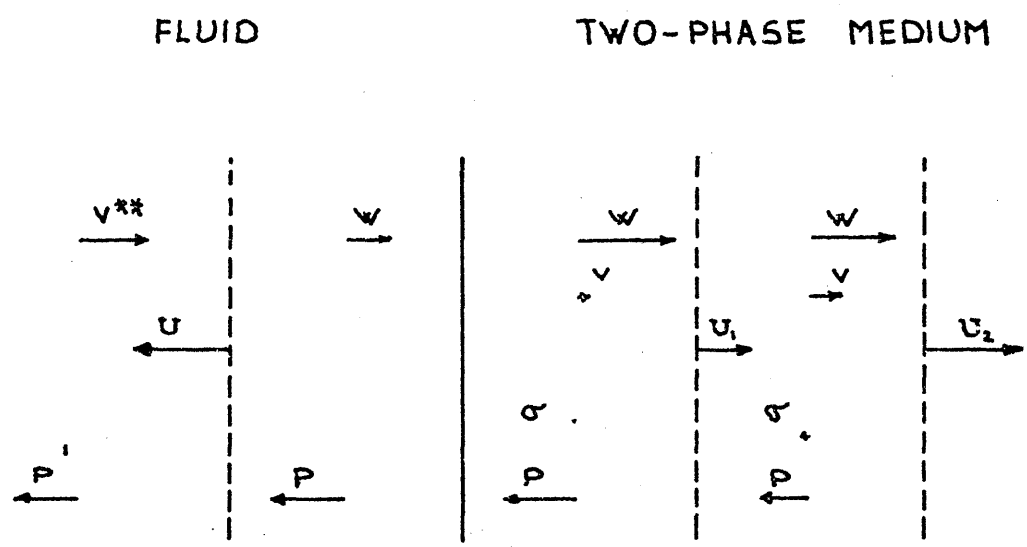

FIG. 16

Hence we conclude that near the interface just after impact, different velocities are being generated in the two-phase medium. The velocity of the grain structure is small and the velocity of fluid is relatively large, and both are in the positive x-direction.

The effective pressure is low and the pore pressure is positive and larger than the original pressure in the fluid. The fact that the effective pressure is small with respect to the pore pressure is important from the point of view of justifying the use of the linearized theory ($K_p \approx$ constant).

If further $w << U_1$, we conclude from chapter J that the non-linearities due to the convective terms are small.

If we use water as a fluid, then the compression modulus K_w is constant until high pressures (Dorsey [44]).

Hence, if $w << U_1$ ($\sim$ 65 m/sec for "practical" values of wet sand) then the use of the linearized theory is justified.

The "fast" discontinuity in the two-phase medium acts merely as a "softening" phenomenon. The differences in velocity and pressure are less than behind the "slow" discontinuity.

Near the interface on the fluid side, just after impact, the pressure is larger and the velocity slower than the original values in the fluid. However, the differences are smaller than in the case of a reflection from a rigid non-porous interface.

M. Constitutive Relations

In the former chapters we used a linearly elastic isotropic model in the linear case as a constitutive equation for the skeleton.

In Chapter B we used the relation $\sigma = \sigma(n)$ for the non-linear case in one dimension. These models will in general not closely describe the behavior of real soils (Scott [34]). Especially the history dependence of the constitutive equations for real soils in the framework of the above formulations forms a barrier for further progress.

We will make an attempt to describe more closely the state and the behavior of a granular material by including additional kinematical variables in a thermodynamic approach to the derivation of the constitutive equation.

We generate a linearized constitutive equation, which will be used for further analysis in the two-phase theory.

M.1 Kinematical Variables

In Chapter B we used the porosity n as a structure variable and we postulated:

$$\sigma = \sigma(n) \tag{M.1.1}$$

For real soils this is not a one to one mapping (Scott [34]).

So the question to be asked is: what variables describe the state of a granular material?

Goodman and Cowin [52] introduced the gradient of the porosity and Mullinger [53] introduced a fabric tensor, representing the distribution of contact points between the grains, as an additional kinematical variable. Both theories contain generalized forces associated with the motion of the additional kinematical variables, which are somewhat hard to explain physically (Jenkins [54]).

Once the state of a granular material is known, one can consider the motion to another state.

Gudehus et al. [55] did work in this area. They defined a state of swept out memory (S.O.M.) and once the material reaches this state the behavior is independent of the initial state.

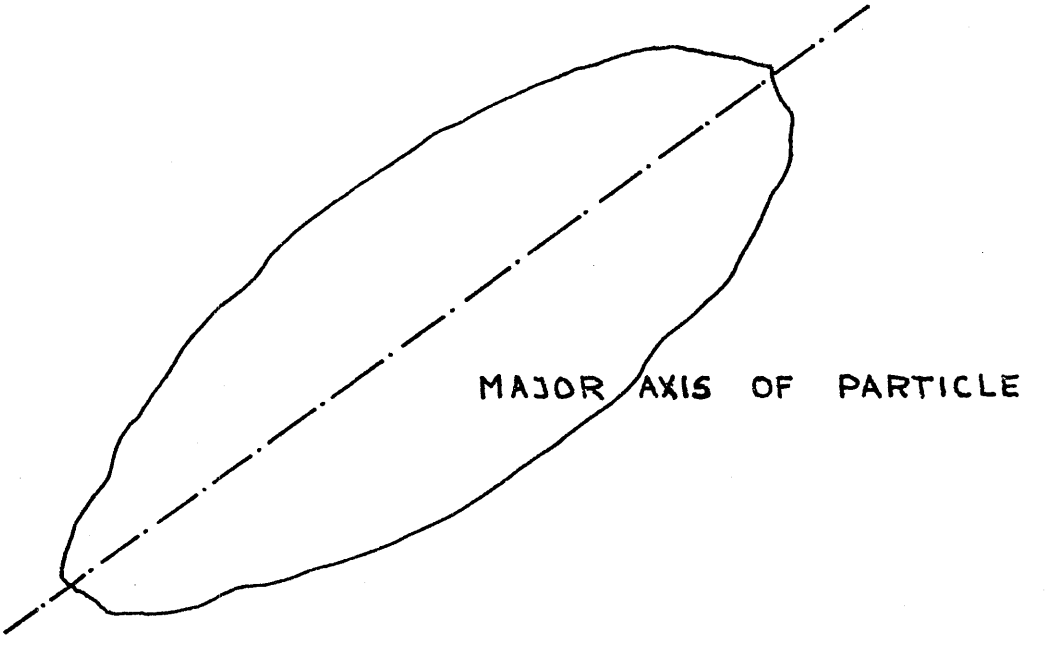

FIG. 17

We will try here to identify the state of a soil in general by introducing additional kinematical variables. For the moment let us restrict ourselves to a two-dimensional case (e.g. a system of rods).

Assume that the state of a granular material is given by the following kinematical variables:

$$n \tag{M.1.1}$$

$$\psi \tag{M.1.2}$$

$$\phi \tag{M.1.3}$$

where n is the porosity ψ and ϕ are scalars.

We choose only two additional kinematical variables in order to generate a simple theory on one hand, and on the other hand hopefully to generate enough information about the grain structure.

Now we have to define the additional kinematical variables in a physical sense.

Oda [56] has shown that the particles in a grain structure orient themselves during stress application. So appropriate choices for the additional kinematical variables seem to be ϕ and ψ, where ϕ is the average angle between the major axis of the particles in an element and the principal stress axes (fig. 17) and ψ is the deviation in an assumed distribution around the average angle ϕ of particles in an element.

An element of particles is defined as that elementary volume by which expansion of that elementary volume does not give any change in n, ϕ and ψ.

The disadvantage of such definitions is that the angle ϕ and the deviation ψ are hard to measure with today's available techniques.

Alternatively one could consider the following definitions: ϕ is the angle between the principal axis of the seepage coefficient and the axis of the principal stress and ψ is the ratio between the principal seepage coefficients.

These variables can be obtained with today's available techniques and give some information about the grain structure. The last definitions look more appropriate for bulky particles.

Other definitions are possible, but the usefulness will depend on the precision and the cost of measurement of these variables.

M.2 Constitutive Assumptions

We restrict ourselves to those materials for which the internal energy per mass ε, the stress $\underset{\sim}{\tau}$ and the temperature θ are functions of the present value of entropy per mass $\eta(\underset{\sim}{X},t)$ and the kinematical variables $\phi(\underset{\sim}{X},t)$, $\psi(\underset{\sim}{X},t)$ and $n(\underset{\sim}{X},t)$.

so:

$$\varepsilon = \varepsilon\ (\eta(\underset{\sim}{X},t),\ \phi(\underset{\sim}{X},t),\ \psi(\underset{\sim}{X},t),\ n(\underset{\sim}{X},t)) \tag{M.2.1}$$

$$\tau = f\ (\eta(\underset{\sim}{X},t),\ \phi(\underset{\sim}{X},t),\ \psi(\underset{\sim}{X},t),\ n(\underset{\sim}{X},t)) \tag{M.2.2}$$

$$\theta = \theta\ (\eta(\underset{\sim}{X},t),\ \phi(\underset{\sim}{X},t),\ \psi(\underset{\sim}{X},t),\ n(\underset{\sim}{X},t)) \tag{M.2.3}$$

The motion of an elementary particle is described by:

$$\underset{\sim}{x} = \underset{\sim}{x}\ (\underset{\sim}{X},t) \tag{M.2.4}$$

where $\underset{\sim}{X}$ is the position of an elementary particle at a reference time.

We use rectuangular Cartesian coordinates throughout. We further assume that the deformation gradient $\underset{\sim}{F}$ is a function of the present value of n, ψ, ϕ and η:

$$\underset{\sim}{F} = \underset{\sim}{F}(n,\psi,\phi,\eta) \tag{M.2.5}$$

where

$$F_{ij} = \frac{\partial x_i}{\partial X_j} \tag{M.2.6}$$

Then (M.2.1) to (M.2.5) together with appropriate balance equations determine the deformation of a body of the given model. We note that

this formulation has the advantage of removing the direct history dependence in the formulation.

From now on we focus our interest on "loading" processes, which means the variables either grow or decay continuously.

In that case we assume that we can write:

$$\phi = \phi(\underset{\sim}{F}) \tag{M.2.9}$$

$$\psi = \psi(\underset{\sim}{F}) \tag{M.2.10}$$

$$n = n(\underset{\sim}{F}) \tag{M.2.11}$$

In order to imply material objectively we pose:

$$\phi(\underset{\sim}{F}) = \hat{\phi}(\underset{\sim}{F}^T \underset{\sim}{F}) \tag{M.2.12}$$

$$\psi(\underset{\sim}{F}) = \hat{\psi}(\underset{\sim}{F}^T \underset{\sim}{F}) \tag{M.2.13}$$

$$n(\underset{\sim}{F}) = \hat{n}(\underset{\sim}{F}^T \underset{\sim}{F}) \tag{M.2.14}$$

M.3 Reduction of the Class of Constitutive Functionals by the Entropy Inequality

Posing the entropy inequality generates information about the dependence of $\underset{\sim}{\tau}$ on $\underset{\sim}{F}$.

The local entropy γ_{local} is given by:

$$\theta\, \gamma_{\text{local}} = \theta\, \dot{\eta} + \frac{1}{\rho}\, \tau_{ij}\, d_{ij} - \dot{\varepsilon} \tag{M.3.1}$$

where

$$d_{ij} = \frac{1}{2}\left(\frac{\partial v_i}{\partial x_j} + \frac{\partial v_j}{\partial x_i}\right) \tag{M.3.2}$$

and

$$v_i = \dot{x}_i \tag{M.3.3}$$

From (M.2.1) and (M.2.9) to (M.2.11) follows:

$$\dot{\varepsilon} = \frac{\partial \varepsilon}{\partial \eta}\, \dot{\eta} + \frac{\partial \varepsilon}{\partial \phi}\, \dot{\phi} + \frac{\partial \varepsilon}{\partial \psi}\, \dot{\psi} + \frac{\partial \varepsilon}{\partial n}\, \dot{n}$$

$$= \frac{\partial \varepsilon}{\partial \eta}\, \dot{\eta} + \frac{\partial \varepsilon}{\partial \phi}\, \frac{\partial \phi}{\partial \underset{\sim}{F}}\, \dot{\underset{\sim}{F}} + \frac{\partial \varepsilon}{\partial \psi}\, \frac{\partial \psi}{\partial \underset{\sim}{F}}\, \dot{\underset{\sim}{F}}$$

$$+ \frac{\partial \varepsilon}{\partial n}\, \frac{\partial n}{\partial \underset{\sim}{F}}\, \dot{\underset{\sim}{F}} \tag{M.3.4a}$$

The entropy inequality states: For all motions $\underset{\sim}{x} = \underset{\sim}{x}(\underset{\sim}{X}, t)$

$\gamma_{\text{local}} \geq 0$.

Substitution of (M.3.4a) in (M.3.1) and posing the entropy inequality gives:

$$\theta \dot{\eta} + \frac{1}{\rho} \tau_{ij} d_{ij} - \frac{\partial \varepsilon}{\partial \eta} \dot{\eta} - \frac{\partial \varepsilon}{\partial \phi} \frac{\partial \phi}{\partial F_{ij}} \dot{F}_{ij}$$

$$- \frac{\partial \varepsilon}{\partial \psi} \frac{\partial \psi}{\partial F_{ij}} \dot{F}_{ij} - \frac{\partial \varepsilon}{\partial n} \frac{\partial n}{\partial F_{ij}} \dot{F}_{ij} \geq 0 \qquad \text{(M.3.4b)}$$

Further we notice:

$$\tau_{ij} d_{ij} = \frac{1}{2} \left(\frac{\partial v_i}{\partial x_j} + \frac{\partial v_j}{\partial x_i} \right) \tau_{ij}$$

$$= \tau_{ij} \frac{\partial v_i}{\partial x_j} \qquad \text{(M.3.5)}$$

$$\dot{F}_{ij} = \frac{\partial}{\partial t} \left(\frac{\partial x_i}{\partial X_j} \right) = \frac{\partial v_i}{\partial X_j}$$

$$= \frac{\partial v_i}{\partial x_k} \frac{\partial x_k}{\partial X_j} = F_{kj} \frac{\partial v_i}{\partial x_k} \qquad \text{(M.3.6)}$$

From (M.3.4) to (M.3.6) follows:

$$\left(\theta - \frac{\partial \varepsilon}{\partial \eta}\right) \dot{\eta} + \left(\frac{1}{\rho} \tau_{ik} - \frac{\partial \varepsilon}{\partial \phi} \frac{\partial \phi}{\partial F_{ij}} F_{kj} \right. \qquad \text{(M.3.7)}$$

$$\left. - \frac{\partial \varepsilon}{\partial \psi} \frac{\partial \psi}{\partial F_{ij}} F_{kj} - \frac{\partial \varepsilon}{\partial n} \frac{\partial n}{\partial F_{ij}} F_{kj} \right) \frac{\partial v_i}{\partial x_k} \geq 0$$

for all $\underset{\sim}{F}(\underset{\sim}{X},t)$ and $\eta(\underset{\sim}{X},t)$.

The inequality (M.3.7) requires that:

$$\theta = \frac{\partial \varepsilon}{\partial \eta} \tag{M.3.8}$$

$$\tau_{ik} = \rho \frac{\partial \varepsilon}{\partial \phi} \left\{ \frac{\partial \phi}{\partial F_{ij}} \quad F_{kj} \right\} + \rho \frac{\partial \varepsilon}{\partial \psi} \left\{ \frac{\partial \psi}{\partial F_{ij}} \quad F_{kj} \right\}$$

$$+ \rho \frac{\partial \varepsilon}{\partial n} \left\{ \frac{\partial n}{\partial F_{ij}} \quad F_{kj} \right\} \tag{M.3.9}$$

We stress here the fact that the above equations have been derived under the assumptions (M.2.9) to (M.2.11), which we assumed to be valid in the case of loading processes. The above derivation is valid for the general non-linear case.

Inspection of (M.3.9) shows that the stress τ_{ik} consists of three parts: those associated with changes in the kinematical variables ϕ, ψ, and n respectively. $\frac{\partial \varepsilon}{\partial \phi}$, $\frac{\partial \varepsilon}{\partial \psi}$, and $\frac{\partial \varepsilon}{\partial n}$ can be viewed as participation factors in the stress due to their ϕ, ψ and n "motion" respectively.

We now linearize the equations; this means that we assume for the motion $\underset{\sim}{x} = \underset{\sim}{x}(\underset{\sim}{X}, t)$ that:

$$\left| \frac{\partial u_i}{\partial X_j} \right| << 1 \tag{M.3.10}$$

where:

$$x_i = X_i + u_i \tag{M.3.11}$$

and u_i is called the displacement.

Then:

$$\frac{\partial x_i}{\partial X_j} = F_{ij} = \delta_{ij} + \frac{\partial u_i}{\partial X_j} \tag{M.3.12}$$

Hence:

$$\phi\ (\underset{\sim}{F}) = \phi(\underset{\sim}{I}) + \frac{\partial \phi}{\partial F_{pg}}\Bigg|_{\underset{\sim}{F}=\underset{\sim}{I}} (F_{pq}-\delta_{pq}) \tag{M.3.13}$$

$$+ \frac{1}{2}\frac{\partial^2 \phi}{\partial F_{pg}\,\partial F_{rs}}\Bigg|_{F=I} (F_{pg}-\delta_{pg})\ (F_{rs}-\delta_{rs}) + \ldots$$

Normalize ϕ such that:

$$\phi\ (\underset{\sim}{I}) = \phi_o \tag{M.3.14}$$

Similar expressions can be derived for ψ and n.

From (M.3.13) follows:

$$\frac{\partial \phi}{\partial F_{ij}} = \frac{\partial \phi}{\partial F_{ij}}\Bigg|_{\underset{\sim}{F}=\underset{\sim}{I}} + \frac{\partial^2 \phi}{\partial F_{ij}\,\partial F_{rs}}\Bigg|_{\underset{\sim}{F}=\underset{\sim}{I}} (F_{rs}-\delta_{rs}) \tag{M.3.15}$$

We note that: (M.3.11)

$$F_{rs} = \delta_{rs} + \frac{\partial u_r}{\partial X_s} \tag{M.3.16}$$

So:

$$\frac{\partial \phi}{\partial F_{ij}} = \frac{\partial \phi}{\partial F_{ij}}\bigg|_{\underset{\sim}{F}=\underset{\sim}{I}} + \frac{\partial^2 \phi}{\partial F_{ij}\,\partial F_{rs}}\bigg|_{\underset{\sim}{F}=\underset{\sim}{I}} \left(\frac{\partial u_r}{\partial X_s}\right) \qquad \text{(M.3.17)}$$

Substituting (M.3.17) into (M.3.9) gives a first term on the right hand side of (M.3.9) as:

$$\frac{\partial \varepsilon}{\partial \phi}\,\rho_o\left\{\frac{\partial \phi}{\partial F_{ij}}\bigg|_{\underset{\sim}{F}=\underset{\sim}{I}} + \frac{\partial^2 \phi}{\partial F_{ij}\,\partial F_{rs}}\bigg|_{\underset{\sim}{F}=\underset{\sim}{I}} \left(\frac{\partial u_r}{\partial X_s}\right)\right\} =$$

$$\frac{\partial \varepsilon}{\partial \phi}\,\rho_o \frac{\partial \phi}{\partial F_{ij}}\bigg|_{\underset{\sim}{F}=\underset{\sim}{I}} + \frac{\partial \varepsilon}{\partial \phi}\,\rho_o \frac{\partial^2 \phi}{\partial F_{ij}\,\partial F_{rs}}\bigg|_{\underset{\sim}{F}=\underset{\sim}{I}} \frac{\partial u_r}{\partial X_s} \qquad \text{(M.3.18)}$$

Similar expressions can be derived for the second and third term of (M.3.9).

So from (M.3.18), the above similar expressions and (M.3.9) there follows:

$$\tau_{ij} = \tau_{ij}^{0} + c_{ijrs} \frac{\partial u_r}{\partial X_s} \tag{M.3.19}$$

where:

$$\begin{aligned} c_{pqrs} &= c_{rspq} \\ c_{pqrs} &= c_{qprs} \\ c_{pqrs} &= c_{pqsr} \end{aligned} \tag{M.3.20}$$

We observe that the material in general behaves as an anisotropic linear elastic material which is prestressed. The result is only valid for the "loading" case with small deviations from the reference state.

From (M.3.12) to (M.3.14) follows:

$$\phi = \phi_o + d_{pq} \frac{\partial u_p}{\partial X_q} + e_{pqrs} \frac{\partial u_p}{\partial X_q} \frac{\partial u_r}{\partial X_s} \tag{M.3.21}$$

We note that this result is formally valid for the two-dimensional case. However including more kinematical variables in the form of (M.2.9) to (M.2.11) in order to describe the grain structure in three dimensions, would have generated equations of the same form as (M.3.19).

When there is no stress in the reference state (M.3.19) becomes:

$$\tau_{ij} = c_{ijrs} \frac{\partial u_r}{\partial X_s}$$

$$= c_{ijrs} \gamma_{rs} \qquad \text{(M.3.22)}$$

where:

$$\gamma_{rs} = \frac{1}{2} \left(\frac{\partial u_r}{\partial X_s} + \frac{\partial u_s}{\partial X_r}\right) \qquad \text{(M.3.23)}$$

Now we consider again a two-dimensional case, then from (M.3.22) follows:

$$\tau_{ij} = c_{ijrs} \gamma_{rs} \qquad \begin{matrix} i,j=1,2 \\ r,s=1,2 \end{matrix} \qquad \text{(M.3.24)}$$

or:

$$\sigma_{xx} = c_{xxxx} \gamma_{xx} + c_{xxxy} 2\gamma_{xy} + c_{xxyy} \gamma_{yy} \qquad \text{(M.3.25)}$$

$$\tau_{xy} = c_{xyxx} \gamma_{xx} + c_{xyxy} 2\gamma_{xy} + c_{xyyy} \gamma_{yy} \qquad \text{(M.3.26)}$$

$$\sigma_{yy} = c_{xxyy} \gamma_{xx} + c_{yyxy} 2\gamma_{xy} + c_{yyyy} \gamma_{yy} \qquad \text{(M.3.27)}$$

From (M.3.20) we conclude that there are six constants in the above constitutive equations.

N. The Propagation of Discontinuities in a Two-Dimensional Two-Phase Medium, Including Dilatancy

So far we have studied the wave propagation through a saturated linearly elastic isotropic porous medium. However a real soil often exhibits dilatancy (Scott [34]). In a dilatant material contraction or expansion takes place during shear. This phenomenon can be taken into account by the use of the derived constitutive equations (M.3.25) to (M.3.27) of the former chapter for the two-dimensional case.

We will consider the case of "dilatant shear". Applying a shear discontinuity at the boundary will generate discontinuities propagating into the two-phase medium. We will derive the jump conditions and an equation for the speed of the discontinuities in a similar way as in the one-dimensional compression case.

We will relate some of the results to the results of the one-dimensional compression case and we will discover that non-propagating discontinuities exist which also occur in a dry material (Appendix VI).

N.1 Field Equations

We assume an orthogonal coordinate system (x,y) and we further assume that the boundary conditions are such that the variables are independent of y.

Then:

$$\gamma_{yy} = \frac{\partial u_y}{\partial y} = 0 \qquad \text{(N.1.1)}$$

So (M.3.25) to (M.3.27) become:

$$\sigma_{xx} = c_{xxxx}\,\gamma_{xx} + c_{xxxy}\,2\gamma_{xy} \qquad \text{(N.1.2)}$$

$$\tau_{xy} = c_{xxxy}\,\gamma_{xx} + c_{xyxy}\,2\gamma_{xy} \qquad \text{(N.1.3)}$$

$$\sigma_{yy} = c_{xxyy}\,\gamma_{xx} + c_{yyxy}\,2\gamma_{xy} \qquad \text{(N.1.4)}$$

Now we write (N.1.2) and (N.1.3) as:

$$\sigma_{xx} = A\,\gamma_{xx} + D\,2\gamma_{xy} \qquad \text{(N.1.5)}$$

$$\tau_{xy} = D\,\gamma_{xx} + F\,2\gamma_{xy} \qquad \text{(N.1.6)}$$

Inspection of (N.1.5) and (N.1.6) shows that the grain structure might expand (γ_{xx} positive) or compress (γ_{xx} negative) by applying a shear stress and hence the possibility of dilatancy is included.

Further:

$$\gamma_{xx} = \frac{\partial u_x}{\partial x}$$

$$2\gamma_{xy} = 2\,\frac{1}{2}\,(0 + \frac{\partial u_y}{\partial x}) = \frac{\partial u_y}{\partial x}$$

Substitution of the above expressions into (N.1.5) and (N.1.6) gives after differentiating with respect to t:

$$\frac{\partial \sigma_{xx}}{\partial t} = A\,\frac{\partial v_x}{\partial x} + D\,\frac{\partial v_y}{\partial x} \qquad \text{(N.1.7)}$$

$$\frac{\partial \tau_{xy}}{\partial t} = D\,\frac{\partial v_y}{\partial x} + F\,\frac{\partial v_y}{\partial x} \qquad \text{(N.1.8)}$$

For the fluid we derive the following storage equation:

$$\frac{\partial w_x}{\partial x} + \frac{1-n}{n}\,\frac{\partial v_x}{\partial x} = -\frac{1}{K_w}\,\frac{\partial p}{\partial t} \qquad \text{(N.1.9)}$$

The derivation is similar to the one in Chapter J. We omit the derivatives with respect to y.

The momentum equations for the fluid are:

$$n\,\rho_w\,\frac{\partial w_x}{\partial t} = -n\,\frac{\partial p}{\partial x} - \frac{n^2}{k_{xx}}\,(w_x - v_x) - \frac{n^2}{k_{xy}}\,(w_y - v_y) \qquad \text{(N.1.10)}$$

$$n\,\rho_w\,\frac{\partial w_y}{\partial t} = - \frac{n^2}{k_{yy}}\,(w_y - v_y) - \frac{n^2}{k_{yx}}\,(w_x - v_x) \qquad \text{(N.1.11)}$$

Again these equations are similar to the ones in Chapter J, but we omit derivatives with respect to y and add terms which represent the forces in the x-direction due to velocity differences in y-direction and vice versa.

In a similar way we derive the momentum equations for the grain structure:

$$(1-n)\ \rho_p \frac{\partial v_x}{\partial t} = \frac{\partial \sigma_{xx}}{\partial x} - (1-n)\frac{\partial p}{\partial x} + \frac{n^2}{k_{xx}}(w_x - v_x) + \frac{n^2}{k_{xy}}(w_y - v_y) \qquad \text{(N.1.12)}$$

$$(1-n)\ \rho_p \frac{\partial v_y}{\partial t} = \frac{\partial \tau_{xy}}{\partial x} + \frac{n^2}{k_{yy}}(w_y - v_y) + \frac{n^2}{k_{yx}}(w_x - v_x) \qquad \text{(N.1.13)}$$

Hence from (N.1.7) to (N.1.13) it follows that the field equations are:

$$\frac{\partial \sigma_{xx}}{\partial t} = A\frac{\partial v_x}{\partial x} + D\frac{\partial v_y}{\partial x} \qquad \text{(N.1.14)}$$

$$\frac{\partial \tau_{xy}}{\partial t} = D\frac{\partial v_x}{\partial x} + F\frac{\partial v_y}{\partial x} \qquad \text{(N.1.15)}$$

$$\frac{\partial w_x}{\partial x} + \frac{1-n}{n}\frac{\partial v_x}{\partial x} = -\frac{1}{K_w}\frac{\partial p}{\partial t} \qquad \text{(N.1.16)}$$

$$n\,\rho_w \frac{\partial w_x}{\partial t} = -\,n \frac{\partial p}{\partial x} - \frac{n^2}{k_{xx}} (w_x - v_x) - \frac{n^2}{k_{xy}} (w_y - v_y) \qquad \text{(N.1.17)}$$

$$n\,\rho_w \frac{\partial w_y}{\partial t} = - \frac{n^2}{k_{yy}} (w_y - v_y) - \frac{n^2}{k_{yx}} (w_x - v_x) \qquad \text{(N.1.18)}$$

$$(1-n)\;\rho_p \frac{\partial v_x}{\partial t} = \frac{\partial \sigma_{xx}}{\partial x} - (1-n) \frac{\partial p}{\partial x} + \frac{n^2}{k_{xx}} (w_x - v_x) + \frac{n^2}{k_{xy}} (w_y - v_y) \qquad \text{(N.1.19)}$$

$$(1-n)\;\rho_p \frac{\partial v_y}{\partial t} = \frac{\partial \tau_{xy}}{\partial x} + \frac{n^2}{k_{yy}} (w_y - v_y) + \frac{n^2}{k_{yx}} (w_x - v_x) \qquad \text{(N.1.20)}$$

The field equations (N.1.14) to (N.1.20) form seven equations for the the seven unknowns v_x, v_y, w_x, w_y, σ_{xx}, τ_{xy} and p.

The independent variables are x and t.

N.2 Derivation of the Jump Conditions

We write (N.1.14) to (N.1.20) in integral form and we assume $x_1 \to x_2$, then:

$$-\frac{d}{dt}\int_{x_1}^{x_2} \sigma_{xx}\, dx + [A\, v_x + D\, v_y] = 0 \qquad \text{(N.2.1)}$$

$$-\frac{d}{dt}\int_{x_1}^{x_2} \tau_{xy}\, dx + [D\, v_x + F\, v_y] = 0 \qquad \text{(N.2.2)}$$

$$\frac{d}{dt}\int_{x_1}^{x_2} p\, dx + [K_w\, w_x + K_w \frac{1-n}{n}\, v_x] = 0 \qquad \text{(N.2.3)}$$

$$\frac{d}{dt}\int_{x_1}^{x_2} n\, \rho_w\, w_x\, dx + [n\, p] = 0 \qquad \text{(N.2.4)}$$

$$\frac{d}{dt}\int_{x_1}^{x_2} \rho_w\, w_y\, dx = 0 \qquad \text{(N.2.5)}$$

$$\frac{d}{dt}\int_{x_1}^{x_2} (1-n)\ \rho_p\ v_x\ dx + [-\sigma_{xx} + (1-n)\ p] = 0 \qquad (N.2.6)$$

$$\frac{d}{dt}\int_{x_1}^{x_2} (1-n)\ \rho_p\ v_y\ dx + [-\ \tau_{xy}] = 0 \qquad (N.2.7)$$

From (N.2.1) to (N.2.7) we derive the following jump conditions:

$$U\ [\sigma_{xx}] \quad + \quad [A\ v_x \quad + \quad D\ v_y] = 0 \qquad (N.2.8)$$

$$U\ [\tau_{xy}] \quad + \quad [D\ v_x \quad + \quad F\ v_y] = 0 \qquad (N.2.9)$$

$$-\ U\ [\ p\ ] \quad + \quad [K_w\ w_x + K_w\ \frac{1-n}{n}\ v_x] = 0 \qquad (N.2.10)$$

$$-\ U\ [\rho_w\ w_x] + \ [\ p\ ] = 0 \qquad (N.2.11)$$

$$-\ U\ [\rho_w\ w_y] = 0 \qquad (N.2.12)$$

$$-\ U\ [(1-n)\ \rho_p\ v_x] + [-\sigma_{xx} + (1-n) \quad p] = 0 \qquad (N.2.13)$$

$$-\ U\ [(1-n)\ \rho_p\ v_y] + [-\ \tau_{xy}] = 0 \qquad (N.2.14)$$

where U is the speed of the discontinuity.

From (N.2.12) it follows that

$$w_{y_1} = w_{y_2} \tag{N.2.15}$$

Now consider the following problem: a discontinuity is propagating into a medium where the variables have the following values (rest state).

$$v_{x_1} = v_{y_1} = w_{x_1} = w_{y_1} = 0 \tag{N.2.16}$$

$$\sigma_{xx_1} = \tau_{xy_1} = p_1 = 0 \tag{N.2.17}$$

Substitution of (N.2.16) and (N.2.17) into (N.2.8) to (N.2.14) gives:

$$- U \sigma_{xx_2} - A v_{x_2} - D v_{y_2} = 0 \tag{N.2.18}$$

$$- U \tau_{xy_2} - D v_{x_2} - F v_{y_2} = 0 \tag{N.2.19}$$

$$U p_2 - K_w w_{x_2} - K_w \frac{1-n}{n} v_{x_2} = 0 \tag{N.2.20}$$

$$U \rho_w w_{x_2} - p_2 = 0 \tag{N.2.21}$$

$$U (1-n) \rho_p v_{x_2} + \sigma_{xx_2} - (1-n) p_2 = 0 \tag{N.2.22}$$

$$U (1-n) \rho_p v_{y_2} + \tau_{xy_2} = 0 \tag{N.2.23}$$

These are six equations for seven variables ($U, \sigma_{xx_2}, \tau_{xy_2}, v_{x_2}, v_{y_2}, w_{x_2}, p_2$).

Hence we have to prescribe one more variable behind the discontinuity, e.g. choose v_{y_2}.

After some algebra we obtain:

$$- D\ U\ \sigma_{xx_2} = -(-A\ U^2\ (1-n)\ \rho_p + AF - D^2)\ v_{y_2} \qquad \text{(N.2.24)}$$

$$\tau_{xy_2} = -\ U\ (1-n)\ \rho_p\ v_{y_2} \qquad \text{(N.2.26)}$$

$$D\ v_{x_2} = \left\{ U^2\ (1-n)\ \rho_p - F \right\} v_{y_2} \qquad \text{(N.2.27)}$$

$$D\ (U^2\ \rho_w - K_w)\ p_2 = U\ \rho_w\ K_w\ \frac{1-n}{n}\ \left\{ U^2\ (1-n)\ \rho_p - F \right\}\ v_{y_2} \qquad \text{(N.2.28)}$$

$$U\ \rho_w\ w_{x_2} = p_2 \qquad \text{(N.2.29)}$$

$$(1-n)^2\ \rho_p^{\,2}\ \rho_w\ U^6$$

$$+\ \{-\ F\ (1-n)\ \rho_p\ \rho_w\ -\ K_w\ (1-n)^2\ \rho_p^{\,2}$$

$$-\ (1-n)^2\ \rho_p\ \rho_w\ K_w\ \frac{1-n}{n}\ -\ A\ (1-n)\ \rho_w\ \rho_p\}\ U^4$$

$$\{F\ K_w\ (1-n)\ \rho_p\ +\ F\ (1-n)\ \rho_w\ K_w\ \frac{1-n}{n}$$

$$+\ K_w\ A\ (1-n)\ \rho_p\ +\ F\ A\ \rho_w$$

$$-\ D^2\ \rho_w\}\ U^2$$

$$+\{-\ F\ K_w\ A\ +\ D^2\ K_w\}=\ 0 \qquad \text{(N.2.30)}$$

Substitution of $V = U^2$ in (N.2.30) shows that we have to solve a third order polynomial in V. We retain only the positive roots of V in order to arrive at real wavespeeds for U.

Assume now that the parameters are such that one pair (positive and negative) of wave speeds U exists, then (N.2.24) to (N.2.29) gives the variables behind the discontinuity in terms of v_{y_2}.

We note that if $D^2 - F A = 0$ there exists a non-propagating discontinuity ($U = 0$). A discussion for this case will be given in Appendix VI for a dry material.

We consider the case $K_w >> A, F, D$ and put (N.2.30) in the following form:

$$ax^3 + 3bx^2 + 3cx + d = 0 \qquad \text{(N.2.30b)}$$

where $x = U^2$.

Then:

$$q = a\,c - b^2 \qquad \text{(N.2.31)}$$

$$z = \frac{1}{2}(3\,abc - a^2\,d) - b^3 \qquad \text{(N.2.32)}$$

Substitution of the coefficients of (N.2.30) into (N.2.31) and (N.2.32) shows:

$$q \approx -b^2 \qquad \text{(N.2.33)}$$

$$r \approx -b^3 \qquad \text{(N.2.34)}$$

So if the parameters are such that there exist three real roots then:

$$x_1 \approx \frac{(-b-b)\ -b}{a} = \frac{-3b}{a} \qquad \text{(N.2.35)}$$

$$x_{2,3} \approx \frac{(-\frac{1}{2}\ (-b-b)\ -b)}{a} = 0 \qquad \text{(N.2.36)}$$

In fact this shows that we solve:

$$ax^3 + 3b\ x^2 \approx 0 \qquad \text{(N.2.37)}$$

Substitution of the coefficients of (N.2.30) into (N.2.35) shows:

$$U^2 \approx \left(\frac{n\ \rho_p + (1-n)\ \rho_w}{n\ \rho_p}\right)\ \frac{K_w}{\rho_w} \qquad \text{(N.2.38)}$$

We note that the speed of the fastest discontinuity in the "dilatant shear" case is equal to the speed of the fastest discontinuity in the one-dimensional compression case (G.2.21).

We note that x_2 and x_3 are small with respect to x_1. In order to associate a propagation velocity with x_2 and x_3 their roots have to be positive. If one of them or both are positive, then the associated speed of a discontinuity is small with respect to the fastest discontinuity (N.2.38).

Hence we conclude that for the case $K_w > A, D, F$ a fast propagating discontinuity is possible and its speed is given by (N.2.38). If the parameters A, D and F are such that one or two propagating discontinuities are possible, then their speed is always small with respect to the fastest discontinuity.

Substitution of (N.2.38) into (N.2.24) to (N.2.29) shows:

$$w_{x_2} = \frac{\rho_p}{\rho_w} v_{x_2} \tag{N.2.39}$$

$$\sigma_{xx_2} = -\frac{A}{K_w}\left(\frac{n \rho_w}{n \rho_p + (1-n) \rho_w}\right) p_2 \tag{N.2.40}$$

$$p_2 = U \rho_w w_{x_2} \tag{N.2.41}$$

We note the similarities between (N.2.39) with (G.2.33), (N.2.40) with (G.2.34) and (N.2.41) with (G.2.32).

Hence for w_{x_2}, σ_{xx_2} and p_2 we conclude that they behave in the same way as the variables behind the fastest propagating discontinuity in the one-dimensional case and the same conclusions for the one-dimensional compression case apply to the dilatant shear case. Additional features in the dilatant shear case, with respect to the one-dimensional compression case, are the generation of a velocity in the y-direction and a shear stress τ_{xy_2} given by:

$$\tau_{xy_2} = \frac{D}{A}\,\sigma_{xx_2} \tag{N.2.42}$$

$$v_{y_2} = + \frac{D}{K_w} \frac{n\,\rho_w}{(1-n)\,(n\,\rho_p + (1-n)\,\rho_w)}\,v_{x_2} \tag{N.2.43}$$

Hence v_{y_2} is always small with respect to v_{x_2} and the ratio of τ_{xy_2} and σ_{xx_2} will be equal to the ratio of D and A. For slightly dilating materials D/A will be small and hence τ_{xy_2} will be small with respect to σ_{xx_2}.

The conclusion is that for $K_w > A, D, F$, behind the fastest propagating discontinuity, the effective stress (τ_{xy_2} and σ_{xx_2}) is small with respect to the pore pressure and velocity differences in x-direction between skeleton and fluid depend on the ratio ρ_p/ρ_w.

A propagating discontinuity or discontinuities are generated by suddenly applied loads or velocities at the boundary. In the case that there exist three discontinuities we can prescribe three variables at the boundary (e.g. $v_x(0,t) = 0$, $w_x(0,t) = 0$ and $\tau_{xy}(0,t) = H(t)$, where H(t) is the stepfunction) and calculate the variables at $t = 0^+$ in the same way as in Chapter L.

O. Wave Propagation in a Laboratory Model

In the theoretical model the saturated granular medium was represented by a two-phase continuum whose stresses and pressures indicate only in an average sense what the sand grains and the pore water are actually doing and, obviously, some significant behavior of the grains and the water are not included in the continuum representation. To throw some light on this behavior experimental studies were undertaken. Our objective here is to obtain additional information especially on those aspects not accounted for in the theoretical model. Notably the discrete character of the solid particles and the ability of the particles to slide along each other or even lose contact will draw our attention.

Furthermore we are interested in interparticle stresses after shock loading. The usual techniques for measuring pore pressures and total pressure (e.g., True and Herrmann [31]) have many drawbacks and calibrating the gages is an elaborate and sometimes questionable process which requires judgement. Therefore we felt the need for another technique to obtain a picture of the changes in intergranular stresses.

At the suggestion of R.F. Scott we chose a photoelastic technique because it permits the direct visualization of stress wave propagation. Two different models are used: (1) Homalite 100 (supplier: Homalite Corp., Wilmington, Delaware), circular discs (diameters: 2 cm and 1 cm, thickness 0.5 cm; two sizes were used to break up the regular pattern) saturated with Pasadena tap water, and (2) crushed Pyrex (sieve $^{+}8\ ^{-}28$) saturated with glycerol.

The first model will give us specific insight into disc movements, relative movements of discs and water, and stress in the discs. The

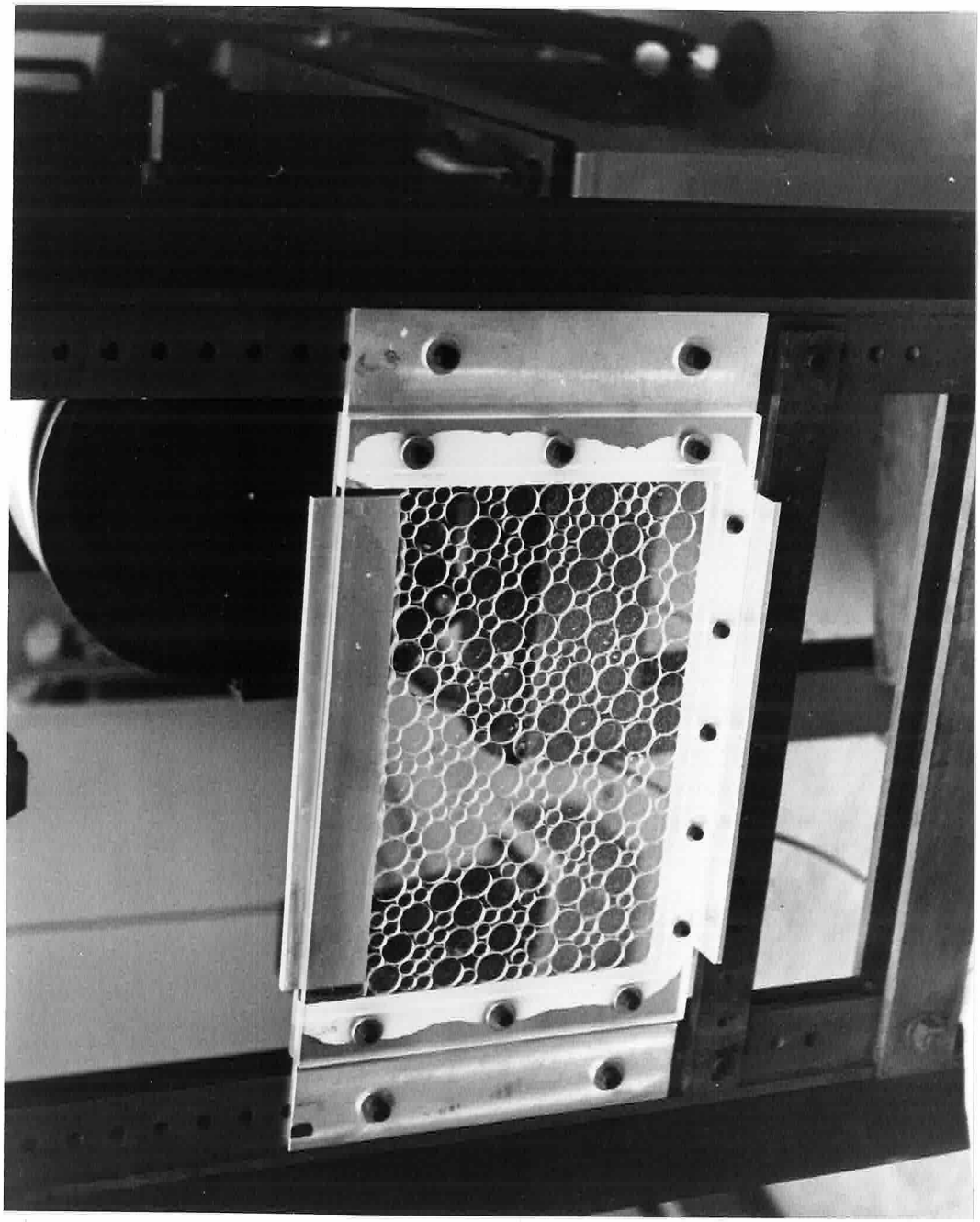

FIG 19

second model gives insight into the stresses in a granular medium which represents more closely the properties of a saturated sand.

Each material was put into a tank (31.5 cm x 22.6 cm x 0.6 cm, inside) which consisted of two Lucite plates, clamped to an aluminum frame (Figure (19)).

0.1 Wave propagation through a disc configuration

Dantu [57], de Josselin de Jong and Verruijt [58], and Drescher and de Josselin de Jong [59] studied the stress and deformation patterns of disc configurations due to applied stresses.

The method consists of projecting polarized light through discs of a photoelastic material. The light patterns on the discs are a measure of the stress in the discs.

Natural light consists of waves vibrating in all directions (Kuske and Robertson [60]). Light passing a polaroid will only vibrate in one direction (the direction of the axis of the polaroid). Natural light passing two polaroids with the axes perpendicular will result in a dark field on a screen behind the last polaroid. Inserting a piece of photoelastic material (the model) between the above polaroids will have the following effect: All points within the model which have principal stress directions parallel to the axes of the polaroids will stay black (these black lines are called isoclinic fringes). Hence the isoclinic fringes determine the principal stress directions.

Polarized light crossing a 1/4 wave plate, which has axes at an angle of 45° with the direction of the incoming polarized light, results in light whose vibration direction rotates.

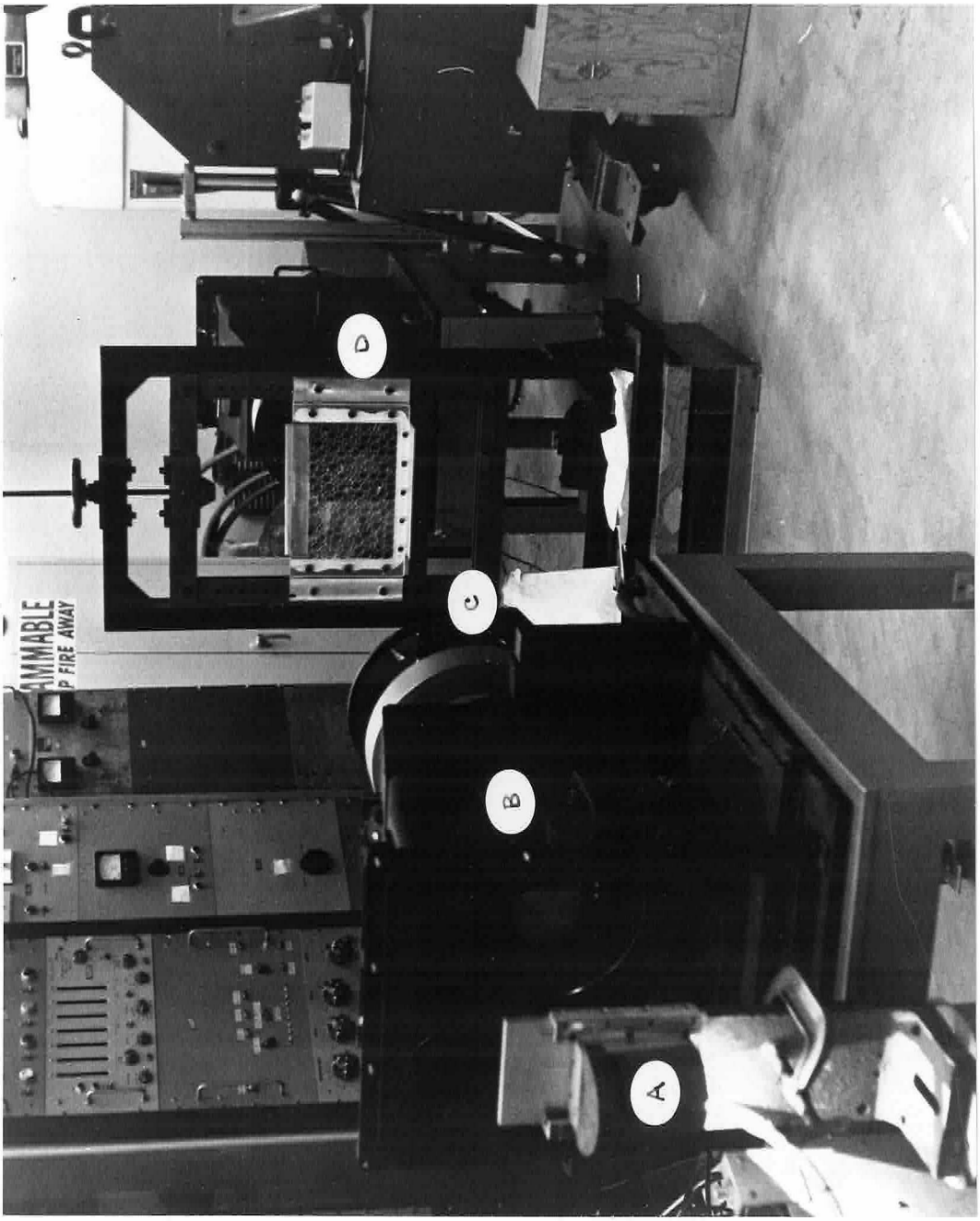

FIG 20

Inserting two 1/4 wave plates between two polarizers (axes perpendicular) in such a manner that the axes of the 1/4 wave plates are perpendicular and make 45° angles with the axes of the polaroids, will result in a dark field on a screen behind the last polarizer (for a monochromatic light source). Inserting the model between the 1/4 wave plates has the following effect: By loading the model a set of dark and light fringes appear. The dark fringes, called isochromatics, give the collection of points where the difference in principal stresses has the same value. No isoclinics appear.

However, when the model is placed between two polarizers (axes perpendicular), isoclinics as well as isochromatics appear on the screen. Frequently one is only interested in the principal stress difference. The isoclinics are then undesirable because they obscure the stress pattern.

It was felt that the photoeleastic technique could be adapted for the study of wave propagation through disc configurations (saturated and dry).

0.2 Experimental Setup

The experimental set-up is as follows (Fig.20): A mercury arc bulb (~150 Watts; A in Fig. 20) generates the light. The light rays are brought parallel by a lens (48 in., f/6.3, B in Fig. 20). The light rays cross the polarizer (1/4-wave plate, C in Fig. 20), tank (D in Fig. 20), (1/4-wave plate), polarizer and a lens, respectively.

Behind the last large lens we placed a high speed camera (type: Hycam, model K20S4E, lens: 25 mm, 1:1.4, film: 16 mm, Kodak RAR film 2498). We set the camera at 5,000 frames per sec. or 10,000 frames per sec.

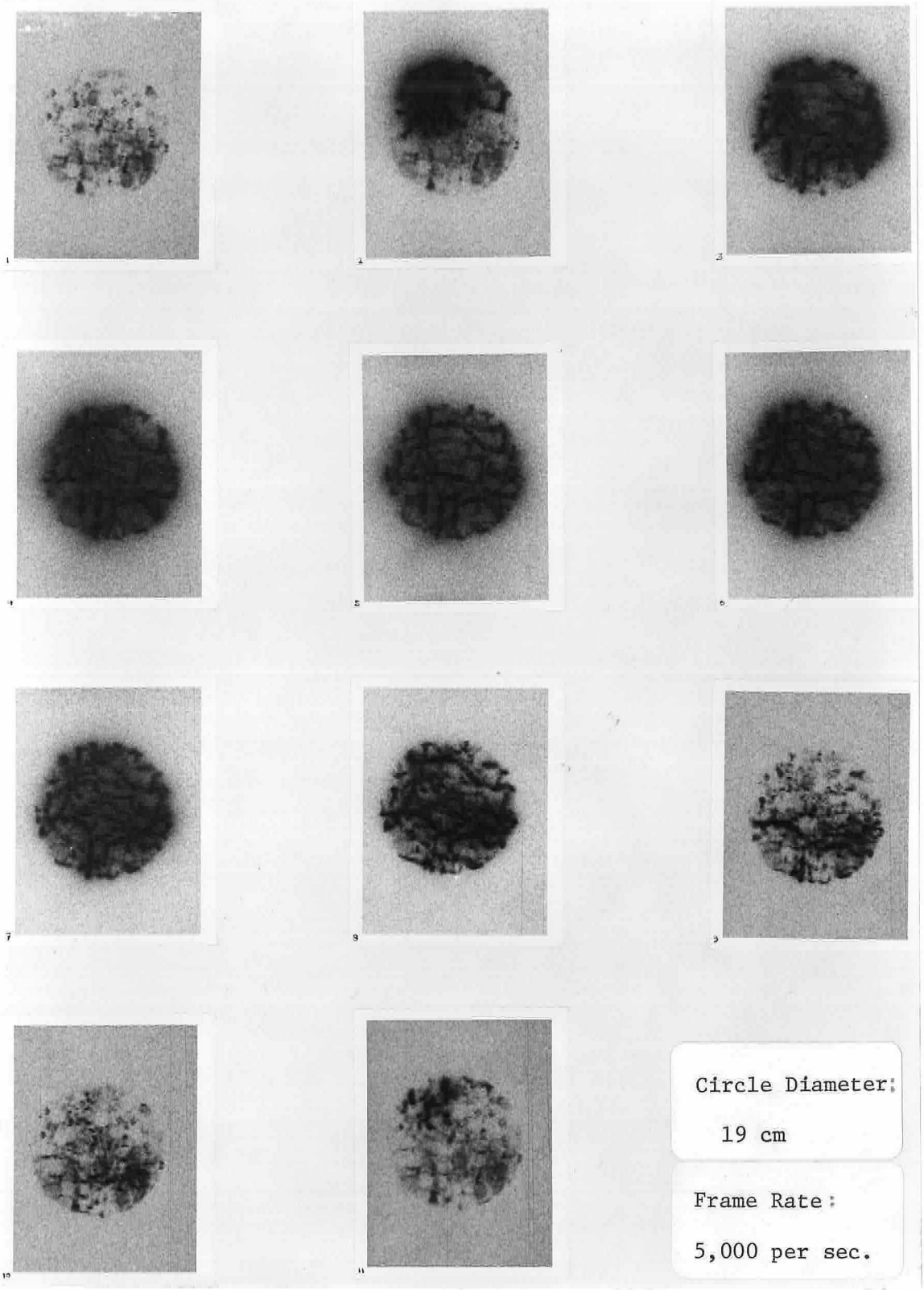

FIG A

0.3 Impacted discs, dry

The tank was randomly filled with discs. On top of the disks was placed an aluminum bar (30.5 cm x 5 cm x 0.5 cm). The top of the bar was struck with a steel strip and a high-speed camera film recorded the subsequent phenomena (5,000 frames per sec.). No 1/4 wave plates were used.

Fig. A.1 shows the unstressed state of the disc configuration. Visible is the part of the tank that was struck by the circular light beam ($\sim$ 19 cm), which was centered on the tank. Figures A.2 to A.11 show the first 10 consecutive frames after impact. In Figure A.2 we can identify a stress front. The front is about halfway down the tank so that, considering the framing rate, this means that the front propagates with at least 5.10^2 m/sec. We notice that in front of the dark-colored fringes a grey area has developed which might indicate some minor stress or disc movement.

Figures A.3 to A.11 show subsequent events. The lighted area stays well-stressed until unloading starts from the top. We note the change in stress patterns, indicating that particles are stressed differently at different times.

From Figures A.8 and A.9 we see that the vertical stress rays disappear faster than the horizontal stress rays during unloading.

Figure A.11 shows a loading wave incoming from the top. In subsequent frames of the original film this loading and unloading behavior took place many times, until it damped out in time. This might be due to the fact that the top bar was hit by a steel strip, which may

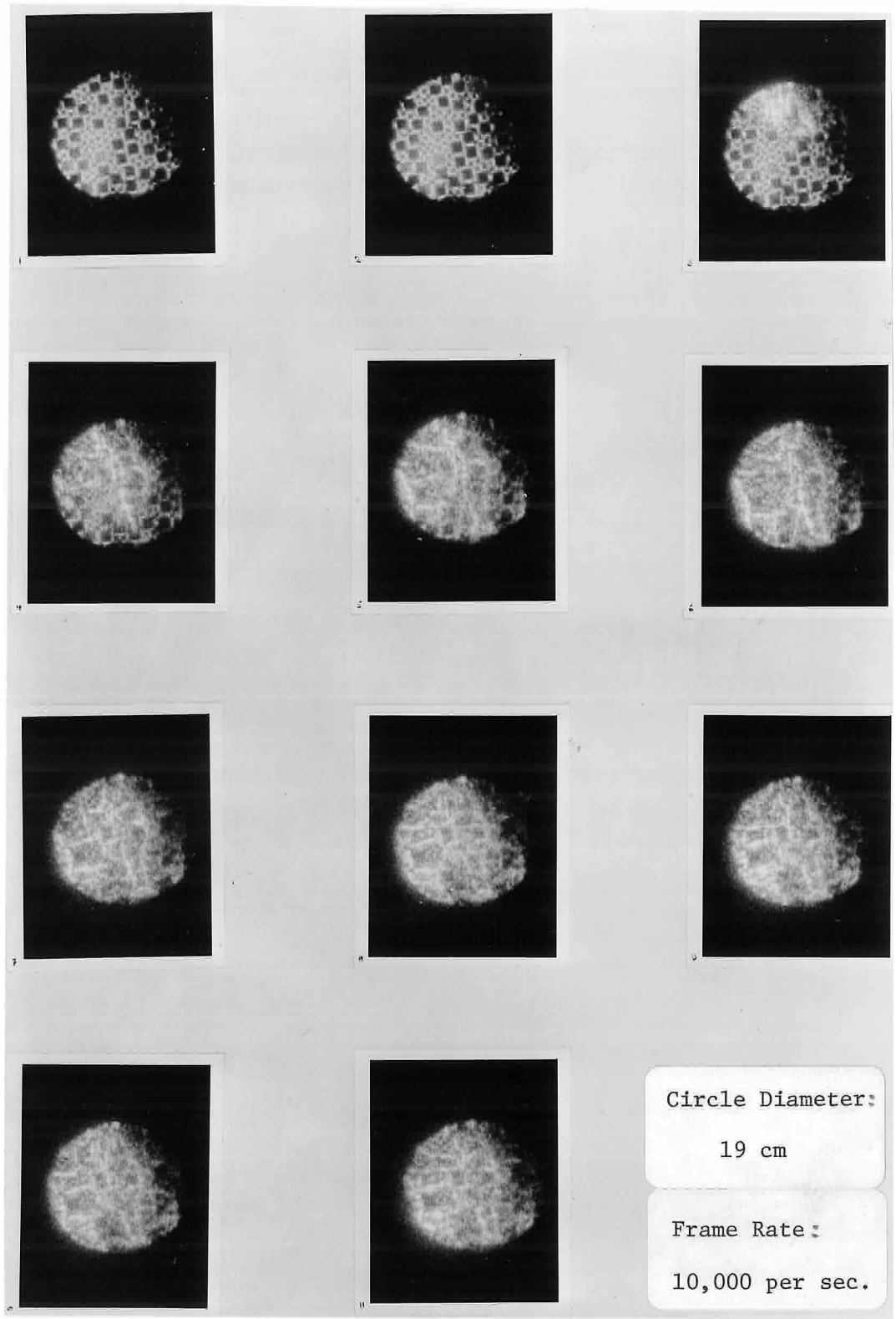

FIG B

have developed a bending vibration around the point where it was clamped (hand) and hence the top bar was possibly subjected to several impacts.

The plate velocity ($= \sqrt{\frac{E}{\rho(1 - \nu^2)}}$) for Homalite 100 plates from which the discs were cut, is in the order of 2.10^3 m/sec. The estimated front velocity was at least 5.10^2 m/sec. The large difference might be due to the tortuosity of the stress transmission path and the possibility of slip between the discs.

0.4 Impacted discs, saturated

This time the tank was filled up with water and discs (Fig. B.1). The aluminum bar was placed on top of the discs and the water level was higher than the lower edge of the bar.

Again the bar was hit by a hammer and a film recorded the subsequent phenomena. The camera speed was set at 10,000 frames per sec. No 1/4 wave plates were used. The first 10 frames after impact are shown in Figs. B.2 to B.11.

In Fig. B.2 the small top disc has changed color, indicating that the disc is stressed. The individual discs are more easily identifiable than in the dry case.

Fig. B.3 shows the progress of the front. The stress "front" is about halfway down. In the stressed area the picture becomes fuzzy and individual discs are not identifiable anymore (which might be due to the movement of discs and/or water). The estimated speed of the "front" is 8.10^2 m/sec, higher than the estimated speed of the front in the dry case.

Fig. B.4 shows the next stage. A definite stress front is not identifiable. A main ray (row of stressed discs) emerges from top to bottom, crossing small particles as well as larger ones. The head of the main ray has propagated approximately half the lighted circle diameter from Figs. B.3 to B.4. The general picture becomes more fuzzy.

Figs. B.5 to B.11 show the subsequent stages. The pictures stay fuzzy and rays of stressed discs are visible. We note the change in location of the rays of stressed discs, indicating a change in stress distribution.

The whole process of loading the discs took about 25 frames; after which stress release in the particles started at the top, progressing in a few frames downwards. The pictures then became less fuzzy and individual particles became again identifiable as in Fig. B.1. Hereafter the pictures stayed stationary; this is in contrast to the dry case in which the process of loading and unloading repeated itself many times. Probably the discs were not loaded anymore by the top bar.

It should be remarked that the discs were in a rather dense configuration and presumably the water contained some air. This, and the fact that the Lucite walls were flexible, probably gave the water an additional compressibility with respect to the compressibility of pure water. Because the walls were flexible the compressibility of the water was not uniform in the tank.

If we estimate the compression modulus of the skeleton from the wave speed ($\sim$500 m/sec) and the dry density and assume that the water

had a compression modulus in the same order as that of the skeleton, then by substituting these values in the equation that determines the speed of the discontinuities (G.2.20), we can actually derive a speed around 800 m/sec for the faster propagating discontinuity and a speed of ∿200 m/sec for the slower discontinuity. The fact that we were unable to identify a definite stress front might partially be caused by the two-wave structure, but we were unable to make definite conclusions.

0.5 Impacted saturated granular medium

Dantu [57] introduced a method of visualizing the stress in a granular medium. It consists of saturating a granular material made of glass (e.g., Pyrex) with a fluid of the same refractive index, so the light is not refracted at the grain boundaries when projected through the saturated medium.

However, when circularly polarized light passes through the stressed saturated medium, a 1/4 wave plate and analyzer in series, small light patterns are visible. Dantu points out that this indicates stress in the granular medium.

R. F. Scott suggested that this technique might be useful for studying effective stress changes in a saturated granular medium due to impact, because the effective stress is indicated in a direct way.

The tank was filled up with a saturated medium, consisting of glycerol and broken Pyrex. An aluminum bar covered the top of the medium and was in contact with the granules. The medium was prestressed by a pair of jacks, placed on top of the bar. Patterns of small lines became visible, mostly concentrated around the edges of the bar.

The patterns disappeared instantaneously after impact; however, the resolution of the film at 5,000 frames per sec. was not high enough to follow this process in detail. Consequently the tests were inconclusive. It should be remarked however that the jacks fell off their supports and hence the eventual disappearance of stress patterns was not unexpected.

Using higher camera speeds, stronger light sources (> 6 amp, mercury arc bulb), and improving the matching of refractive indexes might make it a promising technique for studying liquefaction phenomena due to impact.

0.6 Discs, indirectly loaded

In the foregoing experiments with discs, we got some insight into the stress in discs after impact.

In the dry case the discs were loaded directly by the top bar and in the saturated case the bar rested on the discs and the discs were partly directly loaded by the bar and partly, presumably, by the water. The disc configuration in both cases was rather dense and in general no large relative movement between the discs took place, except in the saturated case where a few small particles, which were not clamped between neighboring particles, moved relative with respect to neighboring particles.

Now we will induce a small water layer above the top discs (± 2 cm) and place a nylon bar on top of it. The nylon bar is fitted close to the Lucite plates at the side. So the discs are not constrained by the bar and can move relatively freely upwards.

The nylon bar was struck and disc displacement and fluid movement observed visually. After impact the following phenomenon occurred: The discs moved upwards and the disc structure expanded so that generally the discs lost contact with each other.

High-speed camera films and particle movement studies showed that in the first stage the discs stay in their positions, but water is flowing downwards around the discs. The downward velocity of the water particles decreases to zero velocity almost simultaneously in the whole tank, then the velocity direction becomes upwards. So far

as could be observed around this point the discs start to move upwards and in general relative to each other.

The same phenomenon was observed in a smaller tank (10 cm X 5 cm x 0.6 cm) with the small size discs, where the walls of the tank were relatively rigid. Experiments in this small tank showed that by using a fluid with a higher viscosity (glycerol-water), the discs moved quickly upwards after which they floated for a while in the viscous fluid.

The upward movement of the top discs and separation of discs after impact on the water layer above the disc layer was also observed in a tank of rectangular cross section (10 cm X 6 cm X 3.5 cm), where the discs were put in randomly in a three-dimensional structure (height disc layer: 4 cm, height water layer: 2 cm).

When a periodic motion of a certain strength was applied to the nylon bar above the water layer in the big tank, a motion of the discs was caused relative to each other. Generally this loosened up the top layers of discs and partially filled up the water layer with discs.

0.7 Summary

Observations showed that behind the downward propagating stress "front" the stress was mainly transmitted perpendicularly to the stress front (that is, approximately vertical), while during unloading the stress was mainly horizontally transmitted. This was true for both the dry and saturated case.

In the saturated case a definite stress front was not identifiable, this might partially be due to a two-wave structure as found in the theory. But no definite conclusions could be made on this aspect.

Relative movement of water and discs was observed for low-frequency cyclic loading and shock loading of saturated disc configurations.

It was observed that indirect shock loading of the discs via a fluid layer on top of the discs was able to induce relative movement of the discs or even cause the discs to lose contact.

P. Summary and Conclusions

The thesis investigation on the wave propagation in saturated porous media was divided in two parts, a theoretical one and an experimental one.

The theoretical model consisted of a continuum with two interacting phases, a fluid and a skeleton. The linear field equations were derived from the non-linear balance laws and constitutive equations for the one-dimensional case. Limiting cases of these field equations yielded well-known results (e.g. fluidization). For "practical" values of wet sand and in the lower frequency range there exist two modes: one in which the phases move almost together (first mode) and one in which the phases move opposite (second mode). In the far field only the first mode survives because the first mode is slightly damped and the second mode is heavily damped. The second mode has to be introduced when we apply boundary conditions other than can be generated by the first mode ($v \approx w$). A larger permeability means a larger area near the boundaries where the second mode can exist. For the first mode and hence in the far field the effective pressure is small with respect to the pore pressure.

If we apply a step loading at the boundary in general, two discontinuities in the variables propagate. We were able to show that for "practical" values of wet sand the jump in the effective stress is always small with respect to the jump in the pore pressure along the fastest propagating discontinuity, regardless of the boundary conditions.

Using a wave front expansion we showed that the discontinuities decay as they propagate. The decay is faster if the permeability is smaller. Including non-linearities due to a non-linear constitutive equation for the fluid opposes the decay of propagating discontinuities in the gradients of the variables.

Equal phase velocities, in general, do not exist unless there is a certain ratio between the compressibilities of the fluid and the skeleton (Equation H.1.18). It was shown that the non-linear convective terms are unimportant if the speed of the discontinuity is high with respect to the phase velocities along the discontinuity.

The theory was extended to more than one dimension in order to allow shear waves to propagate. For an isotropic linear elastic skeleton we demonstrated that for the low frequency range the phases move almost together in the shear mode.

In an attempt to establish a more realistic constitutive equation for a granular material we introduced kinematical variables in order to define the state of a granular material. By using thermodynamic arguments we showed that the stress consists of the sum of stresses due to the "motion" of the kinematical variables. The linearized version of the constructed constitutive relation was used for further analysis in the "dilatant shear" case in the two-phase theory. In this case there exist non-propagating discontinuities, which can also occur in a dry material. For practical values of wet sand we showed some of the similarities and differences with respect to the one-dimensional case.

The speed of the fastest propagating discontinuity is equal for dilatant shear and one-dimensional compression. The jump in the effective stress is small with respect to the jump in the pore pressure and the velocity differences in the direction of propagation depends on the density ratio.

In the one-dimensional model we can apply different boundary conditions, e.g. loading the grains or fluid or both. As an application of the theory of propagating discontinuities we looked at a discontinuity propagating in a fluid and impinging on a two-phase medium at rest. Two discontinuities propagate into the two-phase medium. After the first discontinuity the pore pressure jump is large with respect to the effective pressure jump and both phases compress; however, after the second discontinuity near the boundary the effective stress falls back to zero and the pore pressure rises higher due to the boundary condition. Hence the fluid compresses and the skeleton expands. As indicated in the literature review, True [30], [31] did a series of experiments in which a soil column (saturated, wet and dry) was loaded by an explosion in air above it. True plotted the total pressure, pore pressure and calculated effective pressure as a function of time at depths of 6, 18, 54, 90 and 126 inches below the surface of the sand column and stated that the water pressures measured were probably realistic, but that the total measured and therefore the deduced effective pressures might be affected by wall friction. In the saturated case at a depth of 6 inches the pore pressure followed more or less the input air pressure. The plotted effective pressure

went down to negative reference stress (reference stress is static overburden stress ($\sim$ 1/2 psi)) following an interval of small positive effective stress. For the dry case, again at 6 inch depth, the pore pressure followed more or less the input air pressure, but the positive jump in the plotted effective stress was more pronounced, after which it went down below the static reference stress while the pore pressure was still increasing. Further down in the column the decrease in effective stress was less. True stated that there were indications of a quick condition in some of the tests in the top two feet of the sand column (negative values of effective stress with respect to the reference stress and migration of pressure meters).

A possible interpretation would be that near the top of the column the skeleton first compressed and thereafter expanded. This might have caused "overshoot" in the expanding grain structure to such an extent that the grains lost contact. In the theoretical model compression and expansion of the skeleton directly after impact is due to the existence of two waves in order to satisfy the boundary conditions and hence the question arises as to whether or not the second wave in a saturated granular medium exists and its significance with respect to liquefaction. Therefore, it would be interesting to assess by further experiments whether or not there is compression and expansion of the grain skeleton during such shock loading near the boundary as indicated in the theory. Furthermore it would be interesting to assess whether this phenomenon, if it exists, could initiate liquefaction due to "overshoot" in the expansion of the grain structure.

The experimental model for this thesis consisted of a disc configuration in which the interparticle stresses were visualized by a photoelastic technique. Stress waves in the discs, due to impact, were recorded by a high speed camera film. For the dry case a repeated loading and unloading of the discs took place, while in the saturated case there was apparently only one cycle of loading and unloading in the discs. A definite stress front could be identified in the dry case, but no definite stress front could be observed in the saturated case. Relative movement of fluid and skeleton was observed during impact. Discs that were loaded by impact in an indirect manner via a fluid layer on top of the discs showed a tendency to move upwards and also relative to each other. Whether this phenomenon was mainly due to overshoot of the loaded grain structure or the flow of the fluid is at the moment an open question.

The fact that in the dry case a definite wavefront could be identified, but not in the saturated case, might indicate a two wave structure as found in the theory. In order to assess the existence of the second wave one has to choose the parameters and the boundary conditions in such a manner that the second wave will be generated in at least a part of the field as indicated by the theory. This means a large permeability (in order to reduce the damping) and e.g. only loading the skeleton in the case the parameters take the "practical" values of wet sand (in order to generate the second wave).

Including relaxation effects of the skeleton in the theory, would allow a more detailed description of the change in the variables during rapid loading.

A P P E N D I C E S

Appendix I

Transmission Matrix and Jump Conditions for a Fluid

The transmission matrix and the jump conditions for a fluid system will be derived.

Assume the field equations are given by:

$$\rho_w \frac{\partial v}{\partial t} = - \frac{\partial p}{\partial x} \tag{I.1}$$

$$\frac{\partial v}{\partial x} = - \frac{1}{K_w} \frac{\partial p}{\partial t} \tag{I.2}$$

Equation (I.1) is the momentum equation and equation (I.2) is the continuity equation for the fluid. The pressure and the velocity are represented by p and v respectively. The mass density is ρ_w and the compression modulus is K_w. The independent variables are x and t.

Consider solutions in the form:

$$v(x,t) = V^0 e^{i\omega(t - \frac{x}{c})} = V(x) e^{i\omega t} \tag{I.3}$$

$$p(x,t) = P^0 e^{i\omega(t - \frac{x}{c})} = P(x) e^{i\omega t} \tag{I.4}$$

Substitution of the solution form (I.3) and (I.4) into the field equations (I.1) and (I.2) gives:

$$\rho_w V^0 - \frac{1}{c} P^0 = 0 \tag{I.5}$$

$$- \frac{1}{c} V^0 + \frac{1}{K_w} P^0 = 0 \tag{I.6}$$

For a non-trivial solution we require:

$$\begin{vmatrix} \rho_w & -\frac{1}{c} \\ -\frac{1}{c} & \frac{1}{K_w} \end{vmatrix} = 0 \qquad \text{(I.7)}$$

or:

$$c_{1,2} = \pm \left(\frac{K_w}{\rho_w}\right)^{1/2} \qquad \text{(I.8)}$$

From (I.3), (I.4) and (I.8) follows:

$$V(x) = V_1^0 \, e^{-i\frac{\omega}{c}x} + V_2^0 \, e^{i\frac{\omega}{c}x} \qquad \text{(I.9)}$$

$$P(x) = P_1^0 \, e^{-i\frac{\omega}{c}x} + P_2^0 \, e^{i\frac{\omega}{c}x} \qquad \text{(I.10)}$$

where:

$$c = \left(\frac{K_w}{\rho_w}\right)^{1/2} \qquad \text{(I.11)}$$

Furthermore from (I.5) it follows that

$$P^0 = c\,\rho\,V^0$$

Hence:

$$P_1^{\,0} = c\,\rho\,V_1^{\,0} = \frac{K_w}{c}\,V_1^{\,0} \tag{I.12}$$

$$P_2^{\,0} = -c\,\rho\,V_2^{\,0} = -\frac{K_w}{c}\,V_2^{\,0} \tag{I.13}$$

Substitution of (I.12) and (I.13) into (I.9) and (I.10) gives:

$$V(x) = V_1^{\,0}\,e^{-i\frac{\omega}{c}x} + V_2^{\,0}\,e^{i\frac{\omega}{c}x} \tag{I.14}$$

$$P(x) = \frac{K_w}{c}\,V_1^{\,0}\,e^{-i\frac{\omega}{c}x} - \frac{K_w}{c}\,V_2^{\,0}\,e^{i\frac{\omega}{c}x} \tag{I.15}$$

We now put:

$$V_1^{\,0} + V_2^{\,0} = A \tag{I.16}$$

$$-V_1^{\,0} + V_2^{\,0} = B \tag{I.17}$$

Then (I.14) and (I.15) become:

$$V(x) = A\cos\frac{\omega}{c}x + i\,B\sin\frac{\omega}{c}x \tag{I.18}$$

$$P(x) = -\frac{K_w}{c}\,B\cos\frac{\omega}{c}x - i\frac{K_w}{c}\,A\sin\frac{\omega}{c}x \tag{I.19}$$

so:

$$V(o) = A \tag{I.20}$$

$$P(o) = -\frac{K_w}{c} B \tag{I.21}$$

Substitution of (I.20) and (I.21) into (I.18) and (I.19) gives:

$$V(x) = V(o) \cos \frac{\omega}{c} x \qquad -i \frac{c}{K_w} P(o) \sin \frac{\omega}{c} x \tag{I.22}$$

$$P(x) = -i \frac{K_w}{c} V(o) \sin \frac{\omega}{c} x + P(o) \cos \frac{\omega}{c} x \tag{I.23}$$

or

$$V(L) = V(o) \cos \frac{\omega L}{c} - i \frac{c}{K_w} P(o) \sin \frac{\omega L}{c} \tag{I.24}$$

$$P(L) = -i \frac{K_w}{c} V(o) \sin \frac{\omega L}{c} + P(o) \cos \frac{\omega L}{c} \tag{I.25}$$

The above equation relates the amplitudes at x = o to the amplitudes at x = L. So we have to prescribe two variables at the boundaries in order to solve (I.24) and (I.25).

The jump conditions will be derived as follows: we write the field equations in integral form:

$$\frac{d}{dt} \int_{x_2}^{x_1} \rho_w \, v \, dx - [p] = 0 \tag{I.26}$$

$$\frac{d}{dt} \int_{x_2}^{x_1} \frac{p}{K_w} \, dx - [v] = 0 \tag{I.27}$$

So the jump conditions are:

$$- U \, [\rho_w \, v] + [p] = 0 \tag{I.28}$$

$$- U \, \left[\frac{p}{K_w} \right] + [v] = 0 \tag{I.29}$$

Substitution of (I.29) into (I.28) gives:

$$- U \, \rho_w \, U \, \frac{1}{K_w} + 1 = 0$$

or:

$$U = \pm \left(\frac{K_w}{\rho_w} \right)^{1/2} \tag{I.30}$$

We note that the velocity of the discontinuity has the same speed as the phase velocity.

From (I.28) follows:

$$p_1 - p_2 = U \rho_w (v_1 - v_2) \tag{I.31}$$

This is the jump condition across a discontinuity propagating with a speed given by (I.30).

Appendix II

Speed of Discontinuities for the Case $K_w << K_p$

The speed of the discontinuities for the case $K_w << K_p$ is derived as follows:

In this case equation (G.2.20) reduces to:

$$U^4 \ (1-n) \ \rho_w \ \rho_p \ n - U^2 \ K_p \ \rho_w \ n + n \ K_p \ K_w \approx 0 \qquad \text{(II.1)}$$

From (II.1) follows:

$$U^2 \approx \frac{K_p}{2 \ (1-n) \ \rho_p} \pm \frac{1}{2 \ (1-n) \ \rho_p \ \rho_w \ n}$$

$$\left(K_p^{\ 2} \ \rho_w^{\ 2} \ n - 4 \ (1-n) \ \rho_p \ \rho_w \ n^2 \ K_p \ K_w\right) \qquad \text{(II.2)}$$

Hence:

$$U_{1,2} \approx \pm \left(\frac{K_p}{(1-n) \ \rho_p}\right)^{1/2} \qquad \text{(II.3)}$$

$$U_{3,4} \approx \pm \left(\frac{K_w}{\rho_w}\right)^{1/2} \qquad \text{(II.4)}$$

We note that $U_{1,2}$ and $U_{3,4}$ are the speed of sound in the grain structure and the fluid respectively, viewed as separate materials.

Appendix III

Propagation of Shear Waves in a Two-Phase Medium with a Linearly Elastic Isotropic Skeleton

Consider the case where there are only shear deformations, which are independent of y, due to the applied boundary conditions. Then the field equations (J.3.16) to (J.3.23) reduce to:

$$\frac{\partial \tau_{xy}}{\partial t} = \frac{E}{2(1+\nu)} \frac{\partial v_y}{\partial x} \tag{III.1}$$

$$n \rho_w \frac{\partial w_y}{\partial t} = - \frac{n^2}{k} (w_y - v_y) \tag{III.2}$$

$$(1-n) \rho_p \frac{\partial w_y}{\partial t} = \frac{\partial \tau_{xy}}{\partial x} + \frac{n^2}{k} (w_y - v_y) \tag{III.3}$$

If we consider the harmonic solution:

$$\begin{Bmatrix} \tau_{xy} \\ w_y \\ v_y \end{Bmatrix} = \begin{Bmatrix} T_{xy}(x) \\ W_y(x) \\ V_y(x) \end{Bmatrix} e^{i\omega t} \tag{III.4}$$

and substitute (III.4) into (III.2) we obtain:

$$n\ \rho_w\ W_y\ i\omega\ = -\frac{n^2}{k}\ (W_y - V_y)$$

Hence if: $\rho_w\ \omega\ k \ll 1$, then: $W_y(x) \approx V_y(x)$ (III.5)

So in the lower frequency range:

$$w_y \approx v_y = v \tag{III.6}$$

Substituting (III.6) into (III.2) and (III.3), and then adding (III.2) and (III.3) gives:

$$\left\{(1-n)\ \rho_p + n\ \rho_w\right\}\ \frac{\partial v}{\partial t} = \frac{\partial \tau_{xy}}{\partial x} \tag{III.7}$$

Further from (III.1) follows:

$$\frac{\partial \tau_{xy}}{\partial t} = \frac{E}{2(1+\nu)}\ \frac{\partial v}{\partial x} \tag{III.8}$$

Hence in the lower frequency range the phase velocities are almost equal and the speed of the waves is:

$$c_s = \pm\ \left(\frac{\frac{E}{2(1+\nu)}}{(1-n)\ \rho_p + n\ \rho_w}\right)^{1/2}$$

The propagation of discontinuities is studied in the following way: From (III.1) to (III.3) we derive the following jump conditions in the usual way:

$$- U\,[\tau_{xy}] = \frac{E}{2(1+\nu)}\,[v_y] \tag{III.9}$$

$$- U\,n\,\rho_w\,[w_y] = 0 \tag{III.10}$$

$$- U\,(1-n)\,\rho_p\,[v_y] = [\tau_{xy}] \tag{III.11}$$

Hence:

$$w_{y_1} = w_{y_2} \tag{III.12}$$

$$\tau_{xy_1} - \tau_{xy_2} = - U\,(1-n)\,\rho_p\,(v_{y_1} - v_{y_2}) \tag{III.13}$$

where

$$U = \pm \left(\frac{\frac{E}{2(1+\nu)}}{(1-n)\,\rho_p} \right)^{1/2} \tag{III.14}$$

Hence behind a shear discontinuity the velocity of the fluid does not jump, but the shear stress and the skeleton velocity do.

Appendix IV Liquefied State

If we assume that the interparticle forces are zero ($\sigma=0$), the skeleton does not transmit any forces and hence the constitutive equation for the skeleton may be deleted.

Hence the field equations (B34) to (B37) reduce to:

$$n\,\rho_w \frac{\partial w}{\partial t} = -\,n \frac{\partial p}{\partial x} \qquad -\,\alpha\,(w-v) \tag{IV.1}$$

$$(1-n)\rho_p \frac{\partial v}{\partial t} = -\,(1-n)\,\frac{\partial p}{\partial x} + \alpha\,(w-v) \tag{IV.2}$$

$$\frac{\partial w}{\partial x} + \frac{1-n}{n}\frac{\partial v}{\partial x} = -\,\frac{1}{K_w}\,\frac{\partial p}{\partial t} \tag{IV.3}$$

where:

$$\alpha = \frac{n^2}{k} \tag{IV.4}$$

After some algebra we obtain:

$$\frac{\partial}{\partial t}\left\{ c_f{}^2 \frac{\partial^2 p}{\partial x^2} - \frac{\partial^2 p}{\partial t^2}\right\} + \tau^{-1}\left\{c_0{}^2 \frac{\partial^2 p}{\partial x^2} - \frac{\partial^2 p}{\partial t^2}\right\} = 0 \tag{IV.5}$$

where

$$c_f{}^2 = \frac{K_w\left(n\,\rho_p + (1-n)\rho_w\right)}{n\,\rho_w\,\rho_p} \tag{IV.6}$$

$$c_0{}^2 = \frac{K_w/n}{n\,\rho_w + (1-n)\,\rho_p} \tag{IV.7}$$

$$\tau^{-1} = \frac{n\left\{(1-n)\,\rho_p + n\,\rho_w\right\}}{k\,(1-n)\,\rho_p\,\rho_w} \tag{IV.8}$$

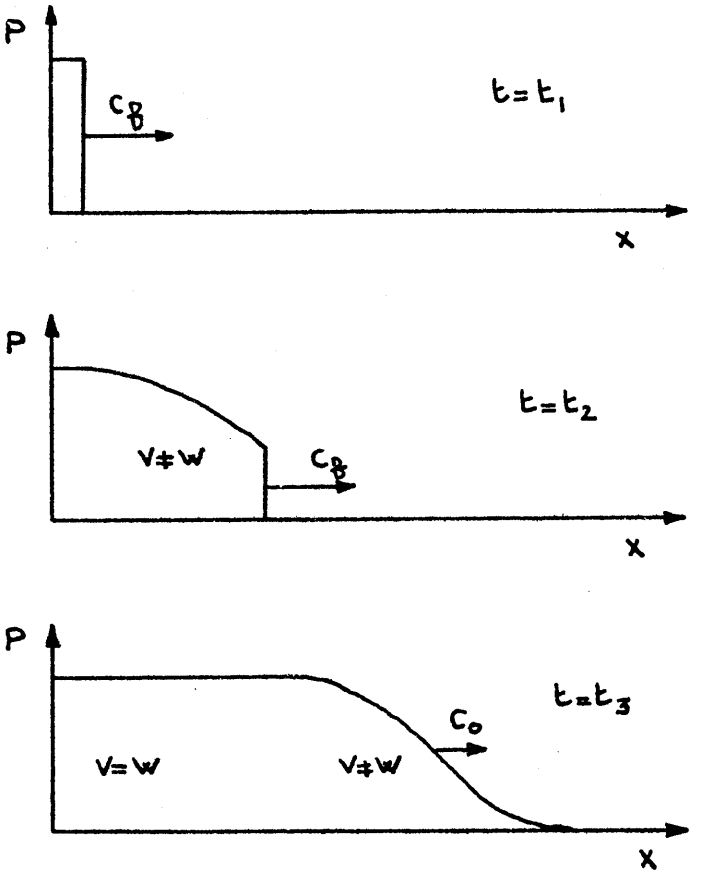

FIG. 21

This is a familiar equation in the theory of the dynamics of mixtures. (e.g. Noordzy and van Wyngaarden [61], Marble [62]). For times $t<<\tau$ the solution consists of waves propagating at speed c_f and for times $t>>\tau$ the solution represents waves propagating with speed c_0.

For a step-loading in the pressure at the boundary we have the following situation: for times smaller than τ the components might have different velocities, but for times greater than τ the component velocities become the same. An initial disturbance propagates with the speed c_f and the strength of this disturbance is being damped exponentially as it propagates. Finally the disturbance has a speed c_0, the equilibrium speed of sound (v=w). This is shown in figure (21).

Inspection of (IV.6) shows that the speed c_f is equal to the fastest propagating discontinuity (G.2.21). The connection is clear when we realize that if we take $K_p \to 0$, the speed and the strength of the slowest propagating discontinuity go to zero and hence we would obtain the same picture if we do the analysis with field equations (B.34) to (B.37) for $K_p \to 0$. Further we note that c_0 is equal to c_1 (C.38) if we take $K_p \to 0$ and $c_2 \to 0$ if $K_p \to 0$ for the lower frequency range.

Nikolaevskii [15] studied the shock wave propagation in a mixture (hence with zero interparticle forces) in the framework of a non-linear theory, for which the solution is stationary in the moving coordinate system $\xi = x - V\,t$ (where V is the shock wave velocity). He concluded that a stationary structure of the front is possible.

For the linearized case he derived an equation in the form of (IV.5).

Appendix V

The generation of some familiar results in soil mechanics with the field equations

V.1 Fluidization

We consider a stationary process in which v=0 (particle velocity).

The momentum equation for the fluid and the skeleton become:

$$0 = - n \frac{\partial p}{\partial x} - \frac{n^2}{k} w - n \rho_w g \qquad (V.1.1)$$

$$0 = - \frac{\partial \sigma}{\partial x} - (1-n) \frac{\partial p}{\partial x} + \frac{n^2}{k} w - (1-n) \rho_p g \qquad (V.1.2)$$

Substitution of (V.1.1) in (V.1.2) gives:

$$\begin{aligned} \frac{\partial \sigma}{\partial x} &= - (1-n) \left\{ - \frac{n}{k} w - \rho_w g \right\} + \frac{n^2}{k} w \\ &\quad - (1-n) \rho_p g \\ &= - (1-n) \left\{ \rho_p - \rho_w \right\} g + \frac{n}{k} w \end{aligned} \qquad (V.1.3)$$

The first term on the right-hand side we call the term due to the buoyancy force and the second term on the r.h.s. we call the term due to the seepage force.

If we assume $\frac{\partial \sigma}{\partial x} = 0$ and assume that the effective stress is zero at the top of the specimen, then $\sigma=0$ throughout. We call this a state of fluidization.

So for fluidization:

$$\frac{n}{k} w = (1-n)\left\{\rho_p g - \rho_w g\right\} \qquad \text{(V.1.4)}$$

Hence in a state of fluidization the seepage force just balances the buoyancy force (Scott [34]).

V.2 Stationary Flow

We assume a steady state, incompressible fluid and fixed position of the skeleton.

The storage equation for the liquid becomes: (J.3.19):

$$\frac{\partial w_x}{\partial x} + \frac{\partial w_y}{\partial y} = 0 \qquad \text{(V.2.1)}$$

The momentum equations for the fluid in x- and y-direction become: ((J.3.20) and (J.3.21) with gravity term)

$$0 = -n \frac{\partial p}{\partial x} - \frac{n^2}{k_x} w_x \qquad \text{(V.2.2)}$$

$$0 = -n \frac{\partial p}{\partial y} - \frac{n^2}{k_y} w_y - n \rho_w g \qquad \text{(V.2.3)}$$

Now we introduce the 'head' h in order to eliminate an explicit gravity term in the equations:

$$\frac{p}{\rho_w g} + y = h \qquad \text{(V.2.4)}$$

Substitution of (V.2.4) into (V.2.2) and (V.2.3) gives:

$$0 = -\frac{\partial h}{\partial x} - \frac{n}{k_x} w_x \qquad \text{(V.2.5)}$$

$$0 = -\frac{\partial h}{\partial y} - \frac{n}{k_y} w_y \qquad \text{(V.2.6)}$$

Substitution of (V.2.5) and (V.2.6) into the continuity equation (V.2.1) gives:

$$k_x \frac{\partial^2 h}{\partial x^2} + k_y \frac{\partial^2 h}{\partial y^2} = 0 \qquad \text{(V.2.7)}$$

This is the well-known quasi-Laplace equation which is used in order to solve stationary flow problems (Scott [34]).

V.3 Consolidation

We assume an incompressible fluid and a slowly varying process, so that we can neglect the inertia forces. In that case the field equations in one dimension become: ((B34) to (B37)).

$$0 = -n \frac{\partial p}{\partial x} - \frac{n^2}{k} (w-v) + n\, g\, \rho_w \tag{V.3.1}$$

$$0 = -\frac{\partial \sigma}{\partial x} - (1-n) \frac{\partial p}{\partial x} + \frac{n^2}{k} (w-v) + (1-n)\, g\, \rho_p \tag{V.3.2}$$

$$\frac{\partial w}{\partial x} + \frac{1-n}{n} \frac{\partial v}{\partial x} = 0 \tag{V.3.3}$$

$$\frac{\partial v}{\partial x} = -\frac{1}{K_p} \frac{\partial \sigma}{\partial t} \tag{V.3.4}$$

Adding (V.3.1) and (V.3.2) gives:

$$\frac{\partial \sigma}{\partial x} = -\frac{\partial p}{\partial x} + n\, g\, \rho_w + (1-n)\, g\, \rho_p \tag{V.3.5}$$

We can write (V.3.1) as:

$$\frac{\partial p}{\partial x} = -\frac{n}{k} (w-v) + \rho_w\, g \tag{V.3.6}$$

Substitution of (V.3.6) into (V.3.5) gives:

$$\frac{\partial \sigma}{\partial x} = -(1-n)\, g\, \rho_w + (1-n)\, g\, \rho_p + \frac{n}{k}(w-v) \qquad \text{(V.3.7)}$$

or:

$$\frac{\partial^2 \sigma}{\partial t\, \partial x} = \frac{n}{k}\, \frac{\partial}{\partial t}(w-v) \qquad \text{(V.3.8)}$$

Further from (V.3.4) follows:

$$\frac{\partial^2 v}{\partial x^2} = -\frac{1}{K_p}\, \frac{\partial^2 \sigma}{\partial x\, \partial t} \qquad \text{(V.3.9)}$$

Substitution of (V.3.9) into (V.3.8) gives:

$$\frac{\partial^2 v}{\partial x^2} = -\frac{n}{k\, K_p}\, \frac{\partial}{\partial t}(w-v) \qquad \text{(V.3.10)}$$

Differentiating (V.3.3) with respect to x gives:

$$\frac{\partial^2 (w-v)}{\partial x^2} + \frac{1}{n}\frac{\partial^2 v}{\partial x^2} = 0 \qquad \text{(V.3.11)}$$

Substitution of (V.3.10) into (V.3.11) gives:

$$\frac{\partial^2 (w-v)}{\partial x^2} = \frac{1}{k\, K_p}\, \frac{\partial}{\partial t}(w-v) \qquad \text{(V.3.12)}$$

Hence we note that the velocity difference between fluid and skeleton satisfies the diffusion equation.

In order to derive an equation for the stresses we proceed as follows:

From (V.3.6) follows:

$$\frac{\partial}{\partial x}(w-v) = -\frac{k}{n}\frac{\partial^2 p}{\partial x^2} \qquad \text{(V.3.13)}$$

and from (V.3.3) follows:

$$\frac{\partial}{\partial x}(w-v) + \frac{1}{n}\frac{\partial v}{\partial x} = 0 \qquad \text{(V.3.14)}$$

Substitution of (V.3.14) into (V.3.13) gives:

$$+\frac{k}{n}\frac{\partial^2 p}{\partial x^2} = \frac{1}{n}\frac{\partial v}{\partial x} \qquad \text{(V.3.15)}$$

From (V.3.4) and (V.3.15) follows:

$$k\,K_p\frac{\partial^2 p}{\partial x^2} = -\frac{\partial \sigma}{\partial t} \qquad \text{(V.3.16)}$$

Further from (V.3.5) follows:

$$\frac{\partial}{\partial x}(\sigma+p) = n\,g\,\rho_w + (1-n)\,g\,\rho_p \qquad \text{(V.3.17)}$$

Hence:

$$\sigma + p = \left\{ n\ g\ \rho_w + (1-n)\ g\ \rho_p \right\} x + \sigma_t(0,t) \qquad \text{(V.3.18)}$$

Substitution of (V.3.10) into (V.3.16) gives:

$$k\ K_p \frac{\partial^2 p}{\partial x^2} = \frac{\partial p}{\partial t} - \frac{\partial \sigma_t\ (0,t)}{\partial t} \qquad \text{(V.3.19)}$$

From (B25) follows:

$$K_p = -\frac{1-n_0}{\beta} = -\frac{1-n_o}{\frac{\partial g}{\partial \sigma}\Big|_{\sigma=\sigma_0}} = -\frac{1-n_0}{\frac{\partial n}{\partial \sigma}\Big|_{\sigma=\sigma_0}} \qquad \text{(V.3.20)}$$

Further we define the void ratio e:

$$e = \frac{n}{1-n} \qquad \text{(V.3.21)}$$

Then:

$$\frac{\partial e}{\partial \sigma}\Big|_{\sigma=\sigma_0} = \frac{\partial n}{\partial \sigma}\Big|_{\sigma=\sigma_0} \frac{1}{1-n_0} - n_0\,(1-n_0)^{-2} \frac{\partial n}{\partial \sigma}\Big|_{\sigma=\sigma_0}$$

or:

$$\frac{\partial e}{\partial \sigma}\Big|_{\sigma=\sigma_0} (1-n_0) = \frac{\partial n}{\partial \sigma}\Big|_{\sigma=\sigma_0} \left\{1 + \frac{n_0}{1-n_0}\right\} = \frac{\partial n}{\partial \sigma}\Big|_{\sigma=\sigma_0} (1+e_0) \qquad \text{(V.3.22)}$$

Substitution of (V.3.22) into (V.3.20) gives:

$$K_p = - \frac{1-n_0}{\frac{\partial e}{\partial \sigma}\Big|_{\sigma=\sigma_0} (1-n_0)} (1+e_0)$$

$$= \frac{1+e_0}{-\frac{\partial e}{\partial \sigma}\Big|_{\sigma=\sigma_0}}$$

$$= \frac{1+e_0}{a_v} \qquad \text{(V.3.23)}$$

where:

$$a_v = - \frac{\partial e}{\partial \sigma} \qquad \text{(V.3.24)}$$

Substitution of (V.3.23) into (V.3.19) gives:

$$k \frac{1+e_0}{a_v} \frac{\partial^2 p}{\partial x^2} = \frac{\partial p}{\partial t} - \frac{\partial \sigma_t\ (0,t)}{\partial t} \qquad \text{(V.3.25)}$$

where

$$k = \frac{k'}{\rho_w\ g}$$

k' = seepage coefficient

$\sigma_t\ (0,t)$ = total stress as a function of time at x=0.

This is the familiar consolidation equation (e.g. Scott[34]).

Appendix VI

Discontinuities in a two-dimensional dilatant material

VI.1 Static

We consider a dilatant material as described by (M.3.25) to (M.3.27). We can put these equations in the following form:

$$\begin{bmatrix} \sigma_{xx} \\ \tau_{xy} \\ \sigma_{yy} \end{bmatrix} = \begin{bmatrix} a & d & b \\ d & f & e \\ b & e & c \end{bmatrix} \begin{bmatrix} \gamma_{xx} \\ 2\,\gamma_{xy} \\ \gamma_{yy} \end{bmatrix} \qquad \text{(VI.1.1)}$$

Where a to f are constants. Now we consider $\tau_{xy}=0$, and hence σ_{xx} and σ_{yy} are principal stresses:

From (VI.1.1) there follows:

$$0 = d\,\gamma_{xx} + f\;2\gamma_{xy} + e\,\gamma_{yy}$$

Hence:
$$2\gamma_{xy} = -\frac{d}{f}\gamma_{xx} - \frac{e}{f}\gamma_{yy} \qquad \text{(VI.1.2)}$$

Substitution of (VI.1.2) into (VI.1.1) gives:

$$\sigma_{xx} = (a - \frac{d^2}{f})\ \gamma_{xx} + (b - \frac{d\ e}{f})\ \gamma_{yy} \qquad \text{(VI.1.3)}$$

$$\sigma_{yy} = (b - \frac{e\ d}{f})\ \gamma_{xx} + (c - \frac{e^2}{f})\ \gamma_{yy} \qquad \text{(VI.1.4)}$$

or:

$$\sigma_{xx} = E\ \gamma_{xx} + B\ \gamma_{yy} = E\ \frac{\partial u_x}{\partial x} + B\ \frac{\partial u_y}{\partial y} \qquad \text{(VI.1.5)}$$

$$\sigma_{yy} = B\ \gamma_{xx} + C\ \gamma_{yy} = B\ \frac{\partial u_x}{\partial x} + C\ \frac{\partial u_y}{\partial y} \qquad \text{(VI.1.6)}$$

Further in the case $\tau_{xy}=0$, the equilibrium equations become:

$$\frac{\partial \sigma_{xx}}{\partial x} = 0 \qquad \text{(VI.1.7)}$$

$$\frac{\partial \sigma_{yy}}{\partial y} = 0 \qquad \text{(VI.1.8)}$$

Now we study the "propagation" of discontinuities in the y-direction in the same way as we studied the propagation in t in the former chapters.

We first put (VI.1.5) and (VI.1.6) in an appropriate form:

$$\frac{\partial \sigma_{xx}}{\partial x} = E \frac{\partial}{\partial x} \frac{\partial u_x}{\partial x} + B \frac{\partial}{\partial x} \frac{\partial u_y}{\partial y} \tag{VI.1.9}$$

$$\frac{\partial \sigma_{yy}}{\partial x} = B \frac{\partial}{\partial x} \frac{\partial u_x}{\partial x} + C \frac{\partial}{\partial x} \frac{\partial u_y}{\partial y} \tag{VI.1.10}$$

From (VI.1.7) to (VI.1.10) we derive the following jump conditions in the x-direction:

$$[\sigma_{xx}] = E \left[\frac{\partial u_x}{\partial x} \right] + B \left[\frac{\partial u_y}{\partial y} \right] \tag{VI.1.11}$$

$$[\sigma_{yy}] = B \left[\frac{\partial u_x}{\partial x} \right] + C \left[\frac{\partial u_y}{\partial y} \right] \tag{VI.1.12}$$

$$[\sigma_{xx}] = 0 \tag{VI.1.13}$$

$$-U^* [\sigma_{yy}] = 0 \tag{VI.1.14}$$

where $U^* = \frac{dx}{dy}$ is the direction of the discontinuity.

From (VI.1.11) to (VI.1.14) there follows: a necessary condition for the existence of a discontinuity in the strains $\frac{\partial u_x}{\partial x}$ and $\frac{\partial u_y}{\partial y}$ is: $(U^* \neq 0)$.

$$EC - B^2 = 0 \tag{VI.1.15}$$

then further:

$$[\sigma_{xx}] = 0 \tag{VI.1.16}$$

$$[\sigma_{yy}] = 0 \tag{VI.1.17}$$

$$\frac{[\frac{\partial u_x}{\partial x}]}{[\frac{\partial u_y}{\partial y}]} = -\frac{B}{E} \tag{VI.1.18}$$

Condition (VI.1.15) for the constitutive equations (VI.1.5) and (VI.1.6) states: strains $\frac{\partial u_x}{\partial x}$ and $\frac{\partial u_y}{\partial y}$ can exist if the stresses σ_{xx} and σ_{yy} are zero. This means the material is in a neutrally stable state.

Hence if condition(VI.1.15) is satisfied then a discontinuity in the strains can exist and the material is in a neutrally stable state.

VI.2 Propagating Discontinuities

We consider now the pore space to be empty. The field equations (N.1.14) to (N.1.20) can be written in the following form:

$$\frac{\partial \sigma_{xx}}{\partial t} = A \frac{\partial v_x}{\partial x} + D \frac{\partial v_y}{\partial x} \tag{VI.2.1}$$

$$\frac{\partial \tau_{xy}}{\partial t} = D \frac{\partial v_x}{\partial x} + F \frac{\partial v_y}{\partial x} \tag{VI.2.2}$$

$$(1-n)\ \rho_p \frac{\partial v_x}{\partial t} = \frac{\partial \sigma_{xx}}{\partial x} \tag{VI.2.3}$$

$$(1-n)\ \rho_p \frac{\partial v_y}{\partial t} = \frac{\partial \tau_{xy}}{\partial x} \tag{VI.2.4}$$

where A , D , F are constants.

We use here the usual convention in solid mechanics (σ_{xx} is positive in tension).

We derive the following jump conditions from (VI.2.1) to (VI.2.4):

$$-U\ [\sigma_{xx}] - A\ [v_x] - D\ [v_y] = 0 \tag{VI.2.5}$$

$$-U\ [\tau_{xy}] - D\ [v_x] - F\ [v_y] = 0 \tag{VI.2.6}$$

$$-U\ (1-n)\ \rho_p\ [v_x] - [\sigma_{xx}] = 0 \tag{VI.2.7}$$

$$-U\ (1-n)\ \rho_p\ [v_y] - [\tau_{xy}] = 0 \tag{VI.2.8}$$

or:

$$\left\{U^2\ (1-n)\ \rho_p - A\ \right\}[v_x] - D\ [v_y] = 0 \quad \text{(VI.2.9)}$$

$$-D\ [v_x] + \left\{U^2\ (1-n)\ \rho_p - F\ \right\}[v_y] = 0 \quad \text{(VI.2.10)}$$

For non-trivial solutions we require:

$$U^4\ (1-n)^2\ \rho_p^{\ 2} - (A+F)\ (1-n)\ \rho_p\ U^2 + (AF-D^2) = 0 \quad \text{(VI.2.11)}$$

or:

$$\tilde{\lambda}^2 - (A+F)\ \tilde{\lambda} + (AF-D^2) = 0 \quad \text{(VI.2.12)}$$

where:

$$U^2 = \frac{\tilde{\lambda}}{(1-n)\rho_p} \quad \text{(VI.2.13)}$$

Hence:

$$\tilde{\lambda}_{1,2} = \frac{A+F \ \pm \left\{(A+F)^2 - 4\ (A\ F - D\ )\right\}^{1/2}}{2} \quad \text{(VI.2.14)}$$

Assuming that A and F are positive, we conclude that there are only two positive roots λ_1 and λ_2 (4 discontinuities) if

$$A\ F\ - D^2\ > 0 \quad \text{(VI.2.15)}$$

$$(A-F)^2 + 4D^2 > 0 \quad \text{(VI.2.16)}$$

Further we note that if:

$$A\,F - D^2 = 0 \tag{VI.2.17}$$

there is only one discontinuity propagating in the positive x-direction and there is one non-propagating discontinuity.

We note further that decreasing the value of $A\,F - D$ until $A\,F - D^2 \to 0$ causes a maximum difference in the speed of the "propagating" discontinuities in the positive x-direction ($\tilde{\lambda}_{max} = A + F$ and $\tilde{\lambda}_{min} = 0$).

For a non-dilating material ($D = 0$) the roots become: $\lambda_1 = A$ and $\lambda_2 = F$.

Now we rewrite (VI.2.1) and (VI.2.2):

$$\sigma_{xx} = A \frac{\partial u_x}{\partial x} + D \frac{\partial u_y}{\partial x} \tag{VI.2.18}$$

$$\tau_{xy} = D \frac{\partial u_x}{\partial x} + F \frac{\partial u_y}{\partial x} \tag{VI.2.19}$$

In a similar way as in Section VI.1 we conclude that condition (VI.2. means that the material is in a neutrally stable condition.

Hence the interpretation becomes clear: when we assume A and F positive ("reasonable" material behavior) and fixed, and we increase D (measure for dilatancy) from zero until:

$$A\,F - D^2 = 0$$

we see the following behavior with respect to the discontinuities:

First (if $D = 0$) two discontinuities propagating in positive x-direction are possible (propagation speed: $U_1 = \left(\frac{A}{(1-n)\,\rho_p}\right)^{1/2}$, pure compression, and $U_2 = \left(\frac{F}{(1-n)\,\rho_p}\right)^{1/2}$, pure shear).

Increasing D will increase the speed of the fastest propagating discontinuity and decrease the speed of the slowest discontinuity (both discontinuities generate now shear and compression).

If $A\,F - D^2 = 0$, then the slowest discontinuity degenerates into a stationary discontinuity. The fastest discontinuity will propagate with speed $U = \left(\frac{A+F}{(1-n)\,\rho_p}\right)^{1/2}$. At that point the material is in a neutrally stable condition.

List of Symbols

ρ_p = mass density of the grain material

ρ_w = mass density of the fluid

w = average fluid velocity

v = average skeleton velocity

p = fluid pressure

σ = effective stress

n = porosity

R = interactive forces

g = acceleration due to gravity

k' = permeability coefficient

ω = frequency

c = wavespeed

K_w = compression modulus of the fluid

K_p = compression modulus of the skeleton

T = period of oscillation

λ = characteristic velocity

$[\,]$ = jump in the expression between the brackets

U = speed of discontinuity

Δ = change in the variable

$v_{x',y',z}$ = average skeleton velocity in x-, y- and z-directions

$w_{x',y',z}$ = average fluid velocity in x-, y- and z-directions

$\sigma_{x',y',z}$ = effective stress in x-, y- and z-directions

$\tau_{xy',xz',yz}$ = shearing stresses on faces of elemental unit volume

E = Young's modulus

ν = Poisson's ratio

$\underset{\sim}{X}$ = position of an elementary particle at a reference time

ψ, ϕ = kinematical variables

F_{ij} = deformation gradient

u_i = displacement in i-direction

ρ = mass density of an elementary particle

ε = internal energy per mass

η = entropy per mass

θ = temperature

e = void ratio

REFERENCES

1. Biot, M. A., 1956, "Theory of Propagation of Elastic Waves in a Fluid-Saturated Porous Solid", Part I, Low-Frequency Range and Part II, Higher Frequency Range, The Journal of the Acoustical Society of America, Vol. 28, pp. 158-191.

2. Biot, M. A., 1962, "Mechanics of Deformation and Acoustic Propagation in Porous Media," Journal of Applied Physics, Vol. 33, No. 4, pp. 1482-1498.

3. Biot, M. A., 1962, "Generalized Theory of Acoustic Propagation in Porous Dissipative Media," The Journal of the Acoustical Society of America, Vol. 34, No. 9, pp. 1254-1264.

4. de Josselin de Jong, G., 1956, "What Happens in the Soil during Pile-Driving," de Ingenieur, No. 25, pp. B.77-B.88, (in Dutch).

5. Ishihara, K., 1968, "Propagation of Compressional Waves in a Saturated Soil," Proc. of the International Symposium on Wave Propagation and Dynamic Properties of Earth Materials, University of New Mexico Press, pp. 195-206.

6. Ishihara, K., 1970, "Approximate Forms of Wave Equations for Water-Saturated Porous Materials and Related Dynamic Modulus," Soils and Foundations, Vol. 10, No. 4, pp. 10-38.

7. Hsieh, L. and Yew, C. H., 1973, "Wave Motions in a Fluid Saturated Porous Medium," Journal of Applied Mechanics, ASME, pp. 873-878.

8. Taub, P. A., 1967, "The Interaction of a Fibre Tangle with an Airflow," Journal of Fluid Mechanics, Vol. 27, Part 3, pp. 561-580.

9. Ghaboussi, J. and Wilson, E. L., 1972, "Variational Formulation of Dynamics of Fluid Saturated Porous Elastic Solids," Journal of the Engineering Mechanics Division, ASCE, Vol. 98, No. EM 4, pp. 947-963.

10. Liou, C. P., 1976, "A Numerical Model for Liquefaction in Sand Deposits," Ph.D. Dissertation, The University of Michigan, Ann Arbor, Michigan.

11. Yew, C. H., and Jogi, P. N., 1976, "Study of Wave Motions in Fluid-Saturated Porous Rocks," Journal of the Acoustical Society of America, Vol. 60, No. 1, pp. 2-8.

12. O'Connell, R. J. and Budiansky, B, 1974, "Seismic Velocities in Dry and Saturated Cracked Solids," Journal of Geophysical Research, Vol. 79, No. 35.

13. Kuster, G. T. and Toksöz, M. N., 1974, "Velocity and Attenuation of Seismic Waves in Two-Phase Media: Part 1, Theoretical Formulations," Geophysics, Vol. 39, No. 5, pp. 587-606.

14. Garg, S. K., Nayfeh, A. H. and Good, A. J., 1974, "Compressional Waves in Fluid-Saturated Elastic Porous Media," Journal of Applied Physics, Vol. 45, No. 5, pp. 1968-1974.

15. Nikolaevskii, V. N., 1964, "On the Theory of Shock Wave Propagation in Soft-Water-Saturated Soils," All-Union Symposium on Elastic-Plastic Wave Propagation in Continuous Media, Baku, FTD-HC-23-240-71 (translated from Russian).

16. Nikolaevskii, V. N., 1964, "On Some Relaxation Processes Connected with Heterogeneity of Continuous Media," Proceedings of the Eleventh International Congress of Applied Mechanics, Munich.

17. Nikolaevskii, V. N., 1966, "Transfer Phenomena in Fluid-Saturated Porous Media," Irreversible Aspects of Continuum Mechanics and Transfer of Physical Characteristics in Moving Fluids, IUTAM Symposium, Vienna.

18. Borisov, S. N., Nikolaevskii, V. N. and Radchenko, V. P., 1967, "Structure of a Shock-Wave Front in Water-Saturated Soil," Izv. AN SSSR. Mekhanika Zhidkosti i Gaza, Vol. 2, No. 3, pp. 55-63 (translated from Russian).

19. Lyakhov, G. M., Okhitin, V. N. and Chistov, A. G., 1972, "Shock Waves in Soils and Water near the Point of Explosion," Zhurnal Prikladnoi Mekhaniki i Tekknicheskoi Fiziki, No. 3, pp. 151-159 (translated from Russian).

20. Lyakhov, G. M. and Okhitin, V. N., 1974, "Spherical Blast Waves in Multicomponent Media," Prikladnoi Mekhaniki i Tekhnicheskoi Fiziki, No. 2, pp. 75-84 (translated from Russian).

21. Wyllie, M. R., Gardner, G. H. F. and Gregory, A. R., 1962, "Studies of Elastic Wave Attenuation in Porous Media," Geophysics, Vol. 17, No. 5, pp. 569-589.

22. Kuster, G. T. and Toksöz, M. N., 1974, "Velocity and Attenuation of Seismic Waves in Two-Phase Media: Part II, Experimental Results," Geophysics, Vol. 39, No. 5, pp. 607-618.

23. Gregory, A. R., 1976, "Fluid Saturation Effects on Dynamic Elastic Properties of Sedimentary Rocks," Geophysics, Vol. 41, No. 5, pp. 895-921.

24. Hardin, B. O., and Richart, F. E., Jr., 1963, "Elastic Wave Velocities in Granular Soils," Journal of Soil Mechanics and Foundation Division, ASCE, Vol. 89, No. SM 1, pp. 33-65.

25. Hall, J. R., and Richart, F. E., Jr., 1963, "Dissipation of Elastic Wave Energy in Granular Soils," Journal of Soil Mechanics and Foundation Division, ASCE, Vol. 89, No. SM 6, pp. 27-56.

26. Seed, H. B., and Lee, K. L., 1966, "Liquefaction of Saturated Sands During Cyclic Loading," Journal of the Soil Mechanics and Foundation Division, ASCE, No. SM 6, pp. 105-134.

27. Castro, G., 1975, "Liquefaction and Cyclic Mobility of Saturated Sands," Journal of the Geotechnical Engineering Division, ASCE, Vol. 101, No. GT-6.

28. Ivanov, P. L., 1967, "Compaction of Noncohesive Soils by Explosions," Leningrad, TT 70-57221, (translated from Russian).

29. Akai, K., Hori, M. and Shimogami, T., 1974, "Study on Stress Wave Propagation Through Saturated Cohesive Soils by Means of Triaxial Shock Tube," Proceedings of the Japanese Society of Civil Engineers, No. 228, pp. 99-108.

30. True, D. G., 1969, "Dynamic Pore Pressure Propagation in Sand, Naval Civil Engineering Laboratory, Port Hueneme, California, Technical Report R 610.

31. True, D. G. and Herrmann, H. G., 1967, "Pore Pressure Propagation in Uniform Rounded Quartz Sand," Technical Note N-889, U.S. Naval Civil Engineering Laboratory, Port Hueneme, California.

32. Perry, E. B., 1972, "Movement of Variable-Density Inclusions in the Wet Sand Under Blast Loading," U.S. Army Waterways Experiment Station, Soils and Pavement Laboratory, Vicksburg, Mississippi, Miscellaneous Paper S-72-37.

33. Whitman, R. V., 1970, "The Response of Soils to Dynamic Loadings," Contract Report No. 3-26, U.S. Army Engineer Waterways Experiment Station, Vickburg, Mississippi.

34. Scott, R. F., 1963, Principles of Soil Mechanics, Addison-Wesley, Inc.

35. Verruijt, A., 1969, "Elastic Storage of Aquifers," in Flow Through Porous Media, Edited by R. J. M. De Wiest, Academic Press.

36. Bear, J., 1972, Dynamics of Fluids in Porous Media, American Elsevier.

37. Terzaghi, K., 1943, Theoretical Soil Mechanics, John Wiley and Sons, Inc.

38. van der Kogel, H., 1973, "System-Theoretical Formulation of Dynamics of Fluid Saturated Porous Elastic Solids," (in Dutch), ir Thesis, Delft University of Technology, Delft, Netherlands.

39. Nikolaevskii, V. N., 1963, "Basic Equations of the Dynamics of Fluid-Saturated Elastic Porous Media," collection: Oil Extraction (in Russian), Izd. Nedra.

40. Herrmann, W., 1969, "Constitutive Equation for the Dynamic Compaction of Ductile Porous Materials," Journal of Applied Physics, Vol. 40, No. 6, pp. 2490-2499.

41. Garg, S. K. and Nur, A., 1973, "Effective Stress Laws for Fluid-Saturated Porous Rock," Journal of Geophysical Research, Vol. 78, No. 26, pp. 5911-5921.

42. Garg, S. K., Brownell Jr, D. H., Prichett, J. W. and Herrmann, R. G., 1974, "Shock-Wave Propagation in Fluid-Saturated Porous Media," Journal of Applied Physics, Vol. 46, No. 2, pp. 702-713.

43. Barkan, D. D., 1962, Dynamics of Bases and Foundations, Mc Graw-Hill Book Company, Inc.

44. Dorsey, N. E., 1940, Properties of Ordinary Water-Substance, Reinhold Publishing Corporation, New York.

45. Gassmann, F., 1951, "Elasticity of Porous Media," Vierteljahrschr. Naturforsch. Ges. Zürich, Vol. 96, pp. 1-21.

46. Brown, J. S. and Korringa, J., 1975, "On the Dependence of the Elastic Properties of a Porous Rock on the Compressibility of the Pore Fluid," Geophysics, Vol. 40, No. 4, p. 608-616.

47. Richart, F. E., Woods, R. D., and Hall, Jr., J. R., 1970, "Vibrations of Soils and Foundations, Prentice-Hall, Inc., Englewood Cliffs, N.J.

48. Pestel, E. C. and Leckie, F. A., 1963, Matrix Methods in Elasto-Mechanics, McGraw-Hill Book Company, Inc., New York.

49. Whitham, G. B., 1974, Linear and Nonlinear Waves, John Wiley and Sons.

50. Courant, R. and D. Hilbert, 1962, Methods of Mathematical Physics, Vol. II, Interscience, New York-London

51. Joyner, W. B., 1975, "A Method for Calculating Nonlinear Seismic Response in Two Dimensions," Bulletin of the Seismological Society of America," Vol. 65, No. 5, pp. 1337-1357.

52. Goodman, M. A. and Cowin, S. C., 1972, "A Continuum Theory for Granular Materials," Arch. Rat. Mech. Anal. 44, 249-266.

53. Mullinger, G., 1974, "A Dipolar Continuum Theory for Granular Media," Ph.D. Thesis, University of Canterbury, Christchurch, New Zealand.

54. Jenkins, J. T., 1975, "Static Equilibrium of Granular Materials", Journal of Applied Mechanics, pp. 603-606.

55. Gudehus, G., Goldscheider, M. and Winter, H., "Mechanische Eigenschaften von Sand und Ton und numerische Integrationsverfahren: einige Fehlerquellen und Genauigkeitsgrenzen," International Symposium on Numerical Methods in Soil Mechanics and Rock Mechanics, University of Karlsruhe, Germany, September 14-20, 1975.

56. Oda, M., 1972, "The Mechanism of Fabric Changes During Compressional Deformation of Sand," Soils and Foundations, Vol. 12, No. 2, pp. 1-18.

57. Dantu, P., 1957, "Contribution à l'Etude Mécanique et Geometrique des Milieux Pulvérulents," Proceedings of the 4th International Conference on Soil Mechanics and Foundation Engineering, London, Vol. 1, Div. 1, pp. 144-148.

58. De Josselin de Jong, G. and Verruijt, A., 1969, "Étude Photo-Élastique d'un Empilement de Disques," Cah. Gr. Franc. Rheol., Vol. 2, pp. 73-85.

59. Drescher, A. and de Josselin de Jong, G., 1972, "Photoelastic Verification of a Mechanical Model for the Flow of a Granular Material," Journal of Mechanics and Physics of Solids, Vol. 20, pp. 337-351.

60. Kuske, A. and Robertson, G., 1974, Photoelastic Stress Analysis, John Wiley and Sons.

61. Noordzy, L. and van Wijngaarden, L., 1974, "Relaxation Effects, Caused by Relative Motion on Shock Waves in Gas-Bubble/Liquid Mixtures," Journal of Fluid Mechanics, Vol. 66, Part 1, pp. 115-143.

62. Marble, F. E., 1970, "Dynamics of Dusty Gases," Annual Review of Fluid Mechanics, Vol. 2, pp. 397-446.

63. Gimalitdinov, F., 1968, "Rates of Propagation and Decay of Weak Discontinuties of Stress and Pressure in a Saturated, Arbitrarily Cemented Porous Medium," Mekhanika Zhidkosti i Gaza, Vol. 3, No. 6, pp. 166-169, 1968 (translated from Russian).